THE UNIVERSITY OF QUEENSLAND

AUSTRALIA

Slime Coating Mitigation on Mineral Surfaces in Froth Flotation by Saline Water

Shengli Zhao

BEng and MEng in Chemistry Science

A thesis submitted for the degree of Doctor of Philosophy at

The University of Queensland in 2017

School of Chemical Engineering

Abstract

Fine and ultra-fine particle flotation is central to the mining industry as a result of the need to treat low grade and difficult ores which require fine grinding to liberate valuable minerals from gangue minerals. However, the flotation of fine and ultra-fine particles is not efficient and a slime coating with slime gangue particles attaching to valuable minerals is one of the most popular barriers. A slime coating prevents the adsorption of collectors on the surface of valuable minerals resulting in low flotation recovery or low product quality.

Saline water is also an important issue in the mining industry. In Western Australia, bore water with a high ionic strength has to be used at mine sites for production, site rehabilitation, and downstream processing because fresh water is not available locally. In Queensland, most mine sites have adopted water re-use as a means for making freshwater savings. However, water re-use results in increased salinity in site water stores, which is driven largely by evaporation and ongoing salt inputs from spoil, minerals and groundwater. Flotation relies on a large amount of water and therefore the impact of saline water on flotation performance has gained more and more attention.

In this research, the role of saline water in the mitigation of slime coatings was studied and a generic approach to improve fine and ultra-fine particle flotation by using saline water was developed, building on the previous research. A model slime coating system was established by using copper minerals in the presence of clay particles. It was found that chalcocite flotation was depressed in the presence of bentonite slimes while chalcopyrite flotation was less affected.

Electrostatic interactions between copper minerals and clay particles were found to be responsible for the different flotation of chalcocite and chalcopyrite in the presence of clay minerals. It was found that surface oxidation occurred during

grinding and changed the surface properties of chalcopyrite and chalcocite. Chalcocite was strongly oxidized while chalcopyrite was slightly oxidized after the grinding with stainless steel media. The different extent of surface oxidation resulted in the different electrical property of chalcocite and chalcopyrite surfaces. The strongly oxidized chalcocite surface became positively charged after grinding at the same pH and electrostatically attractive to bentonite particles resulting in the depressed chalcocite flotation. In contrast, the slightly oxidized chalcopyrite surface remained negatively charged after grinding at pH 9.0 and entropically repulsive from bentonite slime particles. Therefore, bentonite slimes did not influence chalcopyrite flotation as much as chalcocite flotation.

Mitigation of slime coatings on chalcocite in flotation by using electrolytes was further investigated and kaolinite was used to introduce the slime. The results indicated that in tap water, the presence of kaolinite slimes depressed chalcocite flotation. With the addition of electrolytes to the flotation system, the flotation of chalcocite in the presence of kaolinite slimes was improved. The effect of cations (Li^+, Na^+ and K^+) and anions (F^-, Cl^- and I^-) on the mitigation of slime coatings on chalcocite surfaces in flotation was also examined in this study. It was interesting to find that larger size ions improved chalcocite flotation in the presence of kaolinite slimes more than smaller size ions.

Electrochemical impedance spectroscopy (EIS) was developed to investigate how kaolinite coated chalcocite surfaces and how electrolytes with different size ions mitigated this coating. It was found that the impedance of chalcocite in the presence of kaolinite was higher than that in the absence of kaolinite in the low frequency range due to the formation of kaolinite coatings on chalcocite surfaces decreasing the dielectric constant and increasing the impedance of chalcocite. EIS results indicated that the impedance of chalcocite in electrolyte solutions in the presence of kaolinite was lower than that in deionized water reflecting the mitigation of the slime coating. Electrolytes reduced the electrostatic attraction

between kaolinite and chalcocite, resulting in the mitigation of kaolinite fine particles coating on chalcocite surface and consequently the improved chalcocite flotation. In addition, for the cations (Li^+, Na^+ and K^+) and anions (F^-, Cl^- and I^-), the larger ions reduced the impedance of chalcocite more than the smaller ions with less slime coating on chalcocite surfaces presumably due to the greater decrease of electrostatic attraction between chalcocite and kaolinite.

Declaration by author

This thesis is composed of my original work, and contains no material previously published or written by another person except where due reference has been made in the text. I have clearly stated the contribution by others to jointly-authored works that I have included in my thesis.

I have clearly stated the contribution of others to my thesis as a whole, including statistical assistance, survey design, data analysis, significant technical procedures, professional editorial advice, and any other original research work used or reported in my thesis. The content of my thesis is the result of work I have carried out since the commencement of my research higher degree candidature and does not include a substantial part of work that has been submitted to qualify for the award of any other degree or diploma in any university or other tertiary institution. I have clearly stated which parts of my thesis, if any, have been submitted to qualify for another award.

I acknowledge that an electronic copy of my thesis must be lodged with the University Library and, subject to the policy and procedures of The University of Queensland, the thesis be made available for research and study in accordance with the Copyright Act 1968 unless a period of embargo has been approved by the Dean of the Graduate School.

I acknowledge that copyright of all material contained in my thesis resides with the copyright holders of that material. Where appropriate I have obtained copyright permission from the copyright holder to reproduce material in this thesis.

Publications during candidature

Journal Paper Published:

1) Peng,Y., Zhao,S., 2011. The effect of surface oxidation of copper sulfide minerals on clay slime coating in flotation. Minerals Engineering, 24 15: 1687-1693.

2) Zhao,S., and Peng,Y., 2012. The oxidation of copper sulfide minerals during grinding and their interactions with clay particles. Powder Technology, 230: 112-117.

3) Zhao,S., and Peng,Y., 2014. Effect of Electrolytes on the Flotation of Copper Minerals in the Presence of Clay Minerals. Minerals Engineering, 66-68, 152-156.

4) Zhao,S., and Peng,Y., Guo.B., Mai.Y., 2017. An impedance spectroscopy study on the mitigation of clay slime coatings on chalcocite by electrolytes. Minerals Engineering, 101，40-46.

Conference Papers Published:

1) Peng,Y., Zhao,S., Bradshaw.D., 2012. Role of saline water in the selective flotation of fine particles. Water in Mineral Processing: Proceedings of the First International Symposium. 2012 SME Annual Meeting, Seattle, USA, (61-72). 19 - 22 February 2012.

Publications included in this thesis

[1] Peng,Y., Zhao,S., 2011. The effect of surface oxidation of copper sulfide minerals on clay slime coating in flotation. Minerals Engineering, 24 (15): 1687-1693. – incorporated as Chapter 4.

Contributor	Statement of contribution
Author Shengli Zhao (Candidate)	Literature review (50%) Wrote the paper (50%)
Author Yongjun Peng	Literature review (50%) Wrote and edited paper (50%)

[2] Zhao,S., and Peng,Y., 2012. The oxidation of copper sulfide minerals during grinding and their interactions with clay particles. Powder Technology, 230: 112-117. – incorporated as Chapter 5.

Contributor	Statement of contribution
Author Shengli Zhao (Candidate)	Literature review (80%) Wrote the paper (70%)
Author Yongjun Peng	Literature review (20%) Wrote and edited paper (30%)

[3] Zhao,S., and Peng,Y., 2014. Effect of Electrolytes on the Flotation of Copper Minerals inthe Presence of Clay Minerals. Minerals Engineering, 66-68, 152-156. – incorporated as Chapter 6.

Contributor	Statement of contribution
Author Shengli Zhao (Candidate)	Designed experiments (60%) Wrote the paper (70%)
Author Yongjun Peng	Designed experiments (40%) Wrote and edited paper (30%)

[4] Zhao,S., and Peng,Y., Guo.B., Mai.Y., 2017. An impedance spectroscopy study on the mitigation of clay slime coatings on chalcocite by electrolytes. Minerals Engineering, 101，40-46. – incorporated as Chapter 7.

Contributor	Statement of contribution
Author Shengli Zhao (Candidate)	Designed experiments (60%) Wrote the paper (60%)
Author Yongjun Peng	Designed experiments (20%) Wrote and edited paper (20%)
Author Bao Guo	Designed experiments (10%) Wrote and edited paper (20%)
Author Yuliang Mai	Sponsorship

Contributions by others to the thesis

Prof. Yongjun Peng was responsible for setting up the thesis project, organising funding and establishing the initial project goals. He provided the initial idea of effect of clay minerals on copper sulphide flotation using saline water. He also made great contributions to the interpretation of experimental data and critically revised the draft of the thesis.

Statement of parts of the thesis submitted to qualify for the award of another degree

None

Acknowledgements

I would like to thank my principal advisor Prof. Yongjun Peng for his guidances, suggestions, criticisms and supports throughout the course of my research and study. I am very grateful to my supervisors for his always timely critical feedback and comments on the drafts of the papers and the thesis I wrote.

To other group members, including Drs Bao Guo, Bo Wang and Di Liu and Mr. Roy Wei, I am thankful for your help, support. I would also acknowledge the support from my company ALS Metallurgy Burnie.

I gratefully appreciate financial support of this work from Prof. Yongjun Peng's New Start-up Grant awarded from the University of Queensland. The anonymous reviewers are acknowledged for their helpful comments on the peer reviewed papers.

Finally, thanks to my family, especially to my wife Xueqin Zhang. I thank all of them for their understanding, love and support through this journey.

Keywords

Copper sulphide mineral, Chalcocite, Chalcopyrite, Clay, Slime coating, Surface oxidation, Particle-particle interaction, Flotation, Saline water, Electrolyte, Electrochemical impedance spectroscopy (EIS)

Australian and New Zealand Standard Research Classifications (ANZSRC)

ANZSRC code: 091404 Mineral Processing/Beneficiation, 100%

Fields of Research (FoR) Classification

FoR code: 0914, Mineral Processing/Beneficiation, 100%

Table of Content

List of Abbreviations

BSE	Back Scattered Electron
Cryo-SEM	Cryo Scanning Electron Microscopy
EDS	Energy Dispersive Spectrometry
MIBC	Methyl Isobutyl Carbinol
XPS	X-ray Photoelectron Spectroscopy
XRD	X-ray Diffraction
CV	Cyclic voltammetry
DI	Deionized
EIS	Electrochemical impedance spectroscopy
kg	Kilograms
L	Liter
M	Molar (mol dm^{-3})
min	Minute
mL	Milliliter
μm	Micron (10^{-6} m)
P_{80}	80 wt.% passing size
PAX	Potassium amyl xanthate
kΩ	Kiloohm

Chapter 1 Introduction

1.1 Research background and problem statement

Copper sulphide minerals yield most of the copper production throughout the world. They are often associated with precious minerals such as gold and silver. To recover copper sulphide minerals from ores, froth flotation which exploits the difference in surface wettability is normally used to separate them from other gangue minerals.

Clay minerals are naturally fine-grained with particles of colloidal size (Schoonheydt and Johnston, 2006; Kotlyar et al., 1996). It has been well documented that clay slime coatings occur on galena, coal and bitumen surfaces through electrostatic attraction, reduce surface hydrophobicity and then depress the flotation significantly (Gaudin et al., 1960; Arnold and Aplan, 1986; Liu et al., 2005a,b).

The flotation of copper sulphide minerals is also complicated by the presence of clay minerals. The industry is well aware of the difficulty in treating weathered copper ores containing clay minerals. Currently, the only way to treat this type of ores is to blend them at a small proportion with normal ores.

With the depletion of high grade ores, fine and ultra-fine particle flotation is central to the mining industry as a result of the need to treat low grade and difficult ores which require fine grinding to liberate valuable minerals from gangue minerals. However, the flotation of fine and ultra-fine particle is not efficient and the slime coating with slime gangue particles attaching to valuable minerals is one of the most important barriers. A slime coating prevents the adsorption of collectors on valuable minerals resulting in low flotation recovery or low product quality.

Saline water is also a key issue in the mining industry. In Western Australia, bore water with different types of electrolyte and high ionic strength has to be used at mine sites for production, site rehabilitation, and downstream processing because fresh water is not available locally. In Queensland, most mine sites have adopted water re-use as a means for making freshwater savings. However, water re-use results in increased salinity in site water stores, which is driven largely by evaporation and ongoing salt inputs from spoil, minerals and groundwater. Flotation relies on a large amount of water and therefore the impact of saline water with different electrolytes on flotation performance has gained more and more attention. Although salt solutions can have a detrimental corrosive effect on plant hardware, in some cases the occurrence of readily available underground water sources can outweigh this disadvantage, enabling them to be used in flotation.

The previous research work on ultra-fine nickel ore flotation shows that saline water may mitigate serpentine slime coatings on nickel sulphide minerals and improve their flotation significantly (Peng et al., 2012). Saline water may also mitigate clay slime coatings on copper minerals. Therefore, it is important to study the role of electrolytes in saline water in the flotation of copper minerals in the presence of clay minerals and develop a generic approach to improve fine and ultra-fine particle flotation by using saline water.

This study addresses both clay slime coatings and saline water at the same time by linking different types of electrolyte solutions with the mitigation of slime coatings in fine copper mineral particle flotation. Through this research, the flotation mechanisms in saline water and the mechanisms responsible for slime coatings and their mitigation in fine particle flotation may be advanced.

1.2 Research objectives

Based on the above description, the research objectives of this study were to:

1. Establish a model system by using copper sulphide minerals with the coating of slime clay particles;

2. Determine the interaction between slime clay minerals and valuable minerals in saline water.

3. Investigate the role of saline water in the mitigation of slime coatings and mineral flotation;

4. Identify the effect of different salts on the mitigation of slime coatings and mineral flotation.

Chapter 2 Literature review

2.1 Introduction

A comprehensive literature review was conducted based on the research objectives described in Chapter 1. Since the interaction between particles in solution plays an important role in slime coatings, the DLVO theory being used to rationalize forces between charged surfaces in liquid medium was reviewed firstly. Clay properties and slime coatings in mineral flotation were then reviewed to understand the past studies on slime coating mechanisms. The oxidation and flotation of copper sulphide minerals formed the third part of this literature review. In this part, the formation of copper sulphide minerals was firstly introduced. The oxidation on chalcopyrite and chalcocite as the primary and secondary copper mineral, respectively, was then reviewed due to its importance in changing copper mineral surface properties. Then, the previous studies on copper sulphide minerals flotation were outlined, which can assist the understanding and explanation of roles of surface oxidation in copper mineral flotation. The last part of this literature review was the effect of saline water on mineral flotation, outlining the past studies on the influence of saline water on mineral flotation.

This literature review provides an overall picture of current status of studies in these areas and pinpoints the gaps and directions of future researches which were also presented in the end of this chapter. In addition, this study is mainly focused on the chemical mechanisms of electrolytes effect on slime coating mitigation. The nonchemical mechanisms have not been taken into consideration.

2.2 DLVO theory

Slime coatings in flotation mean that fine gangue mineral particles attach to valuable mineral particles driven by attractive forces. The interaction between

particles in solution may play an important role. DLVO theory, developed by Deryagin and Landau (1941) and Verwey and Overbeek (1948), has been used to rationalize forces between charged surfaces interacting in liquid medium.

In DLVO theory, van der Waals forces and electrostatic forces between colloidal particles are considered as the two main sources of interaction. van der Waals forces are almost always present, and result from interactions of the rotating or fluctuating dipoles of atoms and molecules. In most situations, van der Waals forces are attractive.

Deryagin et al. (1982) reported the repulsion between interacting colloids with the same electrical charge in the suspension due to the double layer overlapping. When the interacting colloids have oppositely charged double layers, the attraction occurs.

Double layer model was first put forward by Helmholtz (1853). It refers to two parallel layers of charge surrounding the particle. The first layer is the surface charge layer consisting of ions adsorbed onto the object due to chemical interactions. The second layer is composed of ions attracted to the surface charge via the Coulomb force. It is made of free ions that move in the fluid under the influence of electric attraction and thermal motion rather than being firmly anchored. It is thus called the "diffuse layer". With the development of double layer theory, Stern layer was modelled which further contains Inner Helmholtz Layer (IHL), Outer Helmholtz Layer (OHL). However, traditionally practitioners in this field still call it as “double layer” which actually consists surface charge, stern layer (IHL and OHL), diffuse layer. It will be further discussed in section 2.5.3.

Double layer thickness is referred to the notion of Debye length (κ^{-1}). It indicates the diffuse layer forming the surface where the surface potential has fallen to 1/e of original value (Pashley and Karaman, 2004). Grahame (1947) proposed the

following formula indicating the electrical potential of an ion at distance x from the surface is equal to its bulk value because of the equilibrium between any ion next to a charged surface and the corresponding ions in the bulk solution.

$$C_i(x) = C_i(B)exp\left[-\frac{Z_i q\psi(x)}{kT}\right]$$

$$\psi(x) \cong \psi_0 exp(-\kappa x)$$

where C_i (B) and C_i (x) are the ion concentrations in bulk and at distance x from the charged surface, respectively. *Ziq* is the local density of any ion of charge and ψ is the potential energy.

The counter-ion in the diffuse layer may enter the Stern layer and result in the increase of attraction and decrease in repulsion. The increased ionic strength may also reduce the Debye length making the attractive van der Waals force dominate. This increase of attraction in electrolyte solution can influence the particle interaction in flotation and therefore the recovery of both valuable and gangue minerals.

2.3 Slime coatings on valuable minerals in flotation

A number of studies and industry practices show that slime coatings of clay mineral particles on the surface of valuable minerals dramatically reduce mineral flotation. It is one of the most important barriers for fine and ultra-fine particle flotation in the mining industry. In this section, clay mineral properties and the effect of clay slime coatings on mineral flotation will be reviewed.

2.3.1 Clay minerals

2.3.1.1 Clay mineral structures

Clay minerals are anisotropic and hydrated phyllosilicates with unit cells comprising a layer of one octahedral sheet and either one (such as kaolinite) or two (such as smectite) tetrahedral sheets (Brigatti et al., 2006).

For the octahedral sheet, cations are coordinated with six oxygen atoms or OH groups. These atoms or groups are located around the cations with their centres on the six corners of a regular octahedron. Octahedral cations are normally Al^{3+}, Fe^{3+}, Mg^{2+} and Fe^{2+}. Bergaya (2006) reported that other cations such as Li^{+}, Mn^{2+}, Co^{2+}, Ni^{2+}, Cu^{2+}, Zn^{2+}, V^{3+}, Cr^{3+} and Ti^{3+} could be the octahedral cations.

For the tetrahedral sheet, cations are coordinated with four oxygen atoms which are located around cations with their centres on the four corners of a regular tetrahedron. Si^{4+}, Al^{3+} and Fe^{3+} are the common tetrahedral cations.

Fig 2.1 below shows Bergaya's clay structure model (Bergaya et al., 2006) indicating that the free corners (the tetrahedral apical oxygen atoms, Oa) of all tetrahedral sheets point to the same side of the sheet and connect the tetrahedral and octahedral sheets to form a common plane with octahedral anionic position Ooct (Ooct = OH, F, Cl, O) while Ooct anions lie near to the centre of each tetrahedral 6-fold ring, but are not shared with tetrahedron. The 1:1 layer structure consists of the repetition of one tetrahedral and one octahedral sheet, while in the 2:1 layer structure one octahedral sheet is sandwiched between two tetrahedral sheets. Most clay minerals consist of such layers stacked on top of one another.

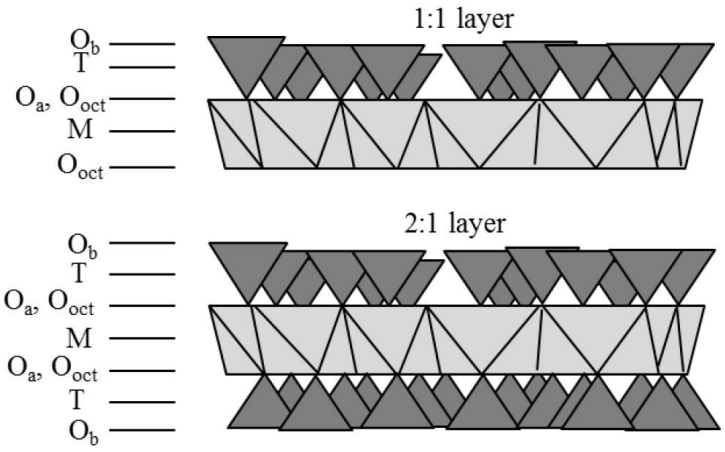

Fig 2.1 Models of 1:1 and 2:1 clay layer structures. Oa, Ob and Ooct refer to tetrahedral basal, tetrahedral apical, and octahedral anionic position, respectively. M and T indicate the octahedral and tetrahedral cation, respectively (reproduced from (Bergaya et al., 2006)).

2.3.1.2 Charges of clay minerals

Electrokinetic studies indicate that clay basal faces carry a constant negative charge at all pH values due to the compensation by the presence of positive counter-ions. In the tetrahedral sheet, trivalent cations (Al^{3+} or Fe^{3+}) may replace Si^{4+}. Divalent cations (Mg^{2+} or Fe^{2+}) may replace Al^{3+} in the octahedral sheet (Luckham and Rossi, 1999). A positive charge deficiency and a negative potential on clay surfaces are created in both cases. The negative potential is compensated by the adsorption of cations on the surface (Luckham and Rossi, 1999).

In the presence of water, these compensating cations diffuse away from the layer surface since their concentrations are often smaller in the bulk solution. On the other hand, they are attracted electrostatically to the charged layers. The result of these opposing trends is the creation of an atmospheric distribution of the compensating cations in a diffuse electrical double layer on the exterior layer surface of a clay particle (Luckham and Rossi, 1999). The compensating cations between the layers of the stack are confined to the narrow space between opposite layer surfaces.

At the edges of the clay layers, the atomic structure is entirely different from that of the flat-layer surfaces. At the edges of the plates, the tetrahedral silica sheets and the octahedral alumina sheets have broken primary bonds. The electrical charge of the edge, arising from hydrolysis reactions from broken Al–O and Si–O bonds, is pH dependent. The edges of clay particles are positively charged in the neutral and acid pH ranges depending on the type of clay minerals (Swartzen-Allen and Egon, 1974).

When the edge surface at tetrahedral sheet is broken, it becomes positively charged in the presence of small amounts of aluminium ions in solution compared with the surface of a silica particle, although silica particles as such are negatively charged. Since the equilibrium solution of clay minerals contain some aluminium ions owing to the slight solubility, the broken silica sheets may possibly carry a positive charge. Moreover, these sheets may be preferentially broken at the points where Si is substituted by Al. Therefore, the edges of clay particles in acid and even in neutral solution carry a positive double layer, in spite of the observed over-all electrophoretic negative charge. When the edge surface at octahedral sheet is broken, which is compared with the surface of alumina particle, alumina particles carry either a positive or a negative charge, depending on the pH of the solution. In acid solution because of Al acting as potential-determining ions and a negative double layer in alkaline solution with hydroxyl ions acting as potential-determining ions, the zero point of charge occurs at some intermediate pH, the position of which depends on the crystal structure of the alumina (van Olphen, 1964).

Zeta potential is known as the electrical potential at the shear plane. It is one of the important electro-osmotic properties of clay minerals. Moayedi et al. (2011) reported that the pH altered the zeta potential of kaolinite shown in Fig 2.2. It indicated that the negative value for the kaolinite system when pH higher than 3.1 due to the net negative surface charge on kaolinite surface. This is agreed with

the measurement in other literatures (Arnold and Aplan, 1986; Vane and Zang, 1997).

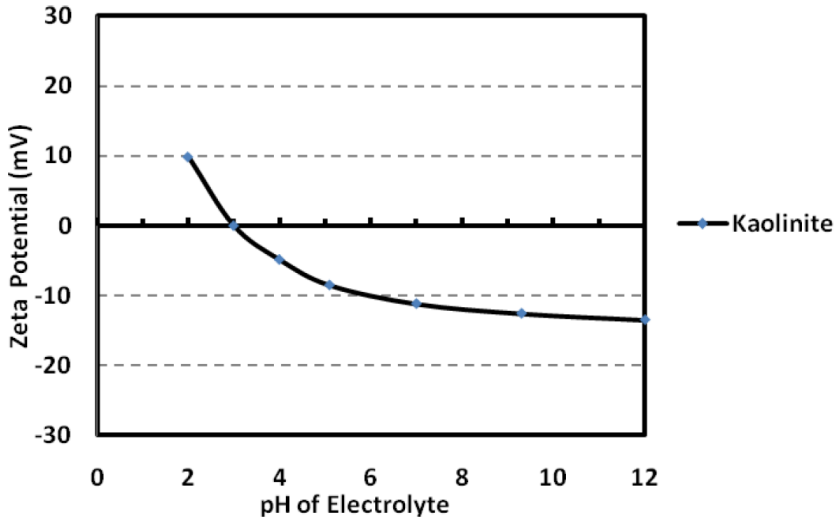

Fig 2.2 Zeta potential - pH relationship for suspended kaolinite in distilled water (Moayedi et al., 2011).

2.3.2 Slime coatings in mineral flotation

2.3.2.1 Slime coatings on mineral surfaces

The electrostatic attraction between gangue and valuable minerals has been reported to attribute to slime coatings. It has been well documented that clay slime coatings occur on galena, coal and bitumen surfaces through the electrostatic attraction, reduce surface hydrophobicity and then depress the flotation significantly (Arnold and Aplan, 1986b; Edwards et al., 1980).

The typical example is the flotation of pentlandite in the presence of serpentine in fresh water. Fig 2.3 shows that in neutral and weakly alkaline solutions, pentlandite is negatively charged, but serpentine is positively charged, resulting in electrostatic interaction between them. The coating of serpentine minerals on pentlandite surfaces explains the poor flotation behaviour of pentlandite as shown in Fig 2.4 (Edwards, G.R., 1980; Bremmell, K.E., 2005). Hydrophilic silicate slime coatings on valuable sulphide minerals reduce surface wettability and thus decrease both the flotation rate and recovery of sulphide minerals. Such flotation

depression actions may reduce the valuable sulphide minerals' flotation rate and recovery (Senior, G.D., 1991; Trahar, W.J., 1981).

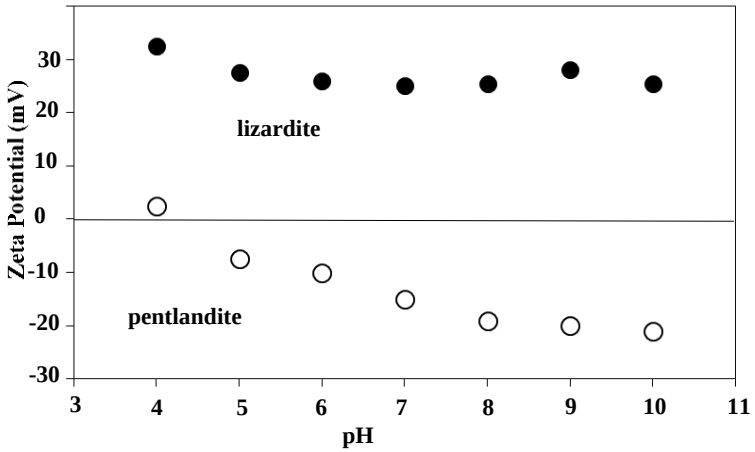

Fig 2.3 Zeta potential of lizardite (a serpentine mineral) and pentlandite (a nickel sulphide mineral) (Bremmell, K.E., 2005).

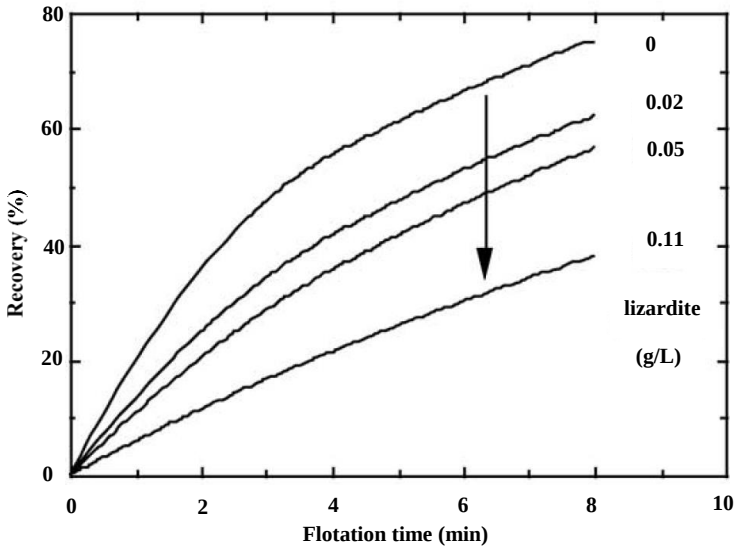

Fig 2.4 Flotation recovery of pentlandite in the presence of different proportion of lizardite (Bremmell, K.E., 2005).

The altered flotation of sphalerite by fine silica minerals has also been contributed to slime coating (Duarte, A.C.P., 2007). In Duarte's work (2007), silica recovery as a function of sphalerite recovery in mixed mineral experiments is presented in Fig 2.5. Sphalerite recovery significantly increased with the addition of both

copper sulphate (1800 g/t) and isopropyl xanthate (1500 g/t). However, silica recovery also increased. An increase in sphalerite recovery, after copper activation, was attributed to the formation of Cu(I)-xanthate species, according to the following reaction:

$$Cu_2S + X^- \longrightarrow CuX + CuS^-$$

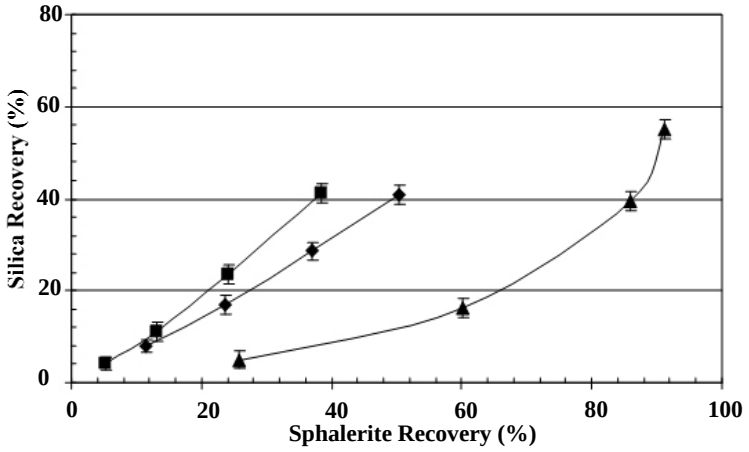

Fig 2.5 Silica recovery as a function of sphalerite recovery at pH 9 in the absence (■) and in the presence of 1800g/t of copper sulphate (CuSO4) (♦), and 1800g/t copper sulphate (CuSO4) +1500g/t isopropyl xanthate (SIPX) (▲) (Duarte, 2007).

Fig 2.6 shows silica recovery as a function of water recovery in a mixed system at pH 9. It indicates that, in the presence of reagents, silica recovery was due to a combination of entrainment and a second mechanism which may be via aggregation with sphalerite. Duarte (2007) found that reagent additions increased sphalerite and silica particle interaction due to the reduction of electrostatic repulsion.

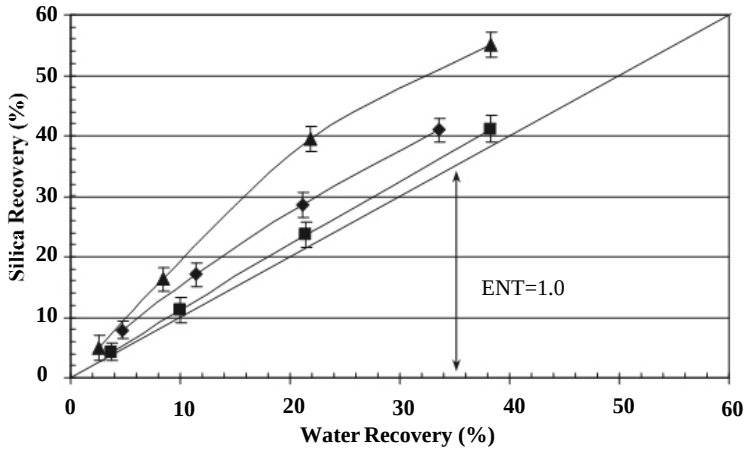

Fig 2.6 Silica recovery as a function of water recovery in a mixed mineral system in the absence of reagents (■), and in the presence of 1800g/t of copper sulphate (CuSO4) (♦), and 1800g/t of copper sulphate (CuSO4) +1500g/t of isopropyl xanthate (SIPX) (▲). Samples were conditioned in 10-3M NaCl at pH 9 prior to reagents addition. (Duarte, 2007).

He et al. (2009) investigated the mechanism of particle interactions and concomitant interfacial chemistry which led to sericite and chalcocite hetero-aggregation. The presence of Cu (II) species in the supernatant, due to oxidation and dissolution of chalcocite, had a striking impact on the interfacial chemistry of sericite particles and hence, caused sericite–chalcocite particle interactions. The specific adsorption of hydrolysed Cu (II) products formed in the pH range 5–11, resulted in the reversal of the sign of sericite surface charge as shown in Fig 2.7. This also led to a noticeable reduction in the magnitude of zeta potential on chalcocite particles. A combination of Cu(II)-mediated mechanisms including: electrostatic/charge patch attraction, van der Waals attraction, adsorbed ion–particle bridging, surface nucleation and cementation was attributed to be responsible for the unexpected attraction. Dispersion conditions which suppressed chalcocite oxidation (e.g., N_2 gas saturation) and dissolution (e.g., pH >7) provided significant electrostatic stabilisation barrier to sericite–chalcocite hetero-aggregation.

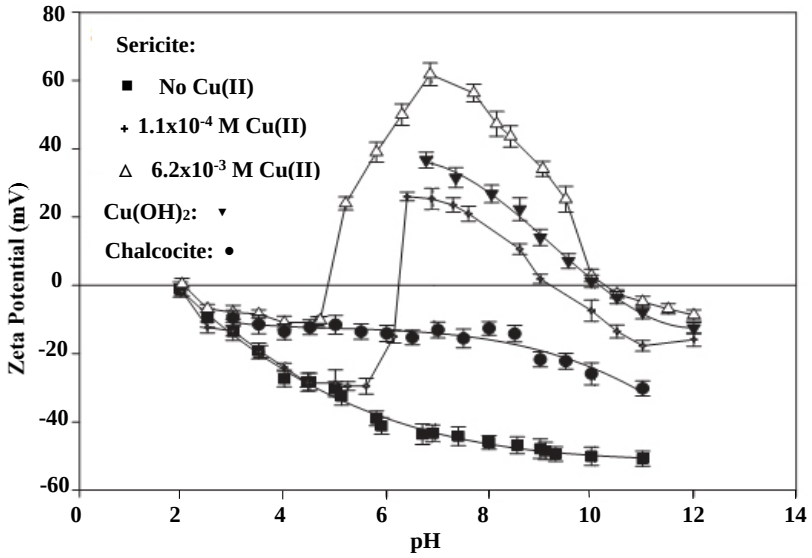

Fig 2.7 Zeta potential of various sericite, chalcocite and Cu(OH)2 (He et al., 2009).

2.3.3 Slime coating mitigation

Since the attractive electrostatic force between fine clay and valuable mineral particles causes slime coatings on mineral surfaces, slime coatings may be mitigated by reducing the attractive electrostatic force.

As an example, CMC (a negatively charged polymer) was used as the dispersant in pentlandite flotation in the presence of lizardite. The attraction between lizardite and pentlandite is changed to electrostatic repulsion as the result of lizardite becoming more negatively charged as CMC adsorbs preferentially on its surface. CMC therefore acts as a dispersant of the hydrophilic lizardite slime particles from the pentlandite surface, which results in the improved Ni recovery observed in the flotation of pentlandite.

Currently, it is common for the mining industry to use charged, low molecular weight polymers as dispersants to prevent the adsorption of silicate or oxide slime particles onto sulphide minerals during grinding and/or flotation. The adsorption of a polyelectrolyte onto mineral particles may increase the magnitude of the particle zeta potential and even result in surface charge reversal (Bandini, 2001;

Bremmell, 2005; Edwards, 1980; Pietrobon, 1997; Song, 2006; Wang, 1992). Reversal of either gangue or valuable mineral particle charge can dramatically alter the particle interactions from initial attraction to repulsion as a result of the emergence of repulsive electrostatic, steric or electro-steric forces which result from repulsive forces between overlapping electron clouds. Consequently, slime coatings can be suppressed or even completely eliminated. Fundamental understanding of polymeric dispersant structure-dependent adsorption behaviour is critical for judicious selection or tailoring of polymer structures for an enhanced mineral dispersing efficiency (Dasgupta, 1991; Israelachvili, 1991; Nsib, 2006,2007; Soga, 2001; Somasundaran, 2003; Tjipangandjara, 1990).

Another case of slime coating mitigation is to control dispersion conditions and pulp chemistry (e.g., via pH modification and speciation) prudently. High intensity conditioning involving vigorous agitation of pulps is one of the approaches used to remove clay slime particles from valuable sulphide mineral surfaces. The strong, destructive shear forces and turbulent eddies which characteristically prevail can, invariably, overcome the attractive interaction force between the slime and sulphide mineral particles (Chen, 1999b; Peng, 2011).

In summary, electrostatic forces play an important role in slime coatings in mineral flotation. The reduction of electrostatic interactions between gangue minerals and valuable minerals contributes to improvement of valuable minerals recovery and grade.

2.4 Oxidation and flotation of copper sulphide minerals

Copper is mainly used for electrical wire (60%), roofing and plumbing (20%), and industrial machinery (15%) (Emsley, 2003). Most of copper production is from copper sulphide minerals. The chemical compositions of different copper-bearing sulphide minerals vary from one mineral to the other one due to different

formation conditions, and these different compositions result in different electrochemical properties.

2.4.1 Formation of copper sulphide minerals

Copper ore bodies are formed when geothermal solutions (superheated under pressure) bring copper dissolved from deep underground to cool near surface environments where the copper and associated metals precipitate as minerals in veins and disseminations within the rock (Sillitoe and Petersen, 1996). Copper is usually deposited as copper sulphide minerals or in some environments as native copper metal. The most common copper minerals in the primary hydrothermal zone are chalcopyrite ($CuFeS_2$) and bornite (Cu_5FeS_4).

During millions of years the mineral deposit may be exposed to oxygen by air penetration, or by oxygen-rich water flowing over it. This oxidation alters the mineralogy, replacing the copper and iron sulphides with carbonates and oxides as the sulphur is oxidized to soluble sulphate and carried away in acid solution (Sillitoe and Petersen, 1996). The most common copper minerals in the oxidized zone are azurite ($Cu_3(CO_3)_2(OH)_2$), cuprite (Cu_2O), malachite ($Cu_2CO_3(OH)_2$) and tenorite (CuO), etc. Beneath the oxidized zone, some dissolved copper is precipitated as secondary or supergene copper minerals. This enriches the sulphides, making a secondary enrichment, or transitional zone. The secondary enrichment replaces iron in the minerals with more copper, further enriching the ore (Sillitoe and Petersen, 1996). The most common copper minerals in the secondary enrichment zone are chalcocite (Cu_2S) and covellite (CuS).

2.4.2 The oxidation on copper sulphide minerals

The oxidation of copper sulphide minerals is an important aspect in mineral processing. Generally mild oxidation results in a surface that is rich in polysulphides with some metal hydroxides present on the surface, due to the dissolution of metal ions from the surface and near surface layers, as observed in

ambient air, acidic and alkaline conditions by X-ray Photoelectron Spectroscopy (XPS) (Buckley and Woods, 1983, 1984). Extensive oxidation results in high quantities of metal hydroxides on the mineral surface (Senior and Trahar, 1991).

2.4.2.1 Chalcopyrite

Chalcopyrite $CuFeS_2$ (Kulikov et al. 1985) is a primarily n-type, less frequently p-type semiconductor. For natural specimens $\rho \approx 10^{-1}$-10^{-5} Ohm· m, the peak of the valent zone is genetically coupled to the 3p-levels of sulphur and the 3d-levels of iron ("genetically" was used to describe the elements of chalcocite such as copper, sulphur and iron). The concentration of carriers is 10^{18}-$10^{19}cm^{-3}$. The activation energy Ea≈0.01-0.03 eV. The crystal structure of chalcopyrite is tetragonal. It is a rectangular prism with a square base (a by a) and height (c, which is different from a). The lattice parameters are: a=5.25Å, c =10.32Å, the XRD main lines are 3.03, 1.85, 1.58, and 1.2. The energy of formation ΔG^0= -178.9 kJ/mol. (Abramov and Avdohin, 1998)

Chalcopyrite ($CuFeS_2$) is an important mineral of copper and an accessory mineral in many igneous rocks (Todd et al., 2003). It is one of the most common and abundant copper-bearing mineral of sulphide ore deposits (Crundwell, 1988). Surface oxidation of chalcopyrite plays an important role in mineral processing. Understanding of the surface chemistry of chalcocite has been widely applied in both flotation and leach process of ores. For example, the collectorless flotation of chalcopyrite can occur under mildly oxidizing conditions (Heyes and Trahar, 1977). Gardner and Woods (1979) reported the electron transfer reactions at a chalcopyrite electrode by employing linear potential sweep voltammetry. It was identified that the products of the oxidation reaction on the surface of chalcopyrite were CuS, $Fe(OH)_3$ and elemental sulphur. It is believed that the elemental sulphur on chalcopyrite surface render chalcopyrite floatable in the absence of collectors in flotation where high chalcopyrite recovery was achieved after

conditioning at high pulp potential. Multilayer quantities of sulphur extraction from chalcopyrite after dry grinding were reported by Kelebek and Smith (1989). Biegler and Horne (1985) also reported a surface layer composed of CuS and S^0 was formed on chalcopyrite electrodes in acid electrolyte solutions.

However, Buckley and Woods (1984) proposed a metal-deficient sulphide lattice rather than elemental sulphur formation by on oxidised chalcopyrite. XPS study indicated an iron hydroxide formation due to iron atoms migrating to surface during chalcopyrite surface oxidation. A sulphur-rich copper sulphide with stoichiometry CuS2 was also formed as well as copper sulphate. The reactions for the oxidation of chalcopyrite in alkaline and acidic solutions had been proposed.

The reaction in alkaline solution:

$$CuFeS_2 + 3/4xO_2 + 3/2xH_2O \rightarrow CuFe_{1-x}S_2 + xFe(OH)_3$$

with $x \approx 1$ for the outermost layers and with the ferric hydroxide covering the sulphur-rich lattice.

The reaction in acidic:

$$CuFeS_2 \rightarrow CuFe_{1-x}S_2 + xFe^{2+} + 2xe^-$$

Zachwieja et al. (1989) studied the oxidation of chalcopyrite agreed with Buckley and Woods (1984) and confirmed that the oxidation of chalcopyrite resulted in the release of iron ions from chalcopyrite. They also found that the floatability of the conditioned mineral was consistent with the hydrophobic sulphur-rich sulphide lattice.

The influence of pulp potential on chalcopyrite oxidation rate and species was also investigated. Vaughan et al. (1997) proposed the sequence of oxidation

reactions with increasing Eh on chalcopyrite surfaces in a solution at pH 9.2 by using cyclic voltammogram together with XPS and XAS:

$2CuFeS_2 + 3xOH^- \rightarrow 2CuFe_{1-x}S_2 + xFe_2O_3 + 3xH^+ + 6xe^-$

$2CuFeS_2 + 6OH^- \rightarrow 2CuS_2* + Fe_2O_3 + 3H_2O + 6e^-$

$CuFeS_2 + 3OH^- \rightarrow 2CuS_2* + Fe(OH)_3 + 3e^-$

$CuS_2* + 2OH^- \rightarrow CuO + 2S + H_2O + 2e^-$

$CuS2* + 2OH^- \rightarrow Cu(OH)_2 + 2S + 2e^-$

Buckley and Woods (1984) proposed the similar first three steps, which was confirmed by Mikhlin et al. (2004). With increasing the potential, these reactions continued, removing iron from deeper within the chalcopyrite. The CuS2 phase decomposed above a critical potential by the further reactions as shown in the last two steps. Similar oxidation pathways were proposed by Yin et al. (2000), who investigated the surface oxidation of chalcopyrite in alkaline solutions of pH 9.2 and 12.7, showing that the oxidation process consisted essentially of three potential-dependent stages.

Fig 2.8 summarizes the possible oxidation species. It is generally agreed that the oxidation starts from the release of iron ions which may form iron oxidation species at alkaline conditions. However, there is no literature about the distribution of O vs S regarding to the conversion of the surface from sulphide to oxide. As a result, a sulphur-rich surface is produced, although there remains an argument whether it is a metal-deficient sulphide lattice, a metal polysulphide or elemental sulphur.

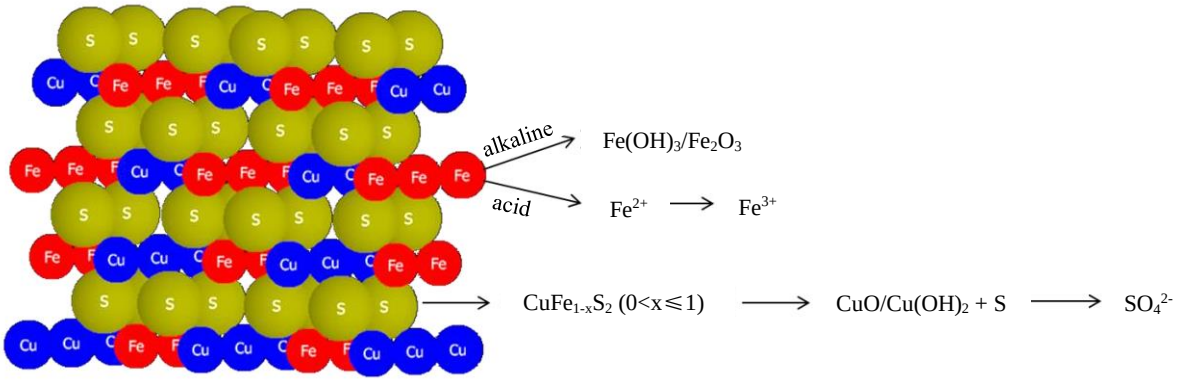

Fig 2.8 Crystal structure of chalcopyrite and schematic representation of some of the possible oxidation species for chalcopyrite oxidation (Chen, 2014).

Due to the oxidation layer thickness may play an important role in particle-particle interactions, researchers also tried to work out the thickness of chalcopyrite surface oxidation layers. For instances, Linge (1976) found that the limiting thickness of the oxidation layer on a chalcopyrite surface in ferric iron leaching was about 5nm. Eadington (1977) found an oxidation layer of 1.2±0.2nm thickness after chalcopyrite was exposed in dry air for 30 min, whereas after exposure in air-saturated deionised water for 1 min, an oxidation layer of 1.5±0.2nm thickness was formed. Yin (1994) reported an oxidation layer of 4nm thickness after chalcopyrite was exposed to atmosphere for 64 hours.

2.4.2.2 Chalcocite

Chalcocite Cu_2S exists in several polymorphous modifications, having variable composition [$Cu_{1.995}S$, $Cu_{1.95}S$ (jarlite), $Cu_{1.85}S$ (digenite)]. This mineral (Samsonov and Drozdova, 1972) is a low-temperature p-type semiconductor and conductivity ρ in natural specimens is $5\cdot10^{-5}$- $4\cdot10^{-2}$ Ohm·m. The activation energy Ea≈0.06–0.13 eV depends on ρ(T). The carrier concentrations of $Cu_{1.995}S$, $Cu_{1.95}S$ (jarlite), $Cu_{1.85}S$ (digenite) are $10^{20}cm^{-3}$, $10^{21}cm^{-3}$, $5\cdot10^{21}cm^{-3}$, respectively. The mobility≈2cm/ (V·s). In chalcocite, the significant ionic conductivity is related to migration of Cu^+; Ea = 0.12-0.26 eV. The parameters of

the crystalline lattice of hexagonal and rhombic chalcocite are a = 3.89Å, c = 6.68 Å; a =11.90 Å, b = 27.28 Å, c = 13.41 Å, respectively. The XRD main lines are 3.14, 2.52, 2.38, 1.96, and 1.64. The energy of formation is -84.6 kJ/mol (Abramov and Avdohin, 1998). Similar to chalcopyrite, the oxidation on chalcocite influences the surface hydrophobicity and the flotation reagent adsorption and hence the mineral floatability.

Walker et al. (1984) used a combination of spectrophotometric and electrochemical techniques for investigation on reactions in the chalcocite-0.05M borate system. They reported that at open circuit, Cu_2S underwent anodic dissolution with the resulting buildup of a soluble copper species and an oxidized sulphur species. The Cu^{2+} has a tendency to form insoluble hydroxides or oxides at alkaline pH.

The oxidation of Cu_2S has been proposed either by:

$$Cu_2S = 2Cu^{2+} + S^0 + 4e^-$$

or by consecutive reactions involving covellite as an intermediate:

$$Cu_2S = Cu^{2+} + CuS + 2e^-$$

$$CuS = Cu^{2+} + S^0 + 2e^-$$

Mielczarski and Suoninen (1988) investigated the oxidation of chalcocite in aerated water and at various pH values at room temperature by using XPS. In acidic solution, an almost monolayer coverage of adsorbed oxygen, water and hydroxide groups was found. While, in neutral and basic solutions, the surface consisted mainly of copper(I) and copper(II) hydroxides and of some copper(II) carbonate. The amount of these products increased with the pH of the solution. However, no oxidized sulphur species were observed on the surface layer.

Abramov and Forssberg (2005) reported that the oxidation products of chalcocite in the region with "more positive" Eh potential values were cupric hydroxycarbonate $Cu_2(OH)_2CO_3$ (pH<9), hydroxide $Cu(OH)_2$ (pH>9), or cuprous oxide Cu_2O and at "more" negative Eh potential values-elemental copper, cuprous, or cupric sulphides. Although the diagram does not have fields of stable simultaneous existence of chalcocite and elemental sulphur, formation of elemental sulphur S^0 on the mineral surface is still possible in acidic and reducing medium. Furthermore, the rate and degree of chalcocite oxidation must increase with an increase in pH value (Abramov and Forssberg 2005). These theoretically calculated results are in a good correlation with experimental measurements of the phase composition of oxidation products at various Eh and pH values undertaken by electron microscope methods (Peabody et al. 1997). It is noted that the primary oxidation product of chalcocite at pH < 5.5 is copper sulphate hydrate $CuSO_4 \cdot Cu(OH)_2$. At pH 5.5-9.5, it is copper hydroxycarbonate $Cu_2(OH)_2CO_3$ which at pH > 9.5 goes over to the hydroxide of bivalent copper $Cu(OH)_2$.

Overall, the oxidation products of chalcocite in a solution are mainly copper oxidation products, such as $CuSO_4 \cdot Cu(OH)_2$, $Cu(OH)_2$ and $Cu_2(OH)_2CO_3$, as summarized in Fig 2.9.

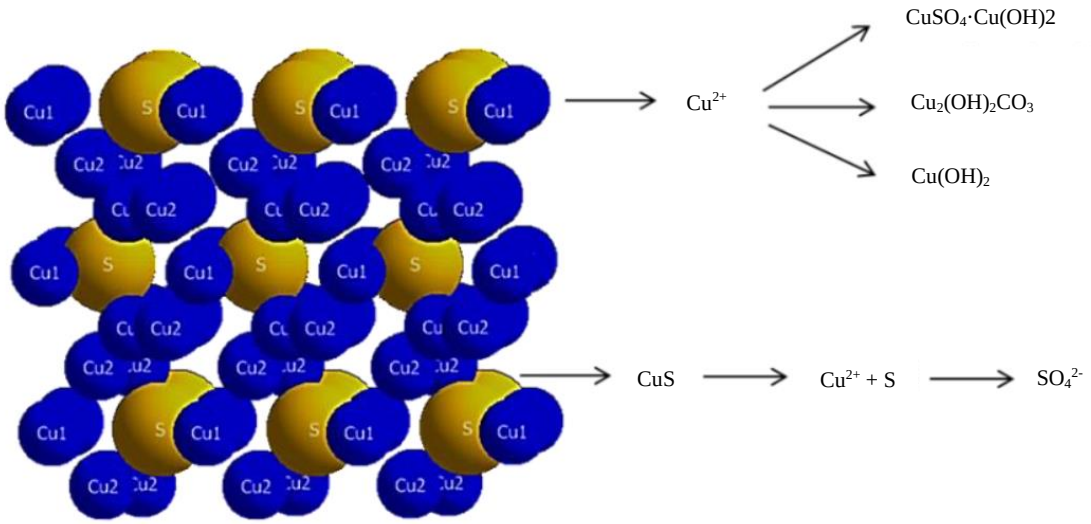

Fig 2.9 Crystal structure of chalcocite and schematic representation of some possible chalcocite oxidation species. (Chen, 2014).

In general, the oxidation behaviours of chalcopyrite and chalcocite are different. By EDTA extraction which removes metal oxidation species instead of metal sulphides, Lascelles and Finch (2002) found that chalcocite produced about 50 times more copper ions than chalcopyrite at the same size fraction (150/212 μm). Fullston et al. (1999) measured the zeta potential of the copper sulphide minerals including chalcocite, covellite, chalcopyrite, bornite, enargite and tennantite as a function of pH and the oxidation condition. They found that the change in zeta potential was governed by a copper hydroxide layer covering a metal-deficient sulphur-rich surface and with the extent of this copper hydroxide coverage increasing with the oxidation condition. They also demonstrated that among these copper sulphide minerals examined, chalcopyrite was the most electrochemically noble while chalcocite was the most electrochemically active (Fullston et al., 1999). Fig 2.10 and 2.11 show the study of Fullston (1999) on the oxidation of chalcopyrite and chalcocite by the measurements of zeta potential.

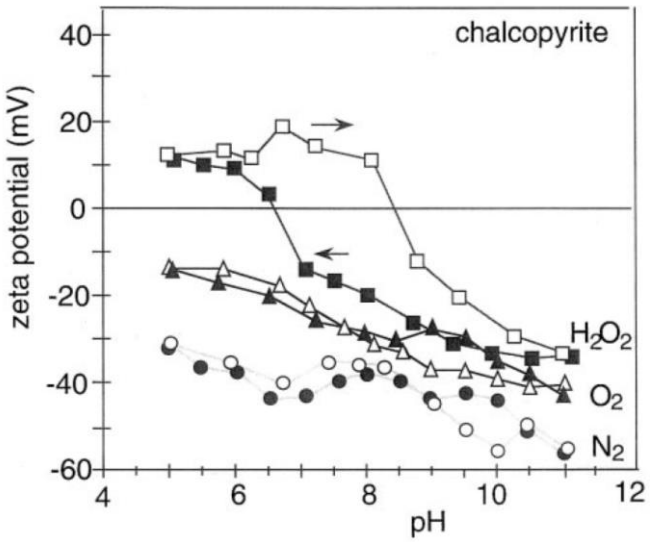

Fig 2.10 Zeta potential versus pH curves of chalcopyrite conditioned at pH 11.0 for 20 min in nitrogen (circle), for 60 min in oxygen (triangle) and for 60 min with H2O2 (square). Filled and empty symbols refer to a pH change from high to low pH values and from low to high pH values, respectively (the arrows show the direction of pH change). (Fullston et al., 1998)

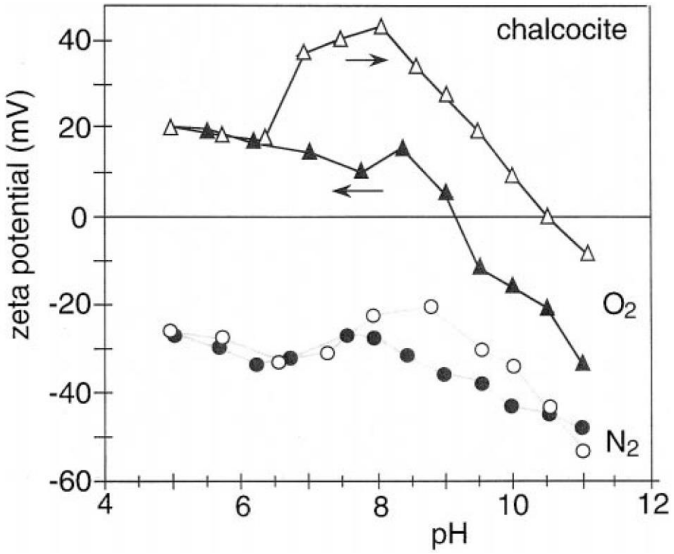

Fig 2.11 Zeta potential versus pH curves of chalcocite conditioned at pH 11.0 for 20 min in nitrogen (circle) and for 60 min in oxygen (triangle). Filled and empty symbols refer to a pH change from high to low pH values and from low to high pH values, respectively (the arrows show the direction of pH change). (Fullston et al., 1998)

2.4.3 Copper sulphide minerals flotation

The flotation of base metal sulphide minerals is always associated with surface oxidation. Surface oxidation not only modifies surface hydrophobicity, but also changes the electrical property on the surface and therefore the interaction with gangue minerals. The oxidation of base metal sulphide minerals produces hydrophobic metal deficient sulphur or polysulphides, and also hydrophilic oxidation products like $S_2O_3^{2-}$; SO_3^{2-} ; SO_4^{2-} and metal hydroxides (Buckley and Woods 1984; Guy and Trahar, 1984). The surface hydrophobicity is actually dependent on the balance of all these species.

Fullston et al. (1999) studied the oxidation of some copper sulphide minerals using zeta potential measurements, and found that the oxidation rate of these copper minerals follows the order: chalcocite > tennantite > enargite > bornite > covellite > chalcopyrite.

2.4.3.1 Chalcopyrite flotation

It is well-known that chalcopyrite can be floated in the absence of collectors under oxidizing conditions, but cannot be floated under reducing environment (Heyes and Trahar 1977). Guy and Trahar (1985) attributed the strong collectorless floatability of chalcopyrite after grinding in an oxidizing environment to chalcopyrite surface oxidation which produced hydrophobic sulphur-rich surfaces. However, an extensive oxidation may result in a production of high quantities of hydrophilic metal hydroxides or sulphates on the mineral surface, decreasing chalcopyrite flotation recovery (Senior and Trahar 1991, Gonçalves et al. 2003, Hirajima et al. 2014). Chander (1991) and Fairthorne et al. (1997) demonstrated that the hydrophobicity of the chalcopyrite surface and the self-induced chalcopyrite flotation were controlled by two oxidation processes, i.e. the metal dissolution that produced a hydrophobic surface and the metal hydroxide precipitation that produced a hydrophilic surface. Flotation results

obtained by Guo and Yen (2003) further proved this process. As shown in Fig 2.12, the chalcopyrite presented a collectorless floatability only in mild oxidizing environments. If the Eh is too high, the floatability will be decreased due to the destruction of metal-deficient sulphur layer.

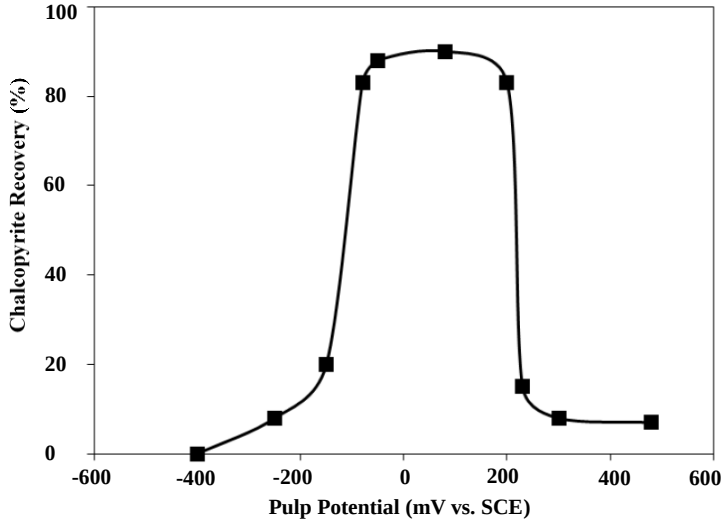

Fig 2.12 Floatability of natural chalcopyrite in pH 10 buffer solution without collector (Guo and Yen 2003).

2.4.3.2 Chalcocite flotation

Walker et al. (1984) correlated the reactions of chalcocite in aqueous solution with its collectorless flotation response. A low collectorless flotation recovery was achieved at open circuit due to the hydrophilic hydroxides formed on the surface. However, the collectorless flotation slightly increased at moderate reducing potential conditions, which may be because the hydrophilic hydroxides can be reduced with the simultaneous reformation of Cu_2S. Maximum natural flotation occurs between -0.03 and 0.0 V, as a result of either elemental sulphur or excess sulphur in the lattice such that the coordination of surface copper with sulphur is maximised. One aspect of this electrochemical study is that the experiments were performed in borate solution. Borate solution was used as a pH 9.2 buffer solution. Due to the borate solution was used in electrochemical study

first, it is appropriate to use it in the flotation test for comparison. As pointed out by Hayes et al. (1987), borate ions can form complexes with frothers, and influence the floatability of minerals. Therefore, it is important to take proper precautions to ensure that it is not a contributor to the apparent hydrophobicity of the system.

The flotation of chalcocite in the absence of collector was also investigated by Heyes and Trahar (1979). It was found that chalcocite displayed a small degree of collectorless flotation over a range of Eh values at pH 11, especially for the fine particles (-10 μm), although the recovery was always much lower than that of chalcopyrite at the same flotation conditions. However, whether the collectorless flotation of chalcocite was induced by sulphur on the mineral surface or by adsorption of frother was not determined in that study. Most of the species on chalcocite surface are hydrophilic, which is believed to be the main reason why chalcocite shows a significantly lower floatability than chalcopyrite in the absence of collectors. Sulphur rich surfaces may be formed at some conditions, which may increase the hydrophobicity, as reported by Walker et al. (1984), however, it has not been confirmed by surface analysis techniques.

Barzyk et al. (1981) identified that chalcocite surface oxidation had a strong effect on both xanthate adsorption and chalcocite floatability, and the most oxidized chalcocite sample required 100 times more collector consumption to obtain the same flotation results than the least oxidized sample. There is a strong relationship between Cu recovery and the electrochemical potential in flotation.

In summary, oxidation alters copper mineral surfaces resulting in different surface hydrophobicity. Chalcopyrite or chalcocite flotation recovery may be well controlled by electrochemical potentials (Tolley et al., 1996).

2.5 The effect of saline water on mineral flotation

Sea water, ground water and recycle water have been commonly used in Australian mining industry due to scarcity of fresh water and stringent regulations on the quality of discharged water. However, these types of water normally contain a high concentration of electrolytes resulting in significant salinity in site water. Since mineral flotation relies on a large amount of water, the impact of saline water on flotation performance has gained more and more attention.

2.5.1 Water structure

2.5.1.1 Pure water structure

It has been well known that liquid water possesses distinctive structural features similar to ice to a certain extent. A proposed resonance scheme for the hydrogen bond in water is shown in Fig 2.13 considering resonance among the three bond structures. The + and - signs represent formal charges, and the resonance (with suitable weighting coefficients) of molecule b between structures I and II represent the ordinary partial polarity of the O-H bond. The mixing-in of a contribution from structure III constitutes the formation of a hydrogen bond (Frank and Wen, 1957).

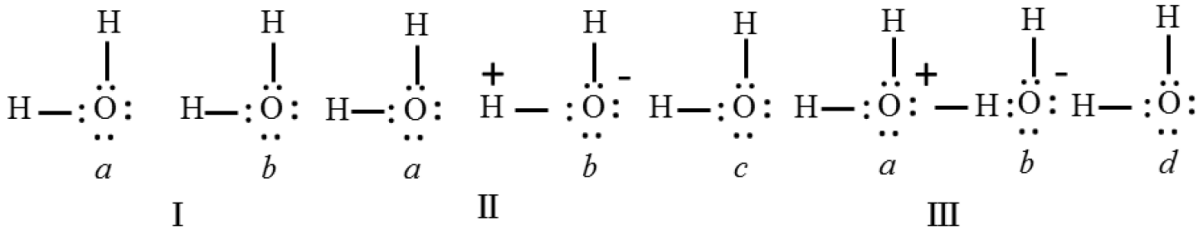

Fig 2.13 Proposed resonance scheme for the hydrogen bond in water (reproduced from (Frank and Wen, 1957)).

However, the liquid state of water structure can be very complex due to the hydrogen bonds may be formed with surrounding molecules. It results in a formation of branched three-dimensional structure of water molecules

interconnected with hydrogen bonds. Various methods were applied to study the properties of water structure such as thermodynamic, viscometric, and conductometric ones as well as X-ray structural analysis, neutron diffraction, NMR, dielectric spectroscopy, Raman spectroscopy, IR spectroscopy, etc. (Nikita et al, 2015). Fig 2.14 shows these hydrogen-bonded chains may form the cluster structure which may be an intrinsic structure of water molecules. The differences among different chains are only the number of molecules containing in them (Pang, 2014).

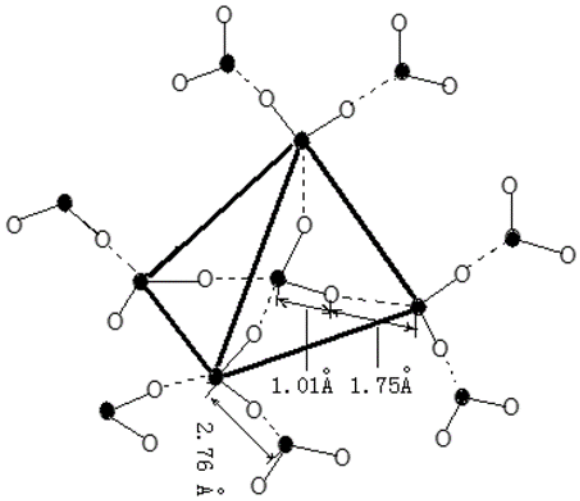

Fig 2.14 The cluster structure of molecules in water based on the hexagonal structure. (Pang, 2014)

2.5.1.2 Saline water structure

Past studies indicate that the electrolytes in solution may influence the water structure. The acknowledgement of Hofmeister effects has been included in this section. Franz Hofmeister published a series of seven papers with the running title 'Lessons on the effects of salts' between 1887 and 1898. He ingeniously separated cationic and anionic effects and established the Hofmeister series for ions by using salts with a common cation or anion (Hofmeister, 1888). Since then, many salts have been studied. The ion orders for cations and anions from weakly

hydrated to strongly hydrated are partially listed here: $K^{+}>Na^{+}>Li^{+}>Mg^{2+}>Ca^{2+}$ and $SCN^{-}>I^{-}>Cl^{-}>F^{-}$ (Duignan, 2014). Hofmeister's explanation for the ionic ordering was eventually framed into the 1930s–1950s theory of structure-making and structure-breaking ions (Jungwirth and Cremer, 2014).

It then has been widely discussed by Ben-Naim (1974), Franks (1972) and Wilhelm et al. (1977) that ionic solutes are attributable to water "structure making" or "structure breaking", while others used "flickering clusters" or "clathration shells" to explain the water structure (Frank and Wen, 1957; Nemethy and Scheraga, 1962; Glew, 1962). These researchers consistently referred the class of inert, nonpolar solutes to as "structure makers". Since then, the terms "structure-maker" and "structure-breaker" have almost universally been adopted to describe the effect of different ions on the surrounding water network (Hribar, 2002; Mancinelli, 2007).

More recently, a hydration model of ions in water has been proposed (Kang, 2014). The hydration model (Fig 2.15) illustrated that a cation has the water molecules oriented toward it with their electron-pair donor atoms, carrying a fractional negative charge, directed at the cation, possibly resulting in a hydrogen bond to form the first hydration shell. These water molecules are polarized by the charge of the cation and are hydrogen-bond donors to other water molecules to form second hydration shell (Marcus, 2015).

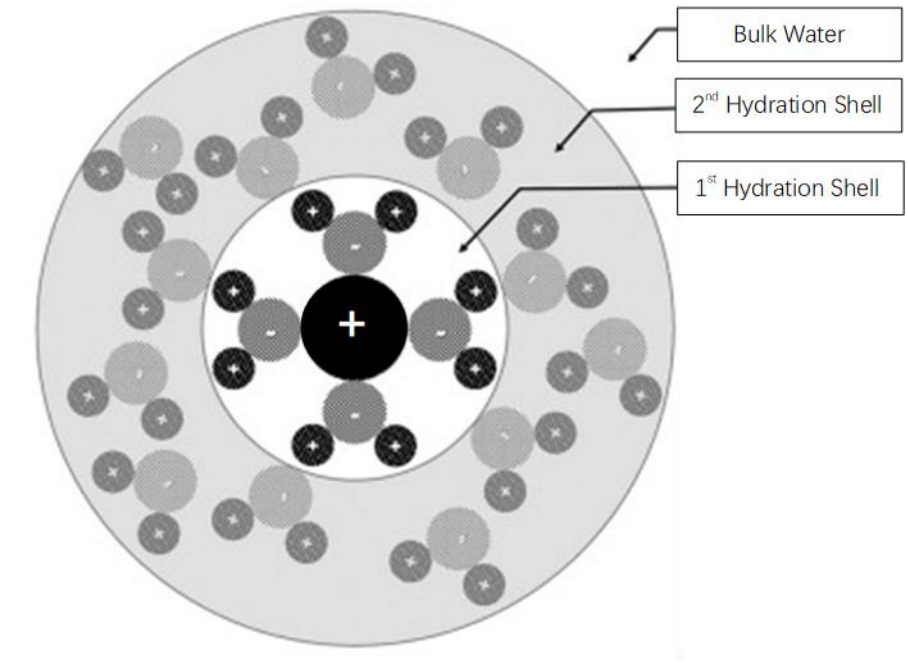

Fig 2.15 Illustrations of hydration model of ions (Reproduced from (Kang, 2014))

The concept of ions being '"structure-maker" and "structure-breaker" has also been challenged (Omta, 2003). It was concluded that the addition of ions had no influence on the rotational dynamics of water molecules outside the first solvation shell which means the effect of ions on water structure is short range. The 2nd hydration shell is normally less than 1nm (Hitoshi, 1993; Martinez, 1999; Spångberg, 2004; Faro, 2010). This result was used to argue that the presence of ions does not lead to an enhancement or a breakdown of the hydrogen bond network in liquid water beyond the first hydration shell of the ions.

Collin (2004) investigated the specific ion effect on water structure and reported that small ions of high charge density are strongly hydrated whereas large monovalent ions of low charge density are weakly hydrated. Kunz (2010) reviewed specific ion effect with many updated experimental data as well as different approaches to explain specific ion effects. They commented that Collins' concept of matching water affinities seems to be a convincing qualitative interpretation for the specific ion effect. However, till today, the saline water structure is still a topic of study.

2.5.2 The effect of saline water on mineral flotation

The flotation of naturally hydrophobic particles in inorganic electrolyte solutions was first documented during the 1930's in the USSR. This work was essentially related to the flotation of coals in saline waters. Following these early studies, many other cases have been reported in the general area of mineral flotation. For example, there are several sulphide mineral systems where it has been clearly demonstrated that different types of inorganic electrolytes can have a profound influence on the flotation kinetics. This area has been reviewed by Wellham et al. (1992), Yoon (1982), and Yarar (1988). A summary indicating the types of electrolytes tested in neutral pH and the characteristics of some of these systems is shown in Table 2.1.

Table 2.1 Examples of salt flotation practice (Paulson and Pugh, 1996)

Electrolyte solution	System floated
Seawater	Zn concentrate from 3.4% to 47.7%
NaCl, $CaCl_2$, Na_2SO_4	Coals; recoveries, 12-83%; grades; 4.5-8.4% ash
NaCl, KCl, $CaCl_2$, saline pit water	Coals; recoveries, ~96%; flotation response is rank-dependent
$Al_2(SO_4)$, Na_2SO_4, NaCl, $CaCl_2$	Coals; recoveries, up to ~90%;Response is Macerel-dependent
NaCl, Na_2CO_3, Na_2PO_4,	
Na_2SO_4, $(NH_4)_2SO_4$, $CuSO_4$,	Coals; recoveries, 50-77%; ash, 11-21%
$FeSO_4$, $Fe_2(SO_4)_3$, $Al_2(SO_4)_3$	
MgCl2, CaCl2, Na2SO4, MgSO4, LaCl3	Graphite; recoveries, up to ~97%

According to these early reviews, several surface chemical mechanisms have been proposed to explain the flotation process in the presence of electrolytes. These range from the action of the electrolytes in (a) disruption of hydration

layers surrounding the particles and enhancing bubble-particle capture, (b) reducing the electrostatic interactions, and (c) increasing the charge on the surface of the bubbles to prevent primary bubble coalescence （Wellham et al., 1992, Yoon, 1982, and Yarar, 1988）. However, none of these appears to satisfactorily explain the experimental behaviour.

In addition, from these studies, the following general observations were noted: (a) the greater the frothing capacity of the inorganic electrolyte, the greater the flotation recovery; (b) the cations play a more important role than the anions in the process efficiency (Paulson and Pugh, 1996) which agreed with Weissenborn (1995) that the inhibition of bubble coalescence in electrolyte solutions appears to be linked to the utilization of water molecules in the hydration of cations and a consequent reduction in water available for gas solubility.

2.5.3 Mechanisms proposed to explain mineral flotation in saline water

2.5.3.1 Double layer compression

From more detailed batch flotation on coal cleaning studied by Yoon (1982) using inorganic electrolyte, it was concluded that flotation kinetics and separation efficiency increased with an increase in salt concentration, and divalent anions such as $S_2O_3^{2-}$ and SO_4^{2-} proved very effective. These workers attributed the mechanism to a reduction in the double layer thickness around the hydrophobic particle enhancing bubble-particle adhesion.

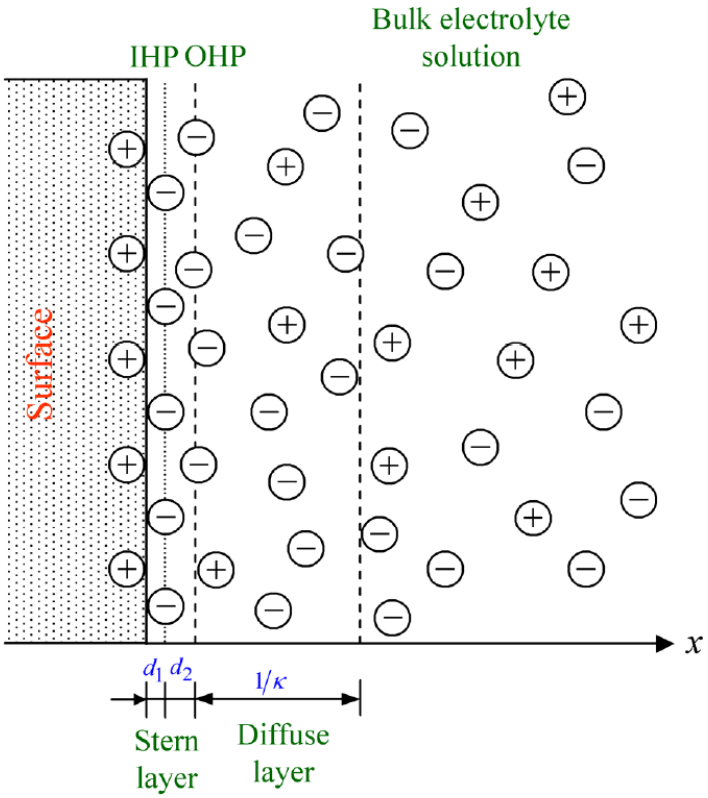

Fig 2.16 Grahame electrostatic double layer model (Grahame, 1947).

According Grahame model (Grahame, 1947) shown in Fig 2.16, the electrostatic attraction by the charged surface groups pulls the counterions back towards the surface, but the osmotic pressure forces the counterions away from the interface resulting in a diffuse double layer. It includes two parts: Stern layer and Gouy-Chapman Diffuse layer. The counterions specifically adsorb on the interface in the inner part of the Stern layer, which is known as inner Helmholtz plane (IHP). The outer Helmholtz plane (OHP) is located on the plane of the centers of the next layer of non-specifically adsorbed ions. The diffuse part of the electrostatic double layer is known as Gouy-Chapman layer. The thickness of the diffuse layer is termed Debye length. It indicates the distance from the OHP into the bulk solution.

The Debye length is reciprocally proportional to the square root of the ion concentration (Russel, 1989). The extent of the double layer decreases with

increase in electrolyte concentration due to the shielding of charge at the solid-solution interface (Ghosh, 2009). When Debye length is comparable or larger than the distance between two identical particles, the overlapping among the particles double-layers can play an important role in their interactions (Plouraboué and Chang, 2010).

The compression of the electrical double layer in saline water enhances the thinning and rupture of the wetting film between bubbles and particles which are a critical step in the formation of a stable bubble-particle aggregate, an important phenomenon in flotation. The compression of the electrical double layer in saline water also promotes particle aggregation in flotation and therefore affects the recovery of both valuable and gangue minerals.

2.5.3.2 Inhibition of bubble coalescence

Craig et al. (1993) assessed the inhibition of bubble coalescence in electrolyte solutions by the application of a combining rule based on the nature of the cationic/anionic pair. This rule enabled one to predict whether or not the electrolyte would inhibit coalescence of gas bubbles in the electrolyte solutions.

The coalescence inhibition depends upon the identities of the ions present. It was demonstrated that by empirically assigning ions a value of either α or β an electrolyte's coalescence inhibition behaviour could be described using simple combining rules (Craig et al., 1993). An electrolyte formed from α cation and α anion will inhibit bubble coalescence as well as an electrolyte formed from a β cation and β anion. However, electrolytes formed from α cation and β anion or β cation and α anion will have no effect. This is more easily understood by referring to Table 2.2, where αα or ββ results in a bubble coalescence inhibition (as indicated by a tick) and αβ or βα results in no inhibition (as indicated by a cross). Researchers have not found any exceptions to these simple predictive rules. Currently it is unclear precisely what properties make an ion as α or β ion.

Table 2.2 Combining rules for effects on bubble coalescence inhibition of selected salts in water

Ion		Ca^{2+}	Mg^{2+}	H^{+}	Li^{+}	Na^{+}	K^{+}	NH_4^{+}	$(CH_3)_4N^{+}$
	assignment	α	α	β	α	α	α	α	β
SCN^{-}	β					X		X	
ClO_4^{-}	β		X	√		X		X	
I^{-}	α				√	√	√		
ClO_3^{-}	β					X			
NO_3^{-}	α	√		X	√	√	√	√	
Br^{-}	α			X		√	√		X
Cl^{-}	α	√	√	X	√	√	√	√	X
CH3COO^{-}	β		√	√		X	X	X	√
SO_4^{2-}	α		√	X	√	√	√		

Christine et al. (2008) proposed that bubble coalescence takes longer in saline water than in pure solution with the bubble lifetime at an interface typically being extended from less than a second to ~5 seconds for a bubble rising to a free interface (Ghosh et al., 2004). Some electrolytes may act to alter the hydrodynamic boundary condition and thereby extend the time required for the growth of bridging capillary waves beyond the typical collision time (Henry et al., 2007).

Weissenborn and Pugh (1995) re-evaluated the coalescence behaviour in terms of the surface tension concentration gradients and the solubility of gases in the electrolyte solutions. Alternative interpretations have also been put forward including Gibbs surface elasticity.

Paulson and Pugh (1996) determined the flotation of model hydrophobic particles in a series of electrolytes under well-defined conditions. These experiments enable current theories of flotation, bubble coalescence, and bubble-particle

attachment to be evaluated. According to their flotation recovery, the electrolytes could be classified into three distinct groups. Fig 2.16 shows that group A electrolytes (such as $LaCl_3$, $MgCl_2$, $MgSO_4$, Na_2SO_4, etc.) were found to give high flotation while group B electrolytes (NaCl, LiCl, KCl, CsCl, NH_4Cl) were found to give an intermediate flotation recovery. Finally group C electrolytes (NaAc, $NaClO_4$, $HClO_4$, HCl, H_2SO_4, $LiClO_4$) produced only low flotation recovery. Paulson and Pugh (1996) proposed that the increased flotation performance of the hydrophobic graphite in electrolytes is linked with the dissolved gas concentration gradients in the electrolyte solutions. Higher flotation recoveries were attributed to an increase in the collision probability with higher concentration of smaller non-coalescing bubbles and a reduction in the electrostatic interactions between particles and bubbles. Though there is no correlation between Paulson and Pugh's electrolyte groups and Craig's αβ rules, it is interesting to find that most of ions in Paulson and Pugh's study followed Craig (1993)'s table (Table 2.2). If Fig 2.17 cited from Paulson and Pugh (1996) was replotted as recovery versus ionic strength rather than molar concentration, it may actually generate 2 groups which will be more agree with Craig's αβ rules.

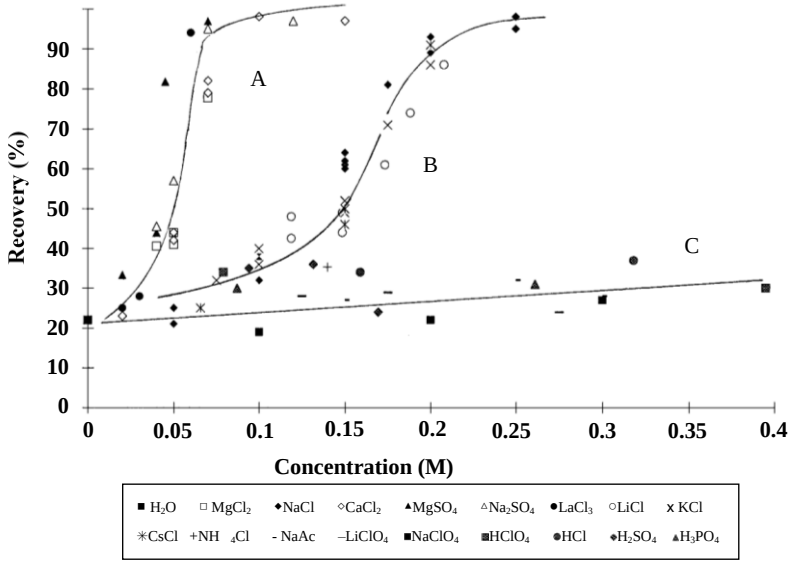

Fig 2.17 Flotation recovery of different electrolytes group (Paulson et al., 1996).

In Harris (2011)'s study, standard plant water (Wiese et al., 2005) was used as the base water quality (1Plant) and the levels of the ions doubled or tripled (2Plant or 3Plant) for the higher ionic strength flotation tests as shown in Table 2.3. They reported that the increase in the ionic strength of the system resulted in an increase in froth stability, leading to increased mass pulls and water recoveries. The effect appears to be directly related to the 2-phase frothing property of the frother rather than changes in the hydrophobicity of the particles entering the froth. The increase in ionic strength had no apparent effect on the recovery of the sulphide minerals as measured by copper and nickel recoveries, however the grades were somewhat decreased as the higher mass pull and water recovery at higher ionic strengths introduced more NFG (non-floatable gangue) to the final concentrate.

Table 2.3 Ions solution system built by Harris (2011)

Water type	Ca^{2+} (ppm)	Mg^{2+} (ppm)	Na^{+} (ppm)	Cl^{-} (ppm)	$SO4^{2-}$ (ppm)	NO_3^{-} (ppm)	CO_3^{2-} (ppm)	TDS	Ionic strength (M)
Tap	19	1.5	12	12	19	17	–	68.5	0.002
1Plant	80	70	153	287	240	176	17	1023	0.0241
2Plant	160	140	306	574	480	352	34	2046	0.0482
3Plant	240	210	459	861	720	528	51	3069	0.0723

The latest investigation on inorganic ions effect on flotation was reported by Ozlem and his colleagues (2012). They found that the dissolved sulfide ions, mainly in the form of SO_4^{2-} and $S_2O_3^{2-}$, influenced both the froth stability and surface chemistry. The froth stability increased in conjunction with the dissolved ion concentration and the degree of entrainment, particularly for pyrite and sphalerite, increased with higher concentrations of dissolved ions in the recycled water. The presence of the dissolved metal ions, such as Cu^{2+} and Pb^{2+}, increased

both the rate and recovery of the copper minerals (mainly chalcopyrite) and sphalerite. This was attributed to the activation of the slow floating, tarnished particles of chalcopyrite and also the sphalerite particles by the metal ions. The activation and depression effects of the ions were simultaneously observed on sphalerite and pyrite flotation performance. Both minerals were activated by the dissolved Cu and Pb ions. The activation effect of metal ions, however, was counteracted by the depressive effect of the sulphide ions.

2.5.3.3 The influence on water structure

Hancer (2001) classified certain ions as “structure breaking” ions. These ions are large inorganic ions, such as Cs^+ and I^-. On the other hand, small inorganic ions, such as Li^+, Mg^{2+}, F^-, and Cl^- are referred to as “structure making” ions as shown in Table 2.4. He proposed that for a collector molecule to adsorb at the salt interface it has to displace interfacial water or penetrate through the structure of water. If the structure of water is strongly hydrogen bonded due to the presence of structure making anions and cations, then collector molecules cannot reach the surface and be adsorbed. Those ions that have a tendency to destroy the structure of water can create a condition for the adsorption of collector molecules and subsequently allow the flotation of soluble salt minerals.

Table 2.4 Structure makers and breakers

	F	Cl	Br	I
Li	F	NF	NF	NF
		STRUCTURE MAKERS		
Na	NF	NF	NF	NF
K	NF	F	F	F
Cs	NF	F	F	F
		STRUCTURE BREAKERS		
Rb	NF	F	F	F

Note, NF, no flotation; F, flotation

It is depicted in Fig 2.18 that on the basis of contact angle measurements, the interfacial water structure at the KI surface has the least stability because the larger anion acts as a structure breaker and tends to destroy the interfacial water structure. It is evident that the KI surface exhibits the least tendency toward surface hydration (contact angle of 25°) and, thus, in a relative sense, a less stable interfacial water structure. On the other hand, the KCl and NaCl surfaces exhibit a greater tendency toward surface hydration (contact angles of 8° and 0°) and, thus, a more stable interfacial water structure.

A micelle is an aggregate (or supramolecular assembly) of surfactant molecules dispersed in a liquid colloid. Due to the hydrophobic nature of surfactants, i.e., polar head and nonpolar chain, they tend to accumulate at interfaces. However, Hancer (2001) reported that in salt solutions the tendency of surfactant molecules to escape the bulk structure of water is also governed by the ability of ions to organize the structure of water. Structure breaking salts allow for the accommodation of the hemimicelle aggregates at the salt surface which may result in promotion of collector adsorption and improvement of flotation. Structure making salts prevent the nucleation and growth of these surface phases. Structure making salts prevent the nucleation and growth which may inhibit collector adsorption and depress flotation, as described in Fig 2.19.

In summary, previous investigations found that saline water could influence minerals flotation behaviors. However, the mechanism of the effect of inorganic ions on flotation is still not certain. Due to the importance of saline water to the mining industry, the effect of electrolytes on flotation needs to be further studied.

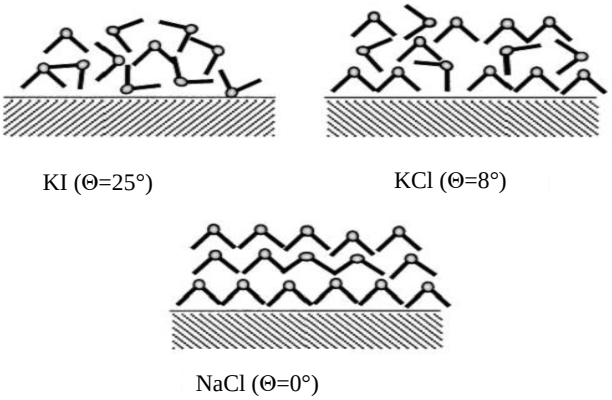

Fig 2.18 Comparison of interfacial water structure at KI, KCl and NaCl surface.

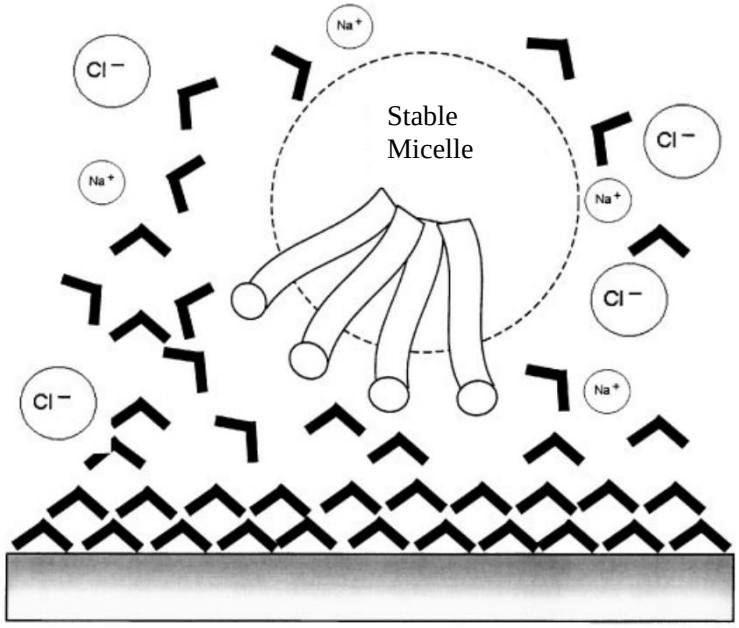

NaCl

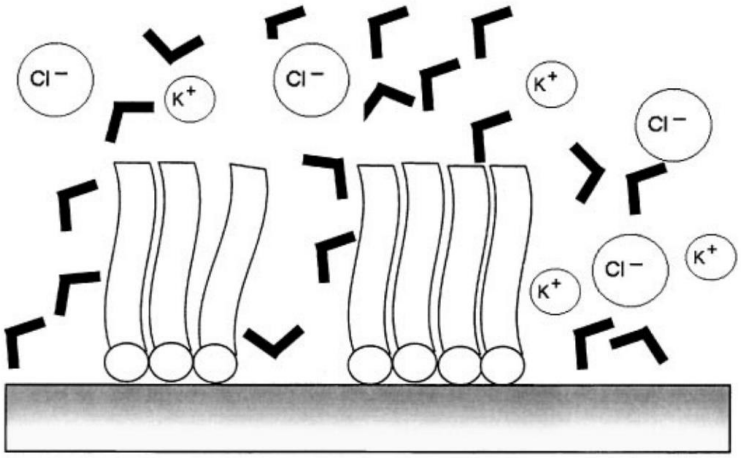

KCl

Fig 2.19 Collector adsorption is inhibited at the NaCl surface (structure maker) due to strong interfacial water structure and stabilization of micelles in the bulk solution. In contrast collector adsorption is promoted at the KCl surface (structure breaker) due to weak interfacial water structure and the stability of the hemimicelle surface state (Hancer et al, 2001).

2.6 Conclusions

Slime coatings with slime gangue particles attaching to valuable minerals is one of the important barriers in fine particles flotation. Slime coatings prevent the adsorption of collectors on valuable minerals resulting in low flotation recovery or low product quality. According to DLVO theory, electrostatic forces may play an important role on slime coatings in flotation. In the mining industry, low molecular weight polymer, controlled dispersion conditions (e.g., high intensity conditioning) and pulp chemistry (e.g., via pH modification and speciation) are applied to mitigate electrostatic interactions between gangue minerals and valuable minerals which may disperse slime coating and improve the flotation.

Copper is one of most important metals. The copper production is mainly yielded from copper sulphide minerals. The oxidation of copper sulphide minerals is a critical issue in mineral processing. Surface oxidation not only modifies surface hydrophobicity, but also changes the electrical property on the surface and therefore the interaction with gangue minerals. The flotation of copper sulphide minerals may be controlled through electrochemical potentials.

Saline water is also a key issue in the mining industry. Previous investigations showed that saline water could influence minerals flotation behaviors. Three mechanisms, double layer compression, inhibition of bubble coalescence, destabilization of hydration layers surrounding the particles, have been proposed to explain how the inorganic ions in saline water improve the mineral flotation. However, these mechanisms are not agreed.

2.7 Research Gaps and Hypotheses

The literature review and project objectives have led to the formation of three gaps which will be addressed in the current research.

1. The slime coating on copper sulphide minerals and its effect on flotation are not clear.

The negative effect of clay slime coatings on galena, coal, and nickel flotation response has been well reported. It may also occur in copper flotation. However, the slime coating effect on primary and secondary copper sulphide ores and underpinning mechanisms are not clear. The investigation on reduction of the interactions between gangue minerals and copper sulphide minerals may contribute to improvement of copper minerals recovery.

2. The influence of surface oxidation on slime coating is not clear.

The electrostatic attraction between gangue and valuable minerals has been reported to attribute to slime coatings which may reduce the hydrophobicity of mineral surface and then significantly depress the flotation (Arnold and Aplan, 1986b; Edwards et al., 1980). Surface oxidation is an important issue for base metal sulphide minerals flotation. It may not only modify surface hydrophobicity, but also change the electrical property on the surface and therefore the interaction with gangue minerals. However, the role of surface oxidation in slime coating has not been investigated.

3. The flotation mechanisms in saline water in the presence of clay mineral and the role of individual ions in solution are not clear.

The use of saline water in Australia is essential. It has been demonstrated that saline water may improve valuable minerals flotation. Different types of inorganic electrolytes can have a profound influence on the flotation kinetics. However, how saline water affects the flotation of valuable minerals with clay minerals slime coatings has not been studied. The effect of individual ions on slime coatings during flotation is still not clear. The mechanism responsible for the process remain unresolved.

The research gaps identified together with the research objective have led us to formulate the following hypotheses to be tested in this study:

Hypothesis one: Clay minerals may coat the surface of copper sulphide minerals and depress their flotation.

Hypothesis two: Oxidation of copper sulphide mineral surfaces may alter the surface property and then enhance the coating of clay minerals on the surfaces.

Hypothesis three: Saline water may reduce the electrostatic interaction between clay minerals and copper sulphide minerals and mitigate the coating of clay minerals,

Hypothesis four: Individual inorganic ions may have different mitigation effects on slime coatings.

2.8 Thesis outline

This thesis is divided into eight chapters to systemically investigate the mitigation of slime coatings from mineral surfaces in froth flotation by saline water, including research outcomes that form the manuscripts of some journal articles.

Chapter 2 is a critical literature review of the existing knowledge relevant to this thesis research. In line with the research objectives, this review is divided into four areas: (1) DLVO theory; (2) slime coatings on valuable minerals in flotation; (3) oxidation and flotation of copper sulphide minerals; (4) effects of saline water on mineral flotation. The literature review provides an overall picture of the current status of studies in this area and pinpoints the gaps in knowledge and hypotheses for future research which are presented at the end of this chapter.

Chapter 3 presents the experimental details of this thesis study, including description of the minerals and reagents used, the grinding and flotation test procedures and the surface analysis techniques used in this study.

Chapter 4 describes an investigation into the flotation behaviours of copper minerals in the presence of clay minerals. In this research, the flotation responses of underground and open pit copper ores were examined firstly followed by the flotation study on single minerals of chalcopyrite and chalcocite in the presence and absence of bentonite. The research described in this chapter was extracted from the work published in Mineral Engineering in 2011(Peng and Zhao, 2011) and Powder Technology in 2012 (Zhao and Peng, 2012).

Chapter 5 details a study which investigated the mechanism of clay slime coatings on copper sulphide minerals in flotation. XPS analyses, zeta potential measurements and CryoSEM-EDS method are applied in this study to reveal how the clay slimes coating occurred on chalcopyrite and chalcocite mineral surface differently. The research described in this chapter was extracted from the work published in Mineral Engineering in 2011 (Peng and Zhao, 2011) and Powder Technology in 2012 (Zhao and Peng, 2012).

Chapter 6 was designed for the presentation of the performed flotation testwork results on chalcocite with the presence of clay in electrolyte solutions. The effect of electrolytes on the flotation of copper minerals in the presence of clay minerals has been investigated. It addresses an important question which is whether the electrolytes can mitigate clay slime coatings and then improve chalcocite flotation. The research described in this chapter was published in the Mineral Engineering in 2014 (Zhao and Peng, 2014).

Chapter 7 details the electrochemical impedance spectroscopy (EIS) study on the mechanism of clay slime coatings mitigation on chalcocite by electrolytes. In this study, for the first time, the electrochemical impedance spectroscopy was applied to investigate the slime coating effect and its mitigation from mineral surfaces by different ions. This chapter explained and interpreted the flotation testwork

results of chapter 6. The research described in this chapter was published in the Mineral Engineering in 2016 (Zhao et al, 2016).

Chapter 8 summarises the major findings from this thesis research based on the proposed hypotheses and provides recommendations for future studies.

Chapter 3 Materials and Methods

3.1 Introduction

The experiments in this thesis were designed and conducted to fundamentally investigate the coating of clay minerals on copper sulphide minerals surfaces and how saline water mitigates this coating. The test work was composed of flotation tests and surface analysis. Test results are reproducible. Grinding and flotation tests were conducted firstly to identify the effect of clay minerals on mineral flotation. Where different flotation behaviours were observed, surface analysis methods were used to examine the surface properties to understand the underpinning mechanisms.

Single minerals were used in most of test work because they were more reliable to study the mineral surface properties and the mineral liberation did not need to be considered. By using single mineral samples, there were no impurities to affect the flotation tests and surface analysis, which may occur if plant samples are used.

Following are the experimental details including the mineral samples and reagents, the grinding and flotation procedures, and surface analyses.

3.2 Materials

3.2.1 Ores and minerals

An underground copper ore and an open pit copper ore were supplied from a copper plant and crushed to a size of -2.36 mm in laboratory before grinding and flotation. The mineral composition of the two ores analyzed by X-ray Diffraction (XRD) is shown in Table 3.1.

Table 3.1 Mineral compositions of the copper ores (wt.%)

	Chalcopyrite	Chalcocite	Pyrite	Geothite	Quarts	Dolomite	Bentonite
Underground ore	1.1	0.2	3.5	2.1	73.8	19.3	-
Open pit ore	0.4	0.8	2.8	1.9	66.1	22.8	5.2

The two ores contain both chalcopyrite and chalcocite. The main copper mineral in the underground ore is chalcopyrite accounting for 85% of the copper minerals. The main copper mineral in the open pit ore is chalcocite accounting 67% of the copper minerals. Another distinct difference in the two ores is the clay mineral (bentonite) in the open pit ore. About 0.5 ppm gold is also associated with the ores, but gold flotation is not considered in this thesis. The head samples of the two copper ores and their flotation products were assayed for total copper and cyanide soluble copper by inductively coupled plasma – optical emission spectroscopy (ICP-OES) using standard methods.

Another copper ore was obtained from an Australian copper plant and crushed to a size of -1.70 mm in laboratory. The copper grade of the ore is about 2.9%. Quantitative XRD analysis indicates that the copper ore contains 0.1% chalcopyrite, 0.4% cuprite, 4.7% chalcocite, 40.6% hematite, 16.4% muscovite and 33.8% quartz. About 91% Cu originates from chalcocite.

Chalcopyrite, chalcocite and bentonite single minerals were obtained from Ward's Natural Science Establishment (US). All of them have more than 98% purity analyzed by XRD. A kaolinite sample was purchased from Sibelco Australia Limited Company and it contains 70.3% kaolinite, 18.8% muscovite and 6.8% quartz based on quantitative XRD analysis.

3.2.2 Reagents and solution preparation

Peroxide and dithionite (AR grade) were used to adjust the oxidation state of chalcopyrite and chalcocite during grinding. High quality of nitrogen and oxygen gases was used to adjust the Eh in the flotation of chalcopyrite and chalcocite.

In copper flotation, potassium amyl xanthate (PAX) was used as collector. It is a commonly used collector in copper flotation in fresh water and saline water for mineral processing industry. Due to this research mainly focused on the slime coating effect on copper flotation and its mitigation by electrolytes, the affinity of different collectors under different electrolyte concentrations to copper minerals is out of topic. The different collector effects have not been compared. Methyl iso-butyl carbinol (MIBC) and IF56 were used as frother. All were industrial grade.

To investigate the effect of electrolytes on the flotation of chalcocite in the presence of kaolinite, sodium chloride (NaCl), lithium chloride (LiCl), sodium fluorite (NaF), potassium chloride (KCl) and sodium Iodide (NaI) of analytical grade were used to make different strengths of solutions. These electrolytes vary in both anion and cation sizes. All solutions were made with AR grade chemicals and deionized (DI) water.

The effects of Mg^{2+} and Ca^{2+} have been widely studied. For instances, Zhang (2013) reported the effects of clay and calcium ions on coal flotation. Castro (2014) showed that molybdenite flotation can be severely depressed by magnesium hydrolysis products, and that in the case of Ca^{2+} the depressing action could be related to the action of $Ca(OH)^{+}$. Uribe (2017) also investigated the role of calcium and magnesium cations in the interactions between kaolinite and chalcopyrite. Therefore, these cations have not been considered in this study.

Tap water was used throughout in the flotation study. Table 3.2 shows the chemical compositions of the water analysed by ICP. The pH of the water was 7.0.

Table 3.2 Chemical compositions of tap water used in this study (mg/L)

TDS	EC	Cl^-	SO_4^{2-}	CO_3^{2-}	Ca	Mg	K	Na
52	110	11	7	24	7.9	0.6	2.8	7.4

3.3 Grinding and flotation

600 gm crushed copper ore sample was ground in a laboratory stainless steel rod mill with stainless steel rods at 40% solids to obtain 80 wt.% particles passing 75 μm. The mill discharge was transferred to a 2.5 L Agitair flotation cell using an agitation speed of 750 rpm and conditioned with 100-300 g/t collector and 20 g/t frother. In the plant, 50 g/t collector was used to float the copper with recycled water in rougher and scavenger flotation. In the laboratory, 100 g/t collector was usually used without recycled water to match the flotation performance in the plant. Lime was used to control pH 9.0 at the end of grinding and during flotation. In flotation, four concentrates were collected after cumulative times of 0.5, 2.0, 4.0 and 8.0 min. Eh and pH were measured in the end of grinding and during flotation. Eh values were converted to the SHE standard.

The chalcopyrite or chalcocite single mineral (100 g) with and without 5 g bentonite was combined with 0.15 dm^3 of de-ionized water and ground in a stainless steel rod mill with stainless steel rods to obtain 80 wt.% particles passing 38 μm. Stainless steel rods were used to represent the inert media in both primary and secondary grinding mills in the mining industry. A small amount of lime was used to control pH 9.0 at the end of grinding. This pH value was normally used in the industry. In the end of grinding, samples were taken for the surface analysis

(Cryo-SEM and X-ray photoelectron spectroscopy analysis) and electrokinetic studies. Flotation of the single minerals was conducted in a 1.5 L Agitair flotation cell using an agitation speed of 500 rpm with 100 g/t collector and 150 g/t frother.

The chalcopyrite or chalcocite single mineral was also ground with the controlled oxidation conditions. Peroxide was added during chalcopyrite grinding with bentonite to maintain 500mV (SHE) while chalcocite was ground at -300 mV (SHE) with addition of dithionite.

The frother concentration required in the flotation of single minerals in this study was much higher than that in the flotation of ore samples probably due to the greater amount of hydrophobic particles to be laden by froth. This is consistent with previous studies where the flotation of galena, chalcopyrite and pyrite single minerals was conducted (Peng et al., 2003a,b; Peng and Grano, 2010). Other conditions were the same in single mineral flotation and copper ore flotation.

3.4 Aqua Regia Method

The total copper digestion method used aqua regia while the cyanide soluble copper digestion used cyanide. Since chalcocite is soluble in cyanide solutions as a secondary copper sulphide mineral but chalcopyrite is insoluble in cyanide solutions as a primary copper sulphide mineral (Scheffel 2002), in this study, the cyanide soluble copper assay relates to the copper mineral associated with chalcocite and the difference between the two assays equates to the copper associated with chalcopyrite. Table 3.3 shows the total copper, cyanide soluble copper and cyanide insoluble copper. The total copper in the underground ore and open pit ore is 0.6% and 0.7%, respectively. In the underground ore, 66% Cu originates from chalcopyrite, while in the open pit ore 86% Cu originates from chalcocite.

Table 3.3 Head copper assays for the copper ores (wt.%)

	Total Cu	Cyanide soluble Cu	Cyanide insoluble Cu
Underground ore	0.6	0.2	0.4
Open pit ore	0.7	0.6	0.1

3.5 EDTA extraction

Ethylene diamine-tetra acetic acid (EDTA) has the ability to solubilise metal oxidation products (e.g. metal oxides, hydroxides, carbonates and sulphate) rather than the metal sulphide, and therefore can be used to determine the amount of oxidation species from minerals and grinding media (Rumball and Richmond 1996). A 3 wt.% solution of AR grade ethylenediamine-tetra acetic acid disodium salt (EDTA) was made up and a sodium hydroxide solution was used to adjust the pH to 7.5. 95 cm^3 of the EDTA solution was placed in a vigorously-stirred reaction vessel and purged with nitrogen for 5 min. 5 cm^3 of slurry sample from the mill discharge was frozen in liquid nitrogen and then added to the EDTA solution, followed by 5 min of conditioning. Nitrogen was continuously purged throughout. The slurry was then filtered through a 0.45 mm Millipore filter. The filtrate was analyzed for metal ions by inductively coupled plasma (ICP) atomic emission spectrophotometry. The solids were retained for chemical analysis for metal ions. The percentage of EDTA extractable copper or iron, a parameter of the degree of surface oxidation, is expressed as the EDTA soluble copper or iron of their insoluble forms in the solids (wt./wt.% Cu or wt./wt.% Fe).

3.6 Zeta potential measurements

Zeta potential measurements were performed by a Rank Brothers Micro-electrophoresis Mark II apparatus. 20 cm^3 of the chalcopyrite or chalcocite slurry from the mill discharge was taken, screened to obtain -38 μm and then

conditioned in a 1.25 dm^3 reaction vessel containing 10^{-3} M KCl solution at pH 9.0 with the nitrogen gas being purged throughout the process to remove dissolved oxygen. The pH value was then changed by using HCl or NaOH solutions and the mineral was conditioned for 5 min. Some suspension was sampled for the zeta potential measurements open to the air. Ten mobility measurements at each of the two stationary planes were performed at each pH. The average mobility was converted to zeta potentials using the Smoluchowski equation. To measure the zeta potential of bentonite, a similar procedure was followed except that the sample was prepared by grinding 2.5 g of bentonite in a ceramic mortar.

3.7 XPS analysis

The chalcopyrite or chalcocite sample for the measurement by X-ray photoelectron spectroscopy was taken after grinding without bentonite. The sample was frozen in liquid nitrogen and stored in a freezer until immediately prior to the analysis. This procedure has been shown to inhibit significant surface speciation alteration (Smart R.St.C, 1991). XPS measurements were carried out with a PHI 5600 spectrometer with an Mg Ka X-ray source operating at 300 W and with a pass energy of 18 eV. The pressure in the analyzer chamber was 10−8 Torr during the analysis. The energy scale was calibrated using the Fermi edge and $3d_{5/2}$ line (BE= 367.9 eV) for silver, while the retardation voltage was calibrated using the position of the Cu $2p_{3/2}$ peak (BE=932.67 eV) and the Cu $3p_{3/2}$ peak (BE=75.13 eV). The measurements were performed at a take-off angle of 45°. The depth of analysis was approximately between 2 and 5 nm. The slurry samples were introduced into the fore-vacuum of the spectrometer. The samples were first examined in survey mode to identify all the elements present then the various elemental regions were scanned in order to extract information on chemical bonding and oxidation stages. Atomic concentrations were determined

from the XPS peak areas, subsequent to Shirley background subtraction, using the elemental sensitivity factors (Wagner C.D., 1979).

3.8 Cryo-SEM-EDS

To detect slime coating on the mineral surface, the cryo-transfer method of sample preparation was used to avoid a structural change caused by surface tension during oven or freeze drying. In the cryo-vitrification SEM analysis, the sample was taken by a large-aperture (>2 mm) pipette directly from the chalcopyrite or chalcocite sample after grinding with bentonite and washed by de-ionized water at pH 9.0. The sample was then mounted onto the top of a 3 mm long copper rivet with outer-diameter 2.4 mm and inner-diameter 1.7 mm. This copper rivet was fixed on a sample holder and plunged into the liquid nitrogen of the cryo-vitrification unit, which reduces the temperature at >800 °C min^{-1} freezing the water without allowing crystallization to ice structures, i.e. vitrifying (Battersby B.J., 1994). The small volume of the sample (about 0.01 cm3) and high heat conductivity of copper minimize shrinkage and distortion of the sample during freezing. The very fast vitrification process avoids crystallization of water to ice and associated volume changes that can alter structures. The sample was then transferred under vacuum to the sample preparation chamber equipped with an Oxford Instrument (CT1500) where the frozen sample was fractured to expose a fresh surface. Then the sample temperature was raised to 173 K to sublimate vitrified water for 7 min. This sublimation process removes fine vitrified water slivers generated during fracture and allows mineral structures to stand out above the glassy background. The sample was eventually coated with platinum plasma for 3 min to avoid charging during the imaging process by a PHILIPS XL30 field emission gun scanning electron microscope (FESEM) normally operated at 20 kV voltages.

The sample was then examined in the SEM. Images were taken in backscattered electron mode (BSE), while elemental analysis was performed by energy dispersive spectrometry (EDS). The combination of BSE and EDS allows the identification of clay coating on the copper mineral surface.

3.9 Electrochemical measurements

A hand-picked natural massive chalcocite specimen of a high purity was used to make a working electrode. XRD analysis also showed little impurities of the chalcocite specimen. The electrode was connected with a copper wire using silver loaded conducting epoxy, and then mounted into a non-conducting epoxy resin, exposing only one side with a geometric surface of approximately 0.1 cm^2 and this value was used to calculate the current density.

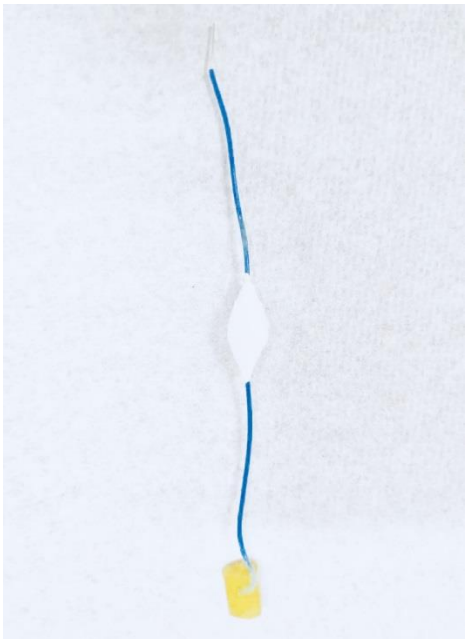

Fig 3.1 Chalcocite electrode.

A fresh electrode surface was prepared between the experimental runs by abrading with silicon carbide abrasive paper (1200 grits), rinsed with deionized water prior to each experiment (Velasquez et al., 2001; Smith et al., 2009). Chalcocite electrode was immersed in clay and/or electrolyte-containing solutions for 2 min under stirring, and then rinsed with DI water. The electrode

was then immediately transferred into the electrochemical cell as a stationary working electrode.

A conventional three-electrode system was employed for the electrochemical measurements. A platinum plate with a surface area of 1 cm^2 was utilised as an auxiliary electrode (counter electrode). Potentials were measured against an Ag/AgCl reference electrode filled with 3M KCl which has a potential of +0.204 V against standard hydrogen electrode (SHE). A Radiometer PGZ100 potentiostat was used in combination with a Frequency Response Analyser (FRA). The background electrolyte performed in all electrochemistry experiments was pH 7 buffer solution (prepared by 0.1 M potassium dihydrogen phosphate). The buffer ions may affect the measurement. However, due to the same buffer background for each test, the buffer ions would not influence the results for comparison. The effect of buffer ions on EIS has not been taken into consideration. EIS was performed in the above buffer solution with a volume of 200 mL at room temperature in the absence and presence of electrolytes and kaolinite individually and in combination. Deionized water (18 MΩ cm) was used in all electrochemical experiments. Open circuit potential was taken as the direct current (DC) voltage (starting potential) of EIS measurements. The alternating current (AC) voltage (amplitude) was 10 mV.

Typically, the working electrode surface was allowed to react with the chemical added for 5 min to enhance the stabilisation at the open circuit potential after which the EIS was obtained. The potential scan rate was 20 mVs^{-1} for all cyclic voltammetry measurements. The variation in the current was recorded as a function of scan potential and reported as current density. Good reproducibility of the electrode pre-treatment and electrolyte preparation was confirmed by carrying out measurements in separate solutions and with freshly abraded electrode.

Chapter 4 The flotation behaviours of copper minerals in the presence of clay minerals

This chapter presents testwork performed to explore flotation behaviour of copper ores in the presence of clay minerals. Batch flotation experiments of copper ores (open pit and underground) and single copper sulphide minerals (chalcopyrite and chalcocite) were designed for investigation.

4.1 Introduction

As outlined in Chapter 2, the flotation of galena, coal and nickel may be depressed in the presence of clay minerals. It is not clear, however, how copper minerals flotation is affected by clay minerals.

In this chapter, the flotation testwork on underground and open pit copper ores containing bentonite was performed under similar conditions to examine flotation responses. Cyanide soluble and insoluble copper recovery analyses were conducted to indicate the flotation recovery of chalcopyrite and chalcocite from the ore. The single mineral flotation of chalcopyrite and chalcocite was then examined with and without the addition of bentonite to identify its effect on the flotation of both chalcopyrite and chalcocite single minerals.

The tests designed in this chapter are expected to answer the following questios: do clay minerals depress copper flotation?

4.2 Flotation of copper ores

4.2.1 Different flotation response between underground and open pit copper ore

Fig 4.1 shows the flotation of underground and open pit copper ores with 100 g/t PAX (Potassium amyl xanthate) as collector. As can be seen, Cu recovery from the flotation of the underground ore was normal, about 87% at the completion of 8 min flotation. The mass pull of the concentrate and water recovery in the end of flotation (not shown in Fig 4.1) were 3.5% and 9.8%, respectively. However, Cu recovery from the flotation of the open pit ore was low, only 56% in the end of flotation although the mass pull of the concentrate and water recovery were increased significantly, being 6.2% and 15.8%, respectively. Obviously, the flotation of copper minerals in the open pit ore was depressed. This is consistent with the practice in the flotation plant where processing the open pit ore on its own is not profitable. It has to be blended at a small proportion with the

underground ore.

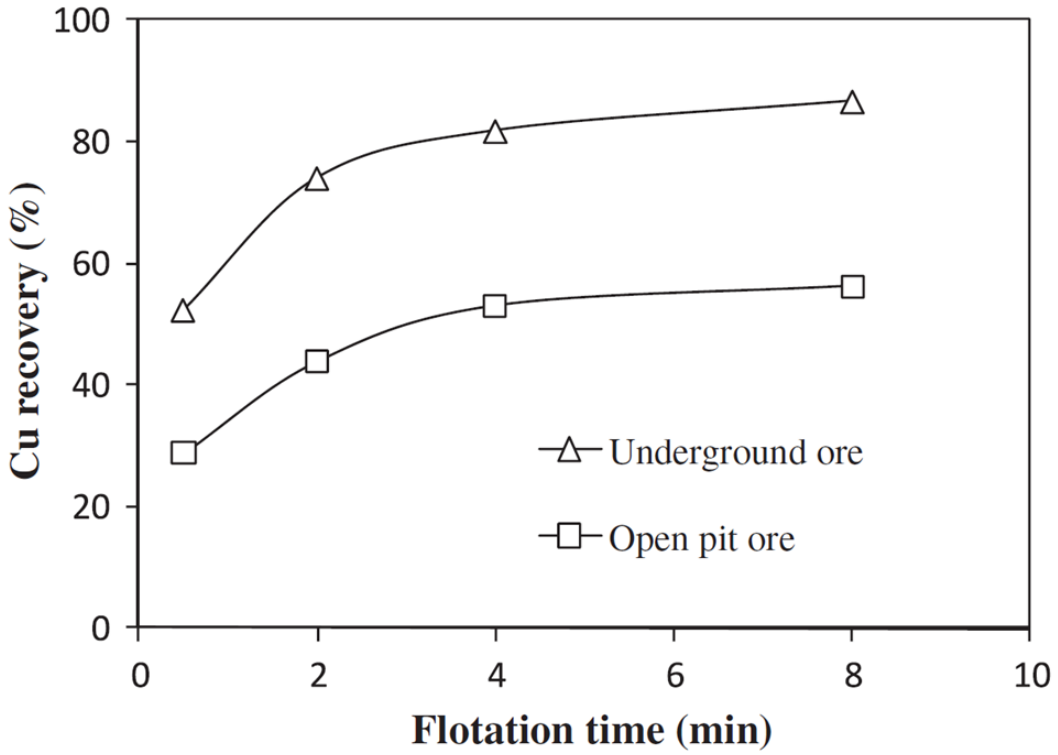

Fig 4.1 Cu recovery as a function of flotation time in the flotation of the underground ore and open pit ore with 100g/t collector.

4.2.2 Cyanide soluble and insoluble copper recovery

When cyanide soluble Cu and insoluble Cu are considered, the flotation behavior of chalcopyrite and chalcocite from the two copper ores may be examined. As shown in Fig 4.2, the recovery of cyanide insoluble Cu was higher than the recovery of cyanide soluble Cu from both ores, indicating that chalcopyrite displayed better floatability than chalcocite. However, the difference between chalcopyrite and chalcocite flotation was much smaller for the underground ore. From the underground ore, chalcopyrite and chalcocite flotation recovery became closer and closer with flotation time. It is also found that the chalcopyrite recovery was slightly higher from the underground ore than from the open pit ore, but the difference in the chalcocite recovery was distinct. The low overall Cu recovery from the open pit ore in Fig 4.1 may be attributed to the low chalcocite recovery.

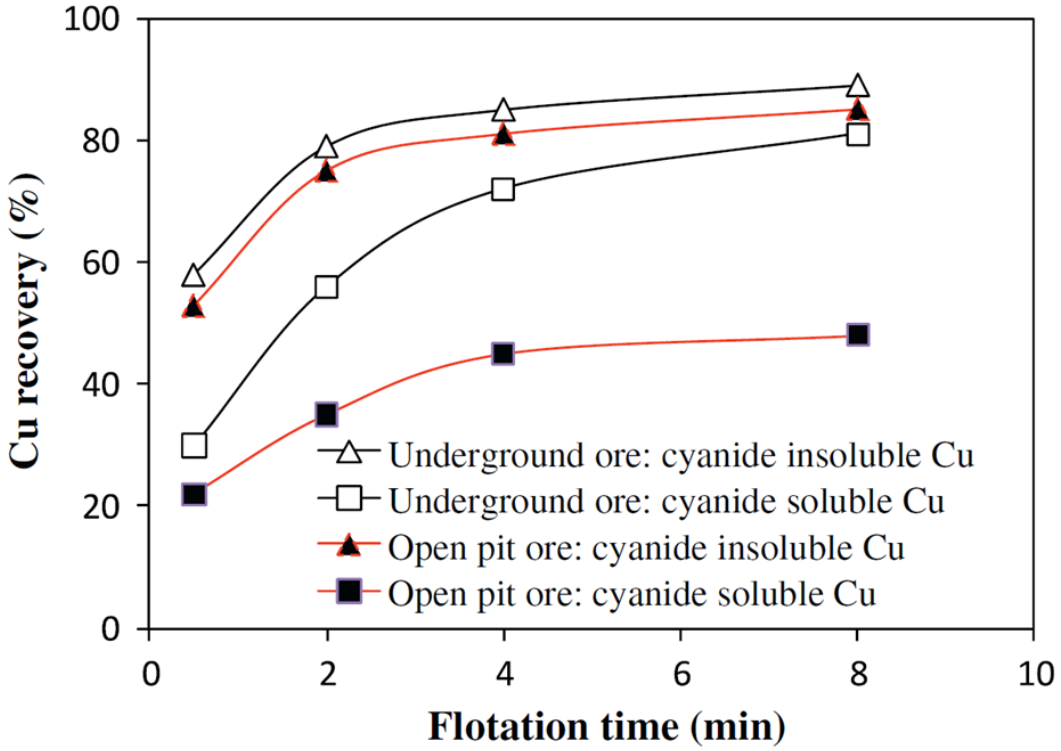

Fig 4.2 The recovery of cyanide insoluble and soluble Cu as a function of flotation time in the flotation of the underground ore and open pit ore with 100g/t collector.

Mielczarski et al. (1998) indicated that if a mineral surface was strongly oxidized, an increased collector addition may be necessary to induce floatability. Tolley et al. (1996) and Ye et al. (2010) increased the flotation of oxidized chalcocite through increasing the collector addition. In this study, 3 times the addition of collector was applied in the flotation of the two copper ores to increase Cu recovery. The results are shown in Fig 4.3. A comparison between Figs 4.2 and 4.3 indicate that when the collector addition was increased from 100 g/t to 300 g/t, only the recovery of cyanide soluble Cu was increased pronouncedly from the underground ore. For example, the recovery was increased from 30% to 46% at the completion of 0.5 min flotation and from 81% to 87% in the end of flotation. The mass pull of the concentrate and water recovery in the end of the flotation of the underground ore were decreased slightly, being 2.8% and 7.5%, respectively, when the collector addition was increased. However, in the flotation of the open pit, the mass pull of the concentrate and water recovery did not change with the

collector addition. As a result, an increased collector addition induced chalcocite floatability in the underground ore but not in the open pit ore.

The results thus far suggest that chalcopyrite displayed a similar behavior in the flotation of the underground ore and open pit ore. Its recovery was high irrespective of the ore type. However, chalcocite flotation was strongly affected by the ore type. In the flotation of the open pit ore, chalcocite recovery was low and a further addition of collector could not restore chalcocite flotation. A potential explanation of this is that bentonite which is only contained in the open pit ore selectively coated on chalcocite surface and depressed its flotation irreversibly.

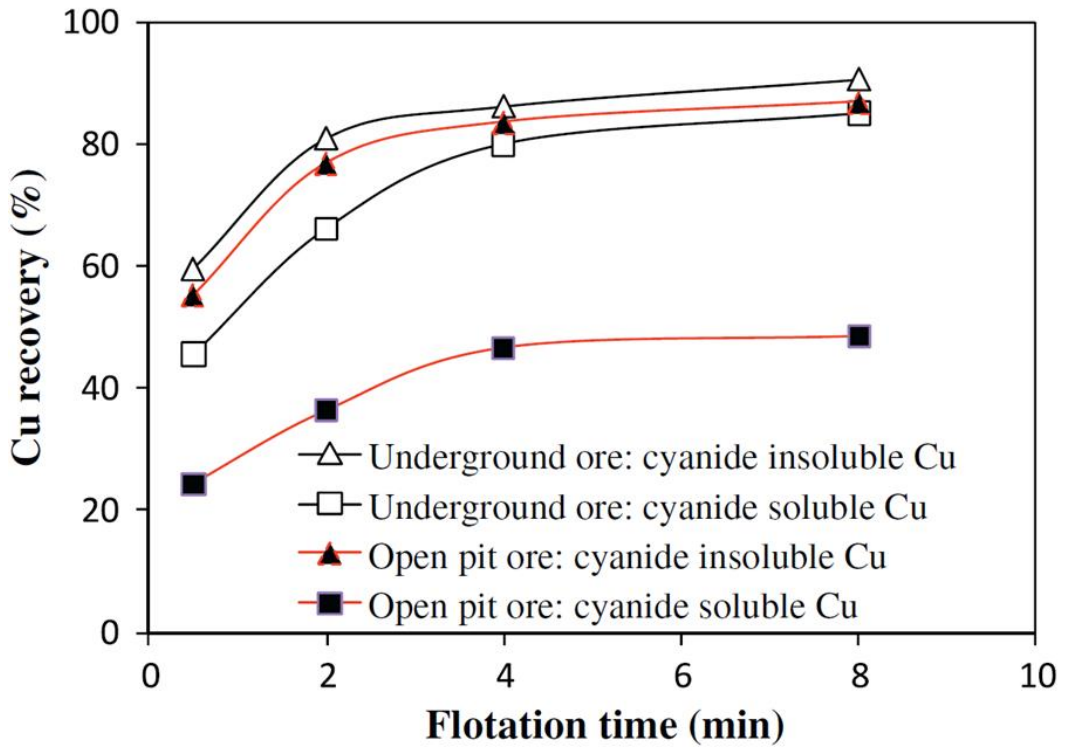

Fig 4.3 The recovery of cyanide insoluble and soluble Cu as a function of flotation time in the flotation of the underground ore and open pit ore with 300g/t collector.

4.3 Flotation of single minerals

The chalcopyrite or chalcocite single mineral was ground and floated by following the same procedure when copper ores were treated. Fig 4.4 shows chalcopyrite and chalcocite flotation in the presence and absence of 5% bentonite.

In the absence of bentonite, chalcopyrite displayed good floatability reaching 91% recovery at the completion of 8 min flotation. The flotation of chalcocite was lower with the recovery of 75% at the same flotation time. The behavior of chalcopyrite and chalcocite in the flotation of single minerals in the absence of bentonite is actually similar to that in the flotation of the underground ore. In the presence of bentonite, chalcopyrite flotation was depressed slightly, but chalcocite flotation was depressed substantially, a phenomenon which is similar in the flotation of the open pit ore containing bentonite.

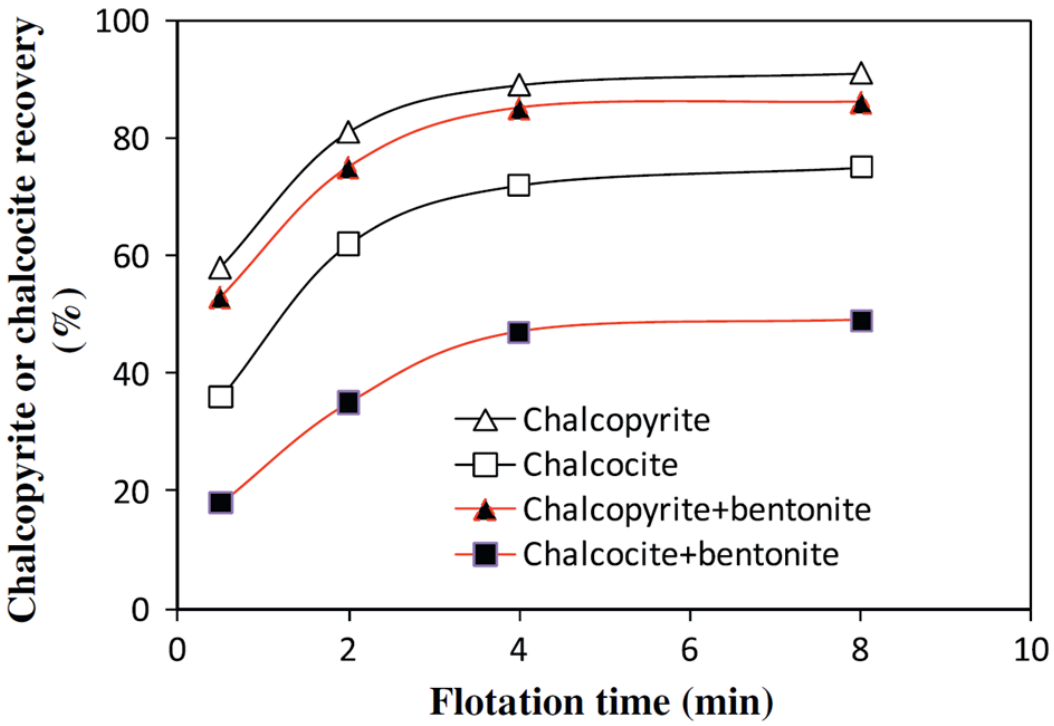

Fig 4.4 Chalcopyrite or chalcocite recovery as a function of flotation time in the flotation of the single mineral.

4.4 Conclusions

The overall copper flotation recovery of open pit ore was lower than that of underground ore indicating the flotation of copper minerals in the open pit ore was depressed. Chalcopyrite displayed better floatability than chalcocite in open pit ore. However, chalcopyrite and chalcocite flotation in underground ore were

similar. Due to only the open pit ore contained bentonite, the low overall Cu recovery from the open pit ore may be attributed to the depression of chalcocite flotation by bentonite.

Further single minerals flotation test results confirmed that chalcocite flotation was much more depressed than chalcopyrite in the presence of bentonite after grinding. However, both chalcopyrite and chalcocite single minerals display good floatability in the absence of bentonite.

Chapter 5 Mechanisms responsible for the effects of clay minerals on copper flotation

This chapter presents testwork performed to evaluate the mechanism responsible for the different effects of clay minerals on the flotation of chalcopyrite and chalcocite.

5.1 Introduction

It is interesting to find in Chapter 4 that bentonite significantly hinders the flotation of chalcocite, but had little effect on the flotation of chalcopyrite after grinding. In mineral processing, grinding not only reduces the particle size and liberates minerals, but also provides differential surface properties on valuable and gangue minerals allowing effective separation of them in the subsequent separation process such as flotation which exploits the difference in surface wettability on valuable and gangue minerals. During grinding of base metal minerals, a number of chemical mechanisms including oxidation of minerals and media, oxygen reduction and galvanic coupling occur and govern the surface properties of minerals (Grano, S., 2009).

The flotation of base metal sulphide minerals is always associated with surface oxidation. Surface oxidation not only modifies surface hydrophobicity, but also changes the electrical property on the surface and therefore the interaction with gangue minerals. The oxidation of base metal sulphide minerals produces hydrophobic metaldeficient sulfur or polysulphides, and also hydrophilic oxidation products like $S_2O_3^{2-}$, SO_3^{2-}, SO_4^{2-} and metal hydroxides (Buckley and Woods 1984; Guy and Trahar, 1984). The surface hydrophobicity is actually dependent on the balance of all these species. In the absence of gangue minerals, the floatability of base metal sulphide minerals may be predicted by the surface oxidation products (Priest et al., 2008). However, in the presence of gangue minerals, the interaction between base metal sulphide minerals and gangue minerals has to be considered.

In the literature outlined in Chapter 2, clay minerals may carry anisotropic charges on edges and basal faces allowing the coating of clay particles on the surface of a range of minerals. However, the interaction of clay minerals with base metal sulphide minerals during grinding has not been studied.

In this chapter, the oxidation of chalcopyrite representing the primary copper sulphide mineral, and chalcocite representing the secondary copper sulphide mineral during grinding was investigated to explore the interaction of oxidized chalcopyrite and chalcocite with bentonite representing the clay mineral.

5.2 The oxidation of chalcopyrite and chalcocite during grinding

5.2.1 XPS surface elements on the chalcopyrite and chalcocite after grinding

The electrochemical potential after grinding of chalcopyrite and chalcocite was about 310 mV (SHE) and 260 mV (SHE), respectively, indicating a strongly oxidizing condition with stainless steel media. The oxidation products on the surfaces of chalcopyrite and chalcocite after grinding were determined by XPS. Table 5.1 shows the type of surface elements and their concentrations. The elemental analyses were normalized to O, Cu, Fe and S only. The major component removed from the elemental accounting by this normalization process was C in the form of adventitious hydrocarbons and Ca added in the form of lime to control grinding pH 9.0. The elemental composition on the chalcopyrite surface was $Cu_{0.46}Fe_{0.61}SO_{0.94}$. Compared with the ideal stoichiometry of chalcopyrite ($Cu_{0.5}Fe_{0.5}S$), the ground chalcopyrite sample deviated from the ideal by Cu 8 at.% and Fe 22 at.% with S being a reference. Obviously, the grinding altered the chalcopyrite surface to some extent. The elemental composition on the chalcocite surface was $Cu_{4.29}SO_{3.04}$. Compared with the ideal stoichiometry of chalcocite (Cu_2S), a dramatic alteration of the surface by grinding was observed as Cu was enriched by 115 at.%. O was detected on both chalcopyrite and chalcocite surfaces with the O concentration being 51.5 at.% on the chalcocite surface and 31.3 at.% on the chalcopyrite surface, respectively. 65 at.% more oxygen concentration was detected on the chalcocite surface. Table 5.1 suggests that grinding modified the elemental composition on both the chalcopyrite and chalcocite surfaces and the chalcocite surface was actually severely changed. The

alteration of the mineral surface is intimately associated with surface oxidation which was indicated by XPS elemental spectra.

Table 5.1 XPS surface elements and their atomic concentrations (at.%) on the chalcopyrite and chalcocite after grinding

Elements	Concentration/at. %	
	Chalcopyrite	Chalcocite
O	31.3	51.5
S	33.3	12.0
Cu	15.2	36.5
Fe	20.2	-

5.2.2 Normalized XPS spectra of the ground chalcopyrite and chalcocite

Fig 5.1 shows the XPS O 1s spectra of the ground chalcopyrite and chalcocite. Both chalcopyrite and chalcocite exhibited two major O components at about 530.5 eV and 533 eV. The component at 530.5 eV is attributed to hydroxyl (OH^-) species, while the component at 533 eV is attributed to attached water (H_2O) (Nesbitt,H.W., 1994; Legrand,D.L., 1997). On the chalcopyrite surface, the attached water accounted for 65 at.% of the O component, while on the chalcocite surface, both the attached water and hydroxyl species were significant with the O emanating from Cu hydroxyl species being about 55 at.%. Fig 5.2 shows the XPS S 2p spectra of the ground chalcopyrite and chalcocite. The XPS S 2p spectra of chalcopyrite are usually composed of three components (Buckley,A.N., 1984). The first component near 161 eV is attributed to sulphide of unoxidized chalcopyrite (S^{2-}). The second component may have a peak located at 162 eV due to metal deficient sulphide (S_2^{2-}) and/or 164 eV due to polysulphide (S_n^{2-}). The third component is for sulfate or thiosulfate (SO_4^{2-} or $S_2O_3^{2-}$) at a higher binding

energy around 168 eV. Fig. 5-2 indicated that the ground chalcopyrite surface exposed sulphide, metal deficient sulphide and polysulphide with S at.% being about 60, 30 and 10%, respectively. No sulfate or thiosulfate was detected on the chalcopyrite surface. The ground chalcocite showed similar S components near 161, 162, 164 and 168 eV, which is consistent with reports in literature (Vela'squez,P., 2001; Mielczarski,J., 1998). However, the proportion of S components was different. The striking difference was the distinct signal of sulfate or thiosulfate, the highest oxidation state of S, detected on the chalcocite surface. S at.% of the unoxidized sulphide was decreased to about 30% on the chalcocite surface from 60% on the chalcopyrite surface.

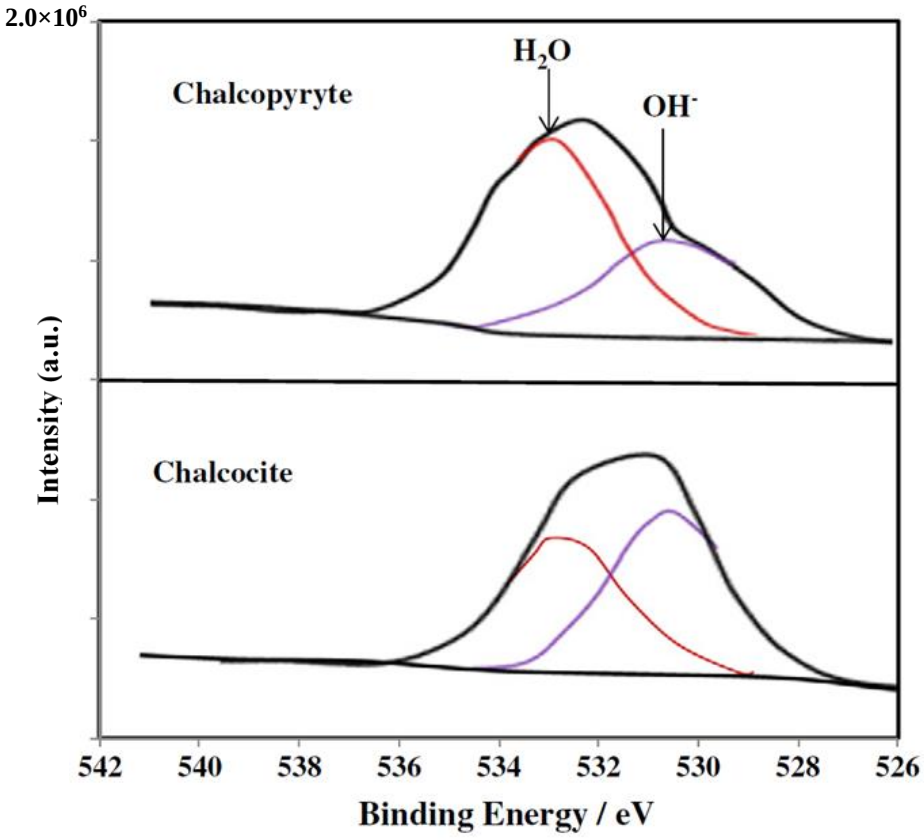

Fig 5.1 Normalized XPS O 1s spectra of the ground chalcopyrite and chalcocite

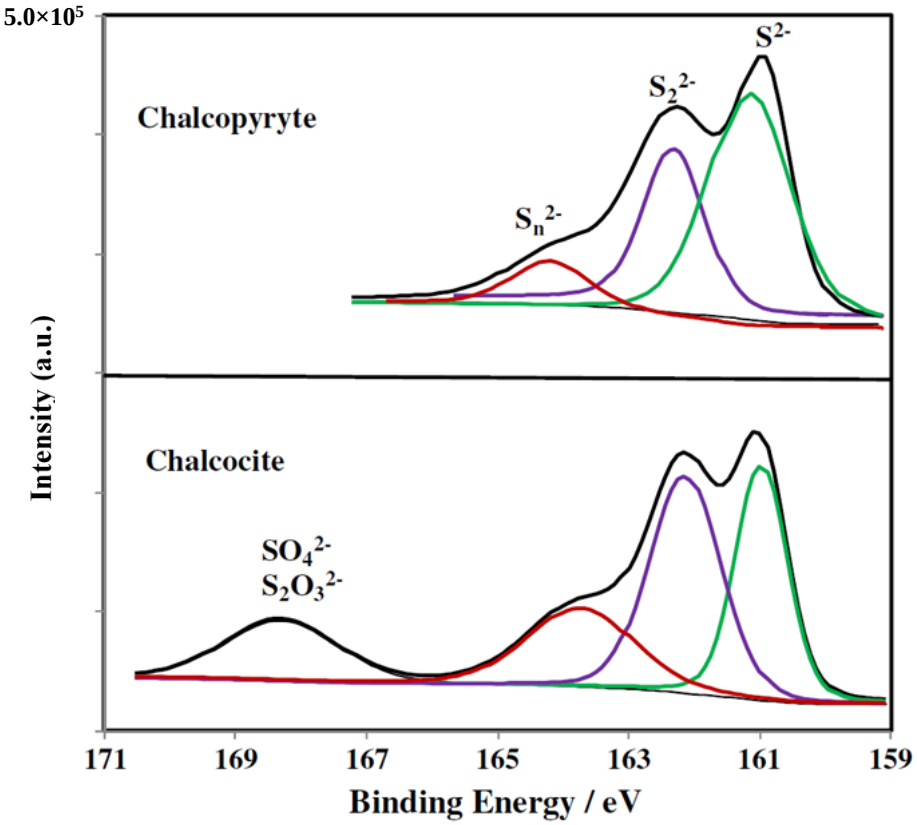

Fig 5.2 Normalized XPS S 2p spectra of the ground chalcopyrite and chalcocite

The XPS Cu 2p spectra (Fig 5.3) show that both Cu^{+} and Cu^{2+} components occurred on the ground chalcopyrite and chalcocite surfaces. The Cu^{+} component was identified in the binding energy range of 932.5 to 932.8 eV attributed to Cu^{+}–S minerals and compounds (McIntyre, N.S., 1975; Deroubaix,G., 1992; Chawla, S.K., 1992). A second component in the binding energy range of 934.3 to 934.6 eV is attributable to Cu^{2+}-hydroxyl species (Fairthorne,G., 1997). The well-known Cu^{2+} related shake-up satellite energy loss structure in the binding energy range of 942.5 to 943.9 eV (Vela'squez,P., 2001) was also clearly observed to be present thus further confirming the presence of Cu^{2+}. The ground chalcopyrite surface consisted of 15.2 at.% Cu (Table 5-1, normalized to Cu, Fe and S) mostly as unoxidized Cu^{+}-sulphide. However, on the ground chalcocite surface, copper from oxidized Cu^{2+}-hydroxyl species was the dominant component.

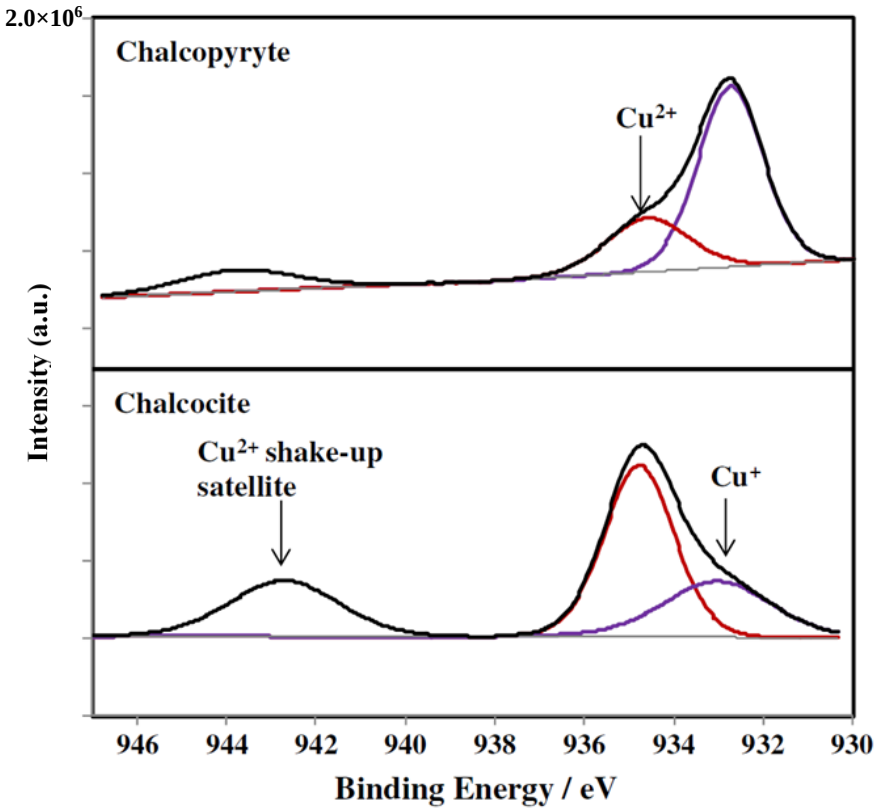

Fig 5.3 Normalized XPS Cu 2p spectra of the ground chalcopyrite and chalcocite

The XPS Fe 2p spectrum of the ground chalcopyrite is shown in Fig 5.4. No obvious Fe signal was detected on the ground chalcocite surface. An iron oxyhydroxide layer was present on the chalcopyrite surface. This is shown by a broad band in the Fe 2p spectrum near 711-712 eV and near 726 eV, while the iron associated with sulfur as in chalcopyrite occurs at about 708 eV (Fairthorne, G., 1998). The Fe component of the chalcopyrite surface was dominated by the unoxidized Fe-S.

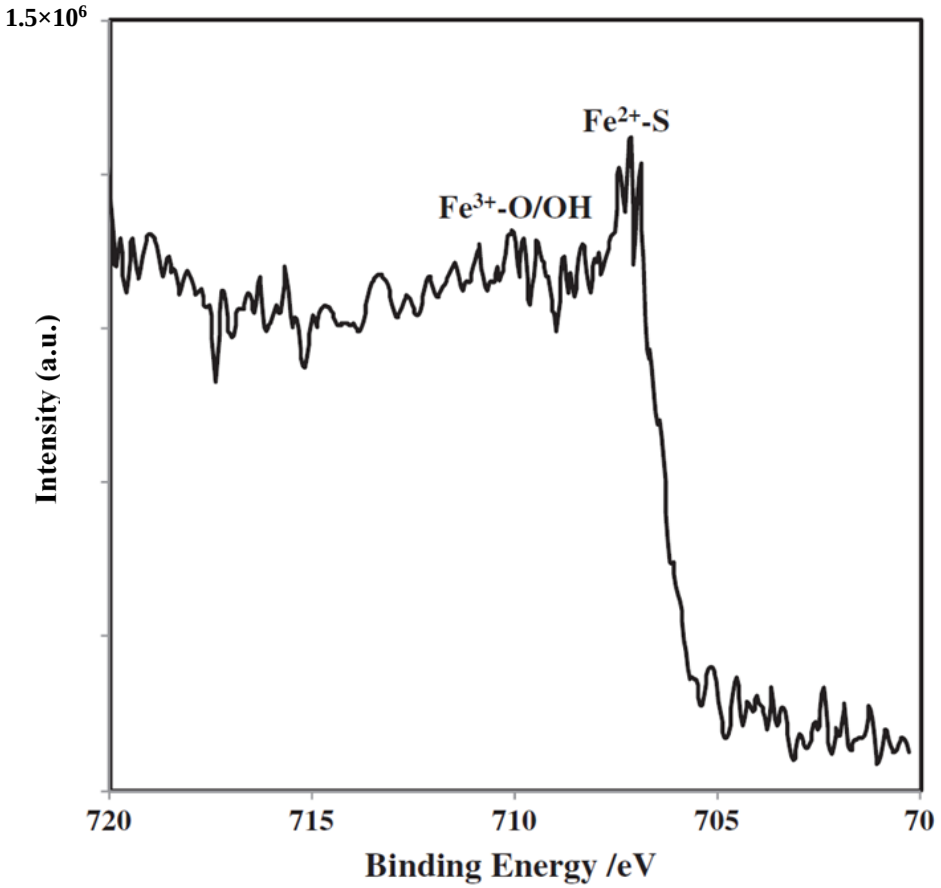

Fig 5.4 Normalized XPS Fe 2p spectrum of the ground chalcopyrite

The XPS analysis indicated that both chalcopyrite and chalcocite surfaces were oxidized after grinding. While the majority of the chalcocite surface was oxidized, only a small proportion of the chalcopyrite surface was oxidized. This is consistent with Lascelles and Finch (Lascelles,D., 2002) who showed that chalcocite produced more EDTA extractable copper ions than chalcopyrite, and Fullston et al. (Fullston,F., 1999) who reported that chalcocite was more electrochemically active than chalcopyrite. The different extent of surface oxidation may be associated with the different interactions of chalcocite and chalcopyrite surfaces with bentonite particles, which is further studied below.

5.3 Zeta potential of chalcocite, chalcopyrite and bentonite after grinding

5.3.1 Normal grinding

Fig 5.5 shows the zeta potential of chalcopyrite and chalcocite after grinding, as well as the zeta potential of bentonite. It was measured in a 10^{-3}M KCl solution at pH 9.0 with the nitrogen gas purging as introduced in Chapter 3. It was found that after grinding, chalcopyrite and chalcocite exhibited a pH isoelectric point at around 4.2 and 9.5, respectively. They were negatively charged at pH values greater than their pH iso-electric points. Fairthorne et al. (1998) found that unoxidized chalcopyrite had a pH iso-electric point at around 1.5. Fullston et al. (1999) measured the zeta potential of chalcocite with nitrogen purging and the iso-electric point was at around 2.0 by extrapolation. They also demonstrated that the oxidation of chalcopyrite, chalcocite and any other base metal sulphide mineral increased their iso-electric points towards the iso-electric points of the corresponding metal hydroxides (Fairthorne et al., 1998; Fullston et al., 1999). For instance, the electrical property of the oxidized chalcopyrite is governed by both iron hydroxides with a pH iso-electric point 6.5 (Fornasiero et al., 1992) and copper hydroxides with a pH iso-electric point 9.5 (Fullston et al., 1999). In this study, it seems that chalcopyrite was slightly oxidized while chalcocite was extensively oxidized after grinding in the stainless steel rod mill with stainless steel rods.

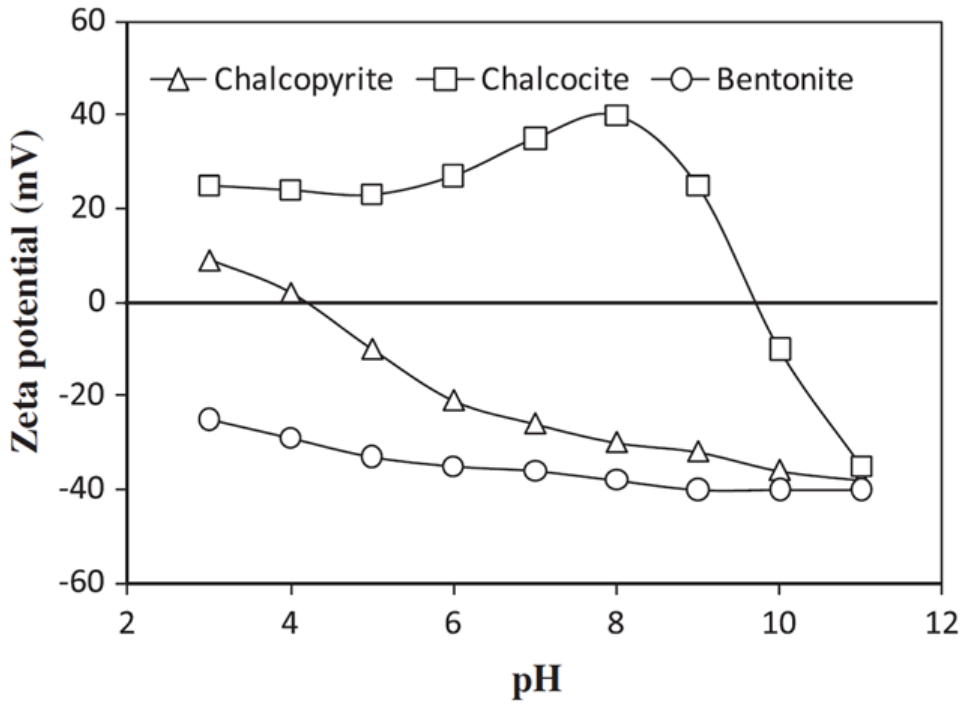

Fig 5.5 Zeta potentials of chalcopyrite and chalcocite after grinding, and zeta potentials of bentonite

The zeta potential measurement of bentonite shows that bentonite was strongly negatively charged across the examined pH range from 3.0 to 11.0. With increasing pH, the zeta potential was decreased slightly. This is in line with the measurement in literature (Arnold and Aplan, 1986; Vane and Zang, 1997). As discussed previously, the basal faces of clay minerals carry a constant negative charge (Luckham and Rossi, 1999; Zhao et al., 2008). The pH-dependent charges of bentonite are therefore a consequence of the existence of hydroxy groups at the edge. Due to the low fraction of the edges in bentonite (less than 1%) (Sondi et al., 1997), the zeta potential in the measurement is predominantly governed by the basal faces. There is a consensus that the point of zero charge of edges of montmorillonites (the determinative components in bentonite), is about 5.0 (Rand et al., 1980; Lagaly, 1993; Permien and Lagaly, 1994). Apparently, at pH 9.0 where the grinding and flotation was operated in this study, both the faces and edges of bentonite are negatively charged.

Theodoor and Overbeek (1990) reported that the entropic repulsion may be the dominant force between the particles with the same surface charge. Fig 5.5 reveals that at pH 9.0, slightly oxidized chalcopyrite is entropically repulsed from bentonite, while oxidized chalcocite is strongly attracted to bentonite. This may explain why bentonite substantially depressed chalcocite flotation through the slime coating but not chalcopyrite flotation. Then it is logical to hypothesize that bentonite may depress the flotation of strongly oxidized chalcopyrite but not the flotation of unoxidized or slightly oxidized chalcocite. This hypothesis was verified by controlling the stage of oxidation on chalcopyrite and chalcocite surfaces during grinding followed by flotation, which is discussed below.

5.3.2 Controlled grinding

Fig 5.6 shows the zeta potential of chalcopyrite and chalcocite ground under the controlled oxidation condition as well as the zeta potential of bentonite. The zeta potential value of chalcocite increased from -25 mV to -15 mV with pH increasing from 5.0 until around pH 9.0 and then decreased thereafter. It was negatively charged across the examined pH range. Obviously, chalcocite was slightly oxidized but without the reversal of the zeta potential and therefore repulsive from bentonite at pH 9.0. Fig 5.6 also shows that chalcopyrite after grinding with peroxide exhibited a pH iso-electric point at around 8.5, indicating strong oxidation. Since chalcopyrite oxidation produces a much higher amount of iron oxidation species than copper oxidation species, the pH iso-electric point of the oxidized chalcopyrite should be predominated by the iron oxidation species. It is also well known that iron oxidation species play a dominant role in depressing mineral flotation (Forssberg et al., 1988; Natarajan, 1996; Peng et al., 2003a). The depressed chalcopyrite flotation in Fig 4.5 may be mainly attributed to the iron oxidation species originated from chalcopyrite oxidation. The oxidized

chalcopyrite was negatively charged at pH 9.0 as well. It is unlikely that bentonite coats on the surface of oxidized chalcopyrite through an electrostatic attraction. Bentonite did not further depress the flotation of heavily oxidized chalcopyrite.

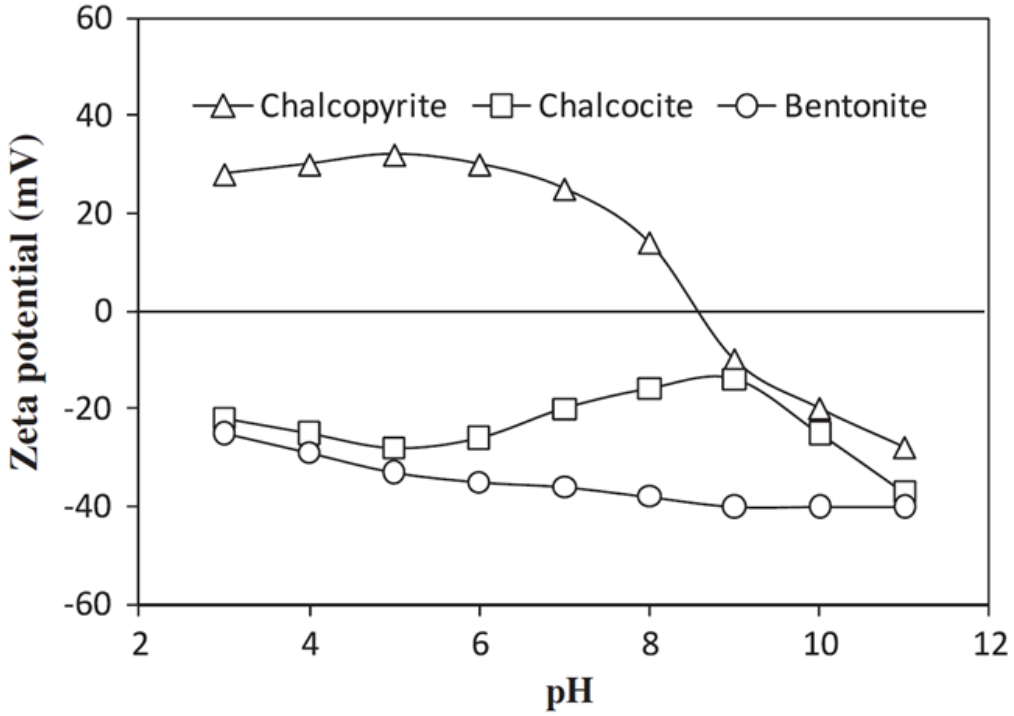

Fig 5.6 Zeta potentials of chalcopyrite and chalcocite after grinding with the controlled oxidation condition and zeta potentials of bentonite: chalcopyrite was ground at 500mV (SHE) while chalcocite was ground at -300mV (SHE).

The results of single mineral flotation experiments suggest two strategies for mitigating the bentonite coating on the chalcocite surface in the flotation of the open pit ore: (1) the control of chalcocite oxidation during grinding to ensure a negative charge on the chalcocite surface at pH 9.0, and (2) increasing the pulp pH to values higher than pH 10.0 where the surface charge of chalcocite is negative. Strategy (1) was tested by adding dithionite during the grinding of the open pit ore to reduce the pulp potential to -300 mV (SHE). In the subsequent flotation the recovery of cyanide soluble Cu was increased to 76% from 48% with the control of oxidation during grinding. Obviously, the adverse effect of bentonite on chalcocite flotation was reduced through the control of the surface

oxidation. Strategy (2) was tested by increasing the pH to 10.0 in the mill and flotation cell. However, the pulp became highly viscous resulting in the worse flotation. The effect of pulp viscosity on the flotation of copper sulphide minerals was reported elsewhere (Peng et al., 2010).

5.4 The interaction of oxidized chalcopyrite and chalcocite with bentonite during grinding

Due to the difference of surface charge across the examined pH range from 3.0 to 11.0 discussed previously, bentonite particles may coat the ground chalcocite surface but not on the ground chalcopyrite surface. The coating of bentonite particles on the ground chalcopyrite and chalcocite surfaces was directly examined by the Cryo-SEM analysis, which is discussed below.

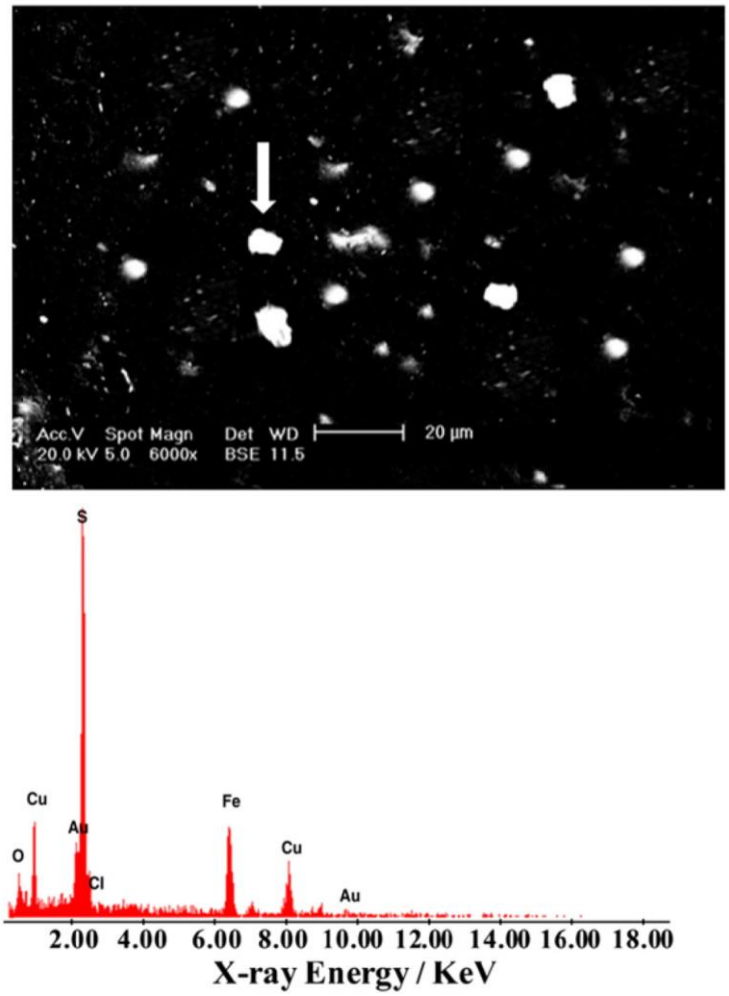

Fig 5.7 The BSE image (top) and EDX analysis on the randomly chosen particle (bottom) of the chalcopyrite sample ground in the presence of bentonite particles.

Fig 5.8 shows the BSE image (top) and EDX analysis on the chosen particle (bottom) of the chalcocite sample ground in the presence of bentonite particles. Again, chalcocite was present as larger particles while bentonite as the smaller dots in the BSE image. EDS analysis confirmed the presence of chalcocite as distinct signals from Cu and S elements were detected on the randomly chosen particle. EDX analysis on the chosen particle also detected distinct signals from Si at about 1.8 keV and Al at about 1.6 keV which were attributed to bentonite. The signal from O was stronger in Fig 5.8 compared to Fig 5.7, but again it might emanate from bentonite, water or mineral oxidation species.

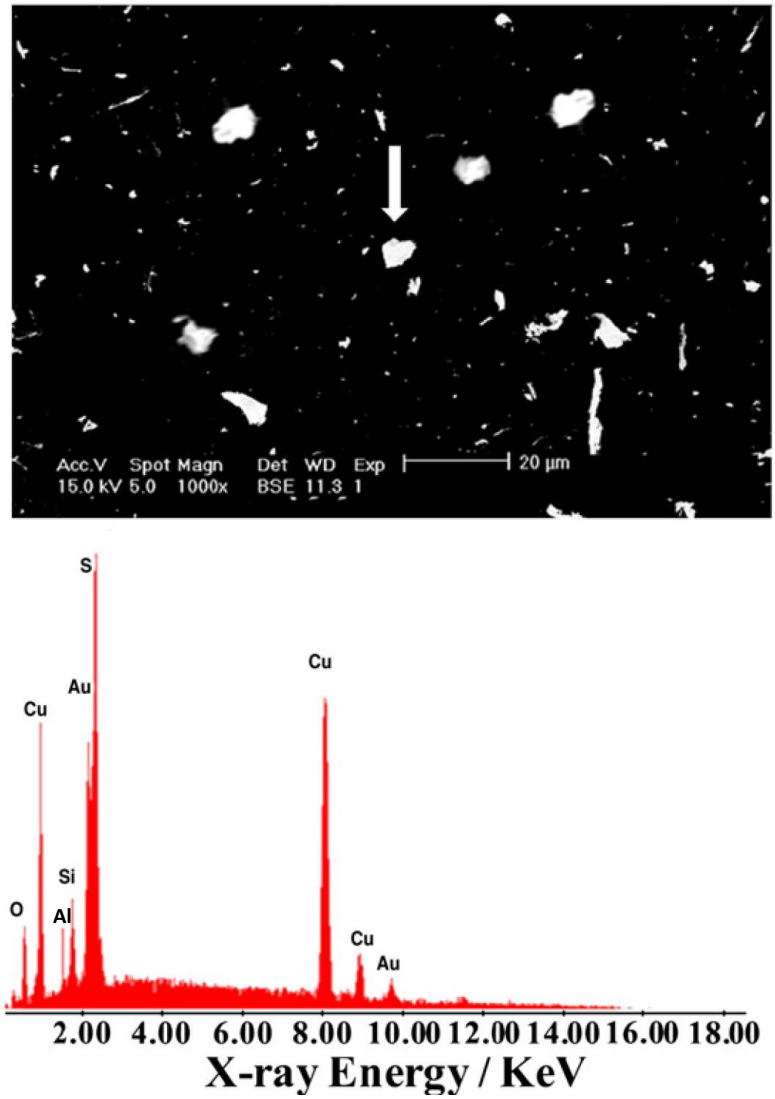

Fig 5.8 The BSE image (top) and EDX analysis on the randomly chosen particle (bottom) of the chalcocite sample ground in the presence of bentonite particles.

5.5 Discussion

It is demonstrated by other researchers that chalcocite is more electrochemically active than chalcopyrite based on the zeta potential measurement (Lascelles,D., 2002). It is also more oxidized producing more EDTA extractable copper ions for the same size fraction (Fullston, F., 1999). This indicates that during grinding to provide a similar size, more chalcocite oxidation should be expected. XPS analysis confirms that during grinding under the same condition, chalcopyrite was

slightly oxidized but chalcocite was strongly oxidized. After grinding, the majority of the chalcocite surface was occupied by oxidation species, while only a small proportion of the chalcopyrite surfacewas oxidized, revealed by XPS atomic compositions and elemental spectra.

Oxidation alters the surface properties of minerals. The iso-electric point of non-oxidized sulphide minerals is similar to that of elemental sulfur at pH between 1 and 2 (Fullston,F., 1999; Fairthorne,G. 1998). Upon oxidation, the sulphide mineral surface becomes increasingly covered with metal oxidation products and the zeta potential versus pH curves of these sulphide minerals become less negative and even positive (Fullston,F., 1999; Fairthorne,G. 1998). The iso-electric point of the oxidized sulphide minerals is therefore increased and lies between that of elemental sulfur and that of the corresponding metal hydroxide species. In this study oxidation during grinding altered the electrical property of both chalcopyrite and chalcocite. Due to mild oxidation, the iso-electric point of chalcopyrite was increased slightly and the chalcopyrite surface was still negatively charged at grinding pH 9.0. However, the strongly oxidized chalcocite showed the electrical property of copper hydroxides and became positively charged at pH 9.0.

The zeta potential of non-oxidized sulphide minerals is comparable to that of elemental sulfur or to a sulphide mineral with a sulfur-rich surface (Fairthorne et al., 1998; Fullston et al., 1999). The pH value where the zeta potential changes sign or the iso-electric point characterizes the electrical property of a mineral. The zeta potential is positive for pH values smaller than the isoelectric point, but negative for pH values greater than the iso-electric point. The iso-electric point of non-oxidized sulphide minerals is similar to that of elemental sulfur at pH between 1 and 2 (Fornasiero et al., 1992). Upon oxidation, the sulphide mineral surface becomes increasingly covered with metal oxidation products and the zeta potential versus pH curves of these sulphide minerals become less negative and

even positive (Fornasiero et al., 1992; Fairthorne et al., 1998; Fullston et al., 1999). The iso-electric point of the oxidized sulphide minerals is therefore increased and lie between that of elemental sulfur and that of the corresponding metal hydroxide species. The zeta potential of clay minerals is negative in alkaline solutions (Arnold,B.J., 1986; Vane,L.M., 1997). At pH 9.0, both the faces and edges of bentonite are negatively charged (Sondi,I., 1997; Rand,B., 1980; Lagaly,G., 1993). It is anticipated that the bentonite coating may occur on the surface of oxidized sulphide minerals due to the electrostatic attraction but not on unoxidized or slightly oxidized sulphide minerals at alkaline pH values. The hydrophilic metal and sulfate oxidation species may also attract bentonite particles by hydrogen bonding. However, the oxidation significantly alters the electrical property of chalcocite being strongly positively charged at pH 9.0. This is probably due to the high amount of copper hydroxides on the surface and their high pH iso-electric point at 9.5 (Fullston et al., 1999). It is likely that bentonite slime coating occurs on the oxidized chalcocite as results of the negative charge of bentonite at pH 9.0 and its natural colloidal size (Schoonheydt and Johnston, 2006; Kotlyar et al., 1996). Consequently, the flotation of oxidized chalcocite is depressed by bentonite. Unlike chalcocite, chalcopyrite flotation is less affected by bentonite. The slightly oxidized chalcopyrite under normal grinding is still negatively charged and entropically repulsive from bentonite. Even with extensive oxidation chalcopyrite may still be negatively charged at pH 9.0 and an electrostatic attraction with bentonite is unlikely. This is confirmed by Cryo-SEM analysis in this study showing that bentonite particles coated the chalcocite surface but not the chalcopyrite surface and also explains why the extraction of chalcocite by flotation was more negatively affected by bentonite than the extraction of chalcopyrite in the previous study in chapter 4.

In this study, the oxidation of chalcopyrite and chalcocite and their interaction with bentonite were investigated under an oxidizing grinding condition by using

stainless steel media. However, in mineral processing, mild steel media is also used and produces a reducing grinding condition and a great amount of iron oxidation species (Peng,Y., 2002; 2010). These iron oxidation species are negatively charged at pH 9.0 (Peng,Y., 2010). It is anticipated that the oxidation of chalcopyrite would be decreased during the grinding with mild steel media resulting in a negatively charged surface which is repulsive from both iron oxidation species and bentonite particles at pH 9.0. Chalcocite is the most electrochemically active among the copper sulphide minerals examined by Fullston et al. (1999) and its oxidation may still be pronounced even under a reducing ground condition produced by mild steel media. It is likely that both iron oxidation species and bentonite particles may be adsorbed on the oxidized chalcocite surface through an electrostatic attraction at pH 9.0. However, how iron oxidation species and bentonite particles compete on the chalcocite surface is not predictable.

5.6 Conclusions

Grinding alters the surface properties of chalcopyrite and chalcocite through surface oxidation. Chalcocite is strongly oxidized while chalcopyrite is slightly oxidized after normal grinding with stainless steel media. The different extent of surface oxidation results in the different electrical property of chalcopyrite and chalcocite surfaces. The slightly oxidized chalcopyrite surface remains negatively charged after grinding at pH 9.0 and entropically repulsive from bentonite slime particles. In contrast, the strongly oxidized chalcocite surface becomes positively charged after grinding at the same pH and electrostatically attractive to bentonite particles.

Chapter 6 The effect of electrolytes on the flotation of copper minerals in the presence of clay minerals

This chapter presents testwork performed to explore the effect of electrolytes on mitigating clay slime coatings in the flotation of chalcocite mineral. Batch flotation experiments of single chalcocite mineral with or without clay minerals in different electrolytes solutions were designed for investigation.

6.1 Introduction

In Chapter 4, the effect of bentonite on the flotation of chalcopyrite and chalcocite in terms of slime coating was investigated. It was found that chalcocite flotation was much more depressed than chalcopyrite in the presence of bentonite after grinding. As outline in chapter 5, the mechanism was found that as a result of the different extent of mineral surface oxidation, chalcopyrite remained negatively charged but chalcocite became positively charged after grinding leading to the different interactions of copper minerals with bentonite particles. The surface of chalcocite was electrostatically attracted to bentonite resulting in bentonite slime coating and the depressed flotation of chalcocite.

As outlined in Chapter 2, Peng and Bradshaw (2012) also reported that serpentine minerals depress pentalandite flotation due to slime coating. They found that bore water with a high ionic strength increased pentlandite flotation recovery. Therefore, the clay slime coating on copper mineral surfaces may also be mitigated by electrolytes.

As reviewed in Chapter 2, the effect of electrolytes on mineral flotation has been studied by other researchers from a different perspective. For instance, Hancer (2001) classified certain ions as “structure breaking” ions or “structure making” ions and proposed that they have different effect on water structure. However, it has not been studied that how the different inorganic ions influence the slime coating in copper minerals flotation. In this chapter, three different cations (Li^+, Na^+ and K^+) and anions (F^-, Cl^- and I^-) were chosen from Hancer’s ion classification table (Table 2.4) for testing as these ions are common in bore water.

Kaolinite is a clay mineral which is more often associated with copper ore deposits. It has similar charge properties to bentonite which can also cause slime coatings on chalcocite surfaces. Therefore, in this chapter, kaolinite was used as

a representative of clay mineral in chalcocite flotation tests. This may also extend to cover the generic clay minerals.

6.2 Chalcocite flotation in tap water

Fig 6.1 shows chalcocite flotation response in the absence and presence of kaolinite in tap water. In the absence of kaolinite, chalcocite displayed a good flotation behaviour with 50% Cu grade and 96% Cu recovery at the end of flotation. The presence of kaolinite decreased chalcocite flotation. Both Cu grade and Cu recovery were decreased when 20% or 30% kaolinite was added and copper flotation kinetics was also decreased. At 30% kaolinite Cu grade and recovery were reduced to 33% and 63%, respectively at the end of flotation.

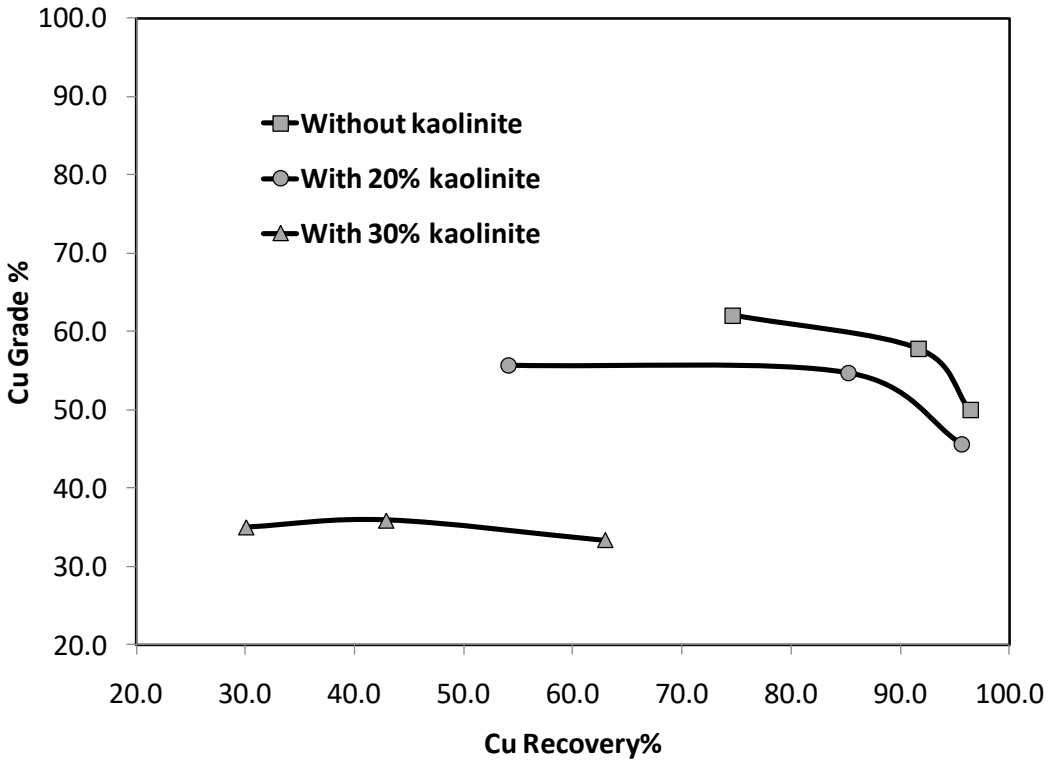

Fig 6.1 Chalcocite flotation in the absence and presence of kaolinite in tap water

In a separate study where the effect of kaolinite on chalcopyrite flotation was investigated, kaolinite had little effect on chalcopyrite flotation. Nor did 30%

weight of kaolinite change the pulp rheology in flotation. In Chapter 4, it was also found that bentonite did not affect chalcopyrite flotation but did influence chalcocite flotation. In that study, both chalcopyrite and chalcocite were ground to -38 μm. Further mechanism study in Chapter 5 attributed the depression of chalcocite flotation by bentonite to the oxidation of the chalcocite surface which was attracted to bentonite resulting in bentonite slime coating. This may explain the depression of chalcocite flotation by kaolinite in the current study using tap water.

6.3 Effect of NaCl addition on chalcocite flotation in the presence of kaolinite

Fig 6.2 shows chalcocite flotation response in the presence of 30% kaolinite in NaCl solutions. With the addition of NaCl, chalcocite flotation was improved. The higher the NaCl concentration, the better the chalcocite flotation response. As shown in Fig. 3, the addition of 0.08 mol/L NaCl increased Cu grade and recovery to 38% and 80%, respectively, at the end of flotation. The addition of 0.34 mol/L NaCl increased Cu grade and recovery to 42% and 90%, respectively, which are close to 50% Cu grade and 96% Cu recovery achieved from the flotation of the chalcocite ore in the absence of kaolinite. Obviously, the addition of NaCl mitigated the negative effect of kaolinite on chalcocite flotation.

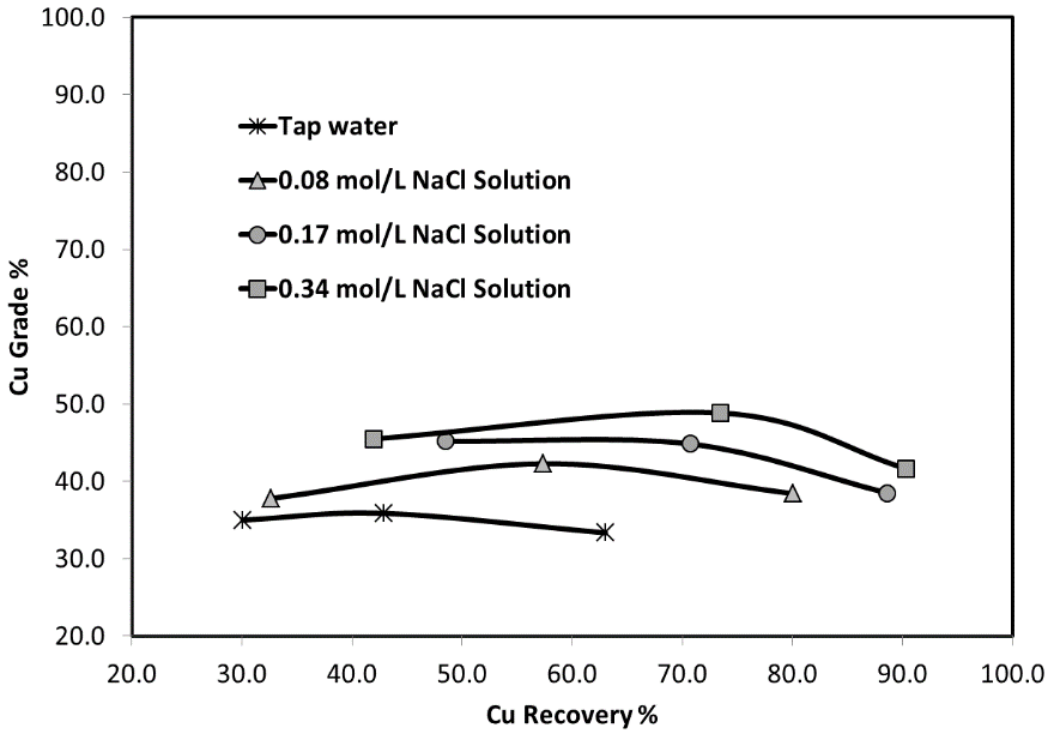

Fig 6.2 Chalcocite flotation in the presence of 30% kaolinite in NaCl solutions

6.4 Effect of cations on chalcocite flotation in the presence of kaolinite

Fig 6.3 shows the effect of different cations on chalcocite flotation in the presence of 30% kaolinite. For a comparison, Cu grade and recovery from chalcocite flotation in tap water and NaCl solutions were also included in the figure. As can be seen, like NaCl, LiCl and KCl mitigated the negative effect of kaolinite on chalcocite flotation. However, the three cations (Na^+, Li^+ and K^+) affected the flotation differently. 0.47 mol/L LiCl and 0.34 mol/L NaCl produced almost identical Cu grade-Cu recovery curves suggesting that Li^+ may be inferior to Na^+ in mitigating the negative effect of kaolinite on chalcocite flotation, reaching similar flotation results but at higher concentration. Meanwhile, 0.27 mol/L KCl produced the best chalcocite flotation with the best Cu grade-Cu recovery results despite the moderate concentration. As a result, K^+ is superior to Na^+ and Li^+ in mitigating the negative effect of kaolinite on chalcocite flotation. Interestingly, it

was found that mitigation effect of these cations on kaolinite slime coating follows Hofmeister effect by the order of $K^+ > Na^+ > Li^+$, based on the influence of the ion on the water in its vicinity (Franks, 2002).

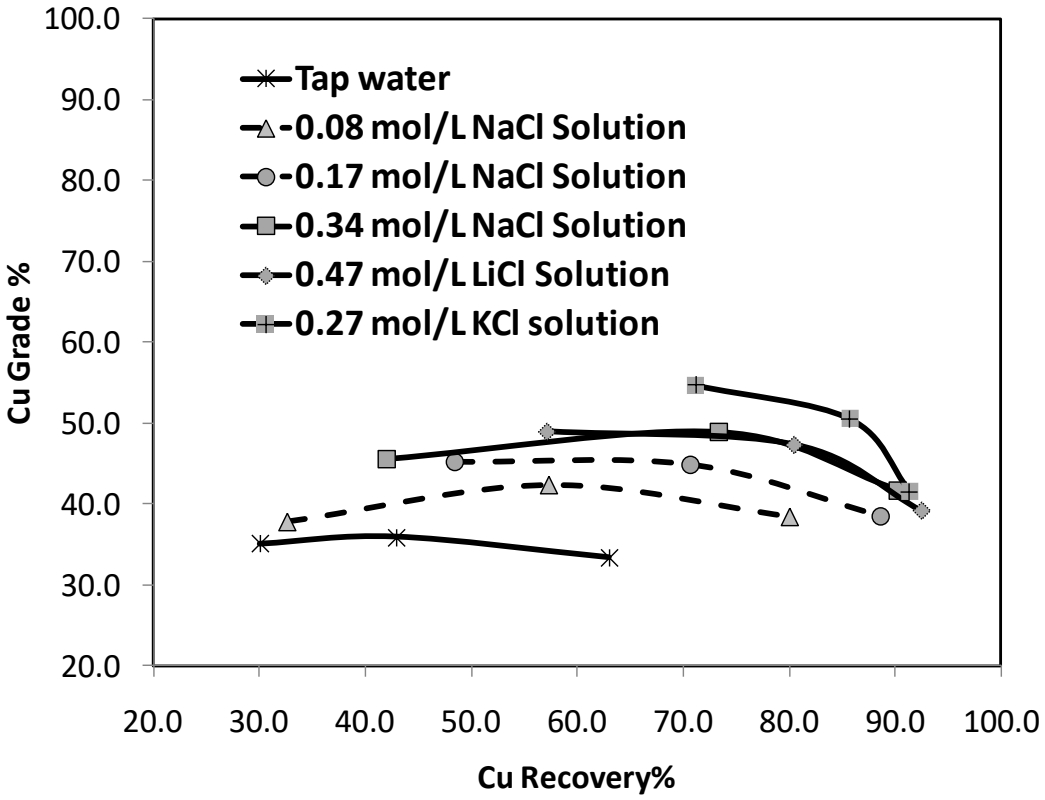

Fig 6.3 Effect of cations on chalcocite flotation in the presence of 30% kaolinite

6.5 Effect of anions on chalcocite flotation in the presence of kaolinite

Similarly, the effect of different anions on chalcocite flotation in the presence of 30% kaolinite was investigated. The results are shown in Fig6.5. Cu grade and recovery from chalcocite flotation in tap water and NaCl solutions were also included in Fig 6.4 for a comparison. Again, the three anions, F^-, Cl^- and I^- mitigated the negative effect of kaolinite on chalcocite flotation. As can be seen from Fig 6.4, F^- improved chalcocite flotation response the least despite the highest concentration, 0.48 mol/L tested. 0.48 mol/L NaF increased Cu recovery from 63% in tap water to 78% without changing the Cu concentrate grade at the

end of flotation. Cl^- produced better flotation than F^- even at a lower concentration. For example, 0.17 mol/L NaCl produced chalcocite flotation concentrate with 39% Cu grade and 89% Cu recovery. I^- improved chalcocite flotation the most. 0.13 mol/L NaI produced a flotation concentrate with 42% Cu grade and 91% Cu recovery.

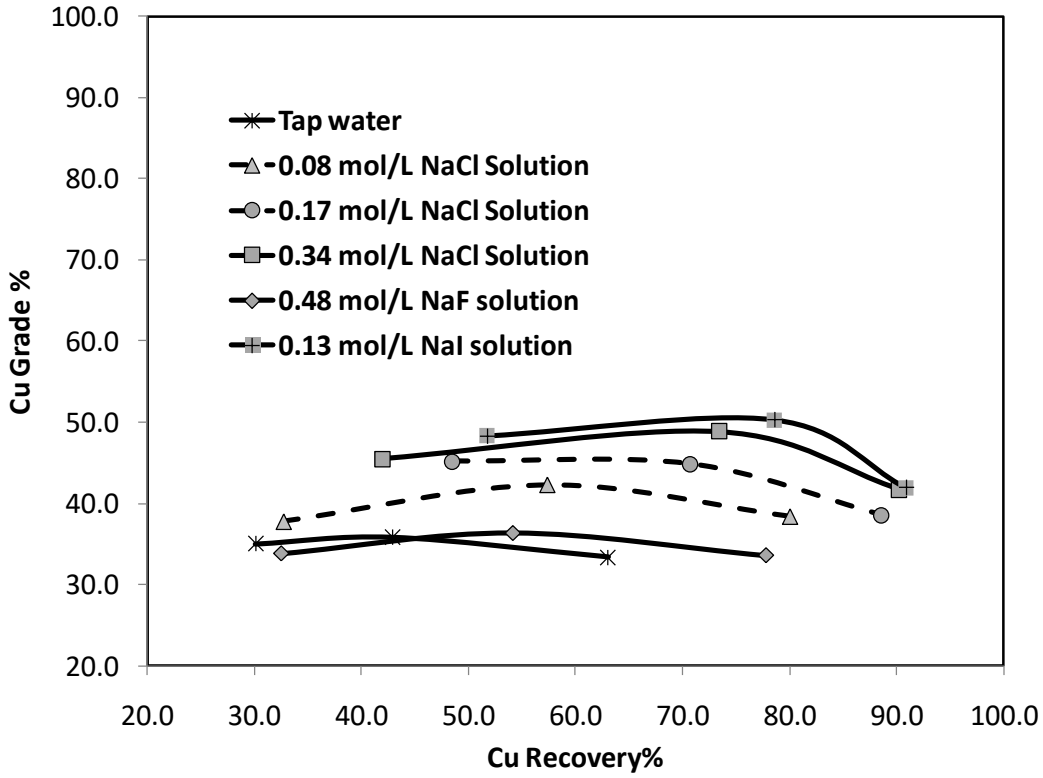

Fig 6.4 Effect of anions on chalcocite flotation in the presence of 30% kaolinite

6.6 Conclusions

The study in this chapter confirmed the effect of kaolinite on chalcocite flotation is similar to bentonite in tap water which depresses the copper flotation by slime coating. Test results indicate that with the addition of electrolytes to the flotation system, the flotation of chalcocite was improved. In addition, it is interesting to find that larger size ions may improve chalcocite flotation in the presence of kaolinite more than smaller size ions.

Chapter 7 Impedance spectroscopy study on the mitigation of clay slime coatings on chalcocite by electrolytes

Testwork presented in this Chapter was designed to explore how the inorganic ions improve chalcocite flotation in the presence of clay mineral by using the electrochemical impedance spectroscopy (EIS). The EIS data are analysed and modelled to identify how the different ions affect the clay slime coating.

7.1 Introduction

Despite the widespread problem of slime coating in mineral flotation, a direct detection of slime coating is not available. Traditionally, zeta potentials on two single minerals are measured to infer the electrostatic attraction which may cause one mineral to coat the other mineral. Cryo-SEM has been used to detect slime coating in chapter 5. The advantage of Cryo-SEM is that samples taken from slurries are snap-frozen to preserve mineral surfaces in the vitrified water without crystallisation as ice (Battersby et al., 1994). Coupled with energy-dispersive X-ray spectroscopy (EDS) to identify the elemental composition of chosen mineral areas, Cryo-SEM can confidently detect slime coating. However, strictly speaking, Cryo-SEM is not an in-situ technique involving a sampling process. It is also sophisticated with limited accessibility.

The electrochemical impedance spectroscopy (EIS) is a sensitive analytical technique with a high accuracy, allowing an in-situ detection of the formation of surface layers on the electrode which is well correlated with the electrode capacitance. The measured impedance data can also reflect the kinetics of surface electrochemical reactions in-situ with a minimum of surface modification (De Wet et al., 1997; Niu et al., 2014). Ekmekçi et al. (2010) used EIS to study the adsorption of CuSO4 and SIBX on pyrrhotite surface and correlated pyrrhotite impedance with its flotation behaviour. Guo et al. (2015) demonstrated that a change in the impedance of pyrite electrode was consistent with the adsorbed xanthate. Mu et al. (2015) reported that the presence of lignosulfonate based biopolymers on pyrite surface was reflected by a change in impedance of pyrite electrode. In this study, for the first time, the EIS was applied to investigate the slime coating and its mitigation on mineral surface. The test method is as outlined in chapter 3. It is expected that the impedance of a mineral electrode in the absence and presence of slime coating is different.

7.2 Cyclic voltammetry studies

The voltammogram of chalcocite electrode in background solution is shown in Fig. 1. Chalcocite voltammograms with surface reactions in aqueous solutions have been frequently reported (Sato, 1960; Velasquez et al., 2001). The peak at 0.15V with the breadth from approximately 0.05 to 0.25 V on the positive-going sweep was attributed to the oxidation of chalcocite resulting in the formation of cupric oxide and a sulfur-rich sub-layer (covellite) as shown in Reaction (1).

$$Cu_2S + 2xOH^- = Cu_{2-x}S + xCuO + xH_2O + xe^- \quad (1)$$

Extensive oxidation of chalcocite to cupric hydroxide and sulphate commences at elevated potential and is much more rapid and electrochemically irreversible. This reaction did not occur in the potential range investigated in this study as shown in Fig 7.1.

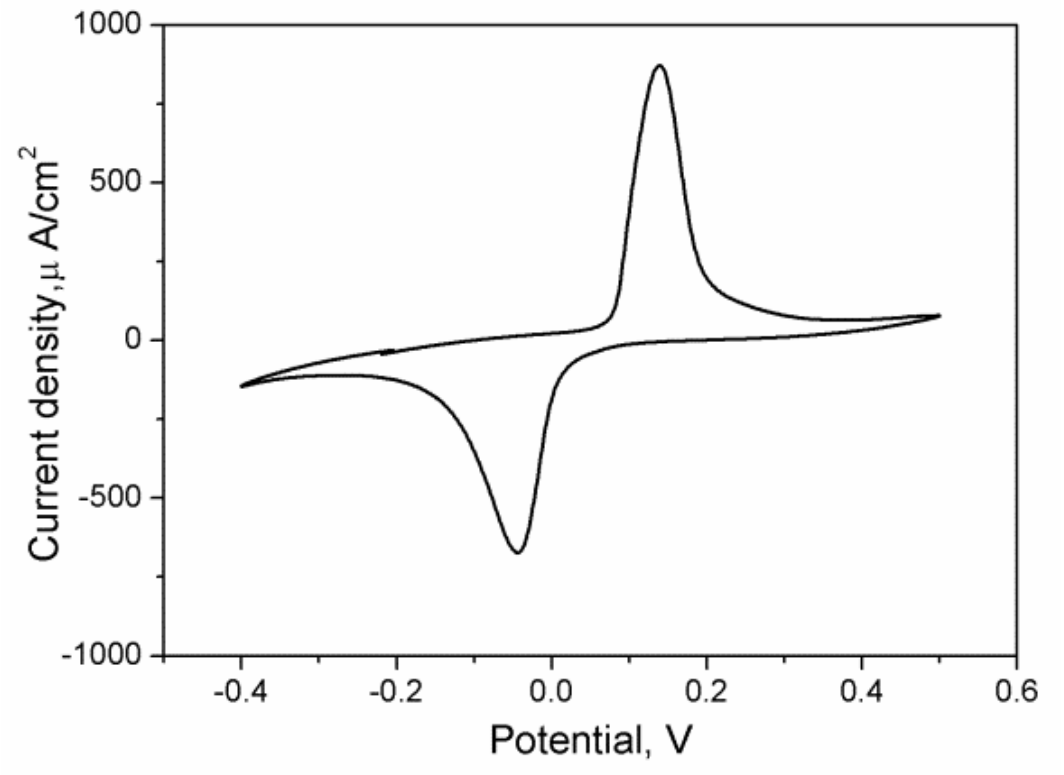

Fig 7.1 Voltammograms of chalcocite electrode in background solution

7.3 Electrochemical Impedance Spectroscopy studies

Impedance measurements were conducted to provide an in-situ detection of possible modification of chalcocite surface exposed to electrolyte solutions in the presence of kaolinite. The impedance spectra are commonly presented as a Bode plot (with log frequency on the X-axis and the impedance absolute value Z on the Y-axis). At a high frequency region (100-10,000 Hz), Z values are low and relatively constant. This is a typical response of a resistor to an AC with high frequency, corresponding to solution resistance. In a low frequency region (0.1-100 Hz), the relationship between Z and frequency becomes linear with a slope of -1. This part corresponds to a capacitive behaviour caused by the electrical double layer at the mineral/solution interface and/or the possible surface layer. In this study, the impedance values indicated in the Bode plots for chalcocite in the presence of kaolinite in different electrolyte solutions were investigated and compared.

7.3.1 EIS Response of chalcocite in DI water in the presence of kaolinite

The formation of surface layer on sulphide mineral surface can be detected by impedance spectroscopy based on the physical properties of the layer. The capacitance of mineral surface in electrolyte solution may include the double layer capacitance （C_{DL}）and the space charge capacitance （C_{SC}）.

According to the Stern model (Bockris and Reddy, 1970; Bard and Faulkner, 1980; Adamson, 1990), the double layer on the solution side consists of several layers: Inner Helmholtz Layer (IHL), Outer Helmholtz Layer (OHL), and Gouy-Chapman (G-C) Diffusion Layer (Fig 7.2). The total capacitance of the electrical double layer, C_{DL}, is given by series combination of Helmholtz capacitance, C_H, and diffusion capcitance, C_G as follows (Bockris and Reddy, 1970):

$$\frac{1}{C_{DL}} = \frac{1}{C_H} + \frac{1}{C_G} \quad (1)$$

For semiconductor, another term is introduced in the double layer capacitance owing to diffuse charge region (the Garrett-Brattain Space Charge) inside an intrinsic semiconductor (Fig 7.2).

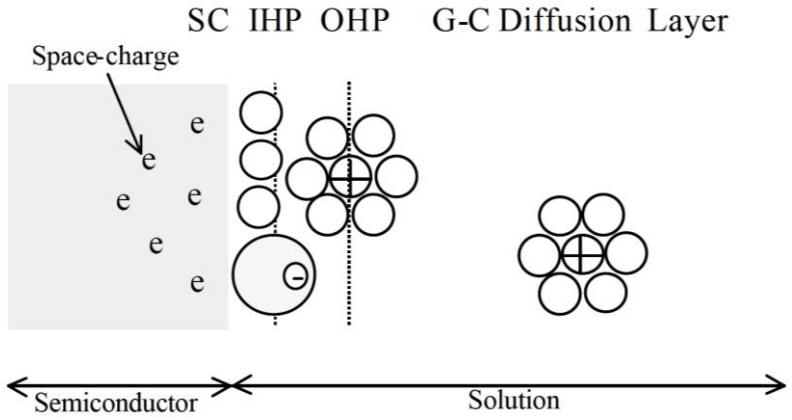

Fig 7.2 Excess charge distribution in the Garrett-Brattain space charge region and the double layer for a semiconductor in an electrolyte (Bockris and Reddy, 1970).

Therefore, the observed capacitance is resultant of two capacitors in series: the space charge capacitor, C_{SC}, and the double layer capacitance in the solution phase (Bockris and Reddy, 1970):

$$\frac{1}{C_{obs}} = \frac{1}{C_{SC}} + \frac{1}{C_{DL}} = \frac{1}{C_{SC}} + \frac{1}{C_H} + \frac{1}{C_G} \quad (2)$$

In a strong electrolyte solution $C_G \gg C_H \gg C_{SC}$, therefore the measured capacitance is given by $C_{obs} \approx C_{SC}$ (Neeraj K. M., 2000). In this research, the electrolytes selected from Hancer's ion classification table (2001) were strong. The change of double layer capacitance will have little effect on the C_{obs}, compared with slimes coating on the mineral surface. Therefore, the double layer capacitance has not been taken into consideration.

Due to the observed capacitance can be determined by the space charge capacitance which can be considered as the capacitance of a parallel plate capacitor (Bockris and Reddy, 1970), it can be determined by the dielectric

constant with the material that forms on mineral surface. A capacitor forms when two conducting plates are separated by a non-conducting medium, called the dielectric. The value of the capacitance C can be described as Eq. (3):

$$C = \varepsilon_0 \varepsilon_r A/d \quad (3)$$

where ε_0 is the dielectric constant of free space which is a physical constant, ε_r is the dielectric constant varying with material, d is the distance between two plates, and A is the surface area of the plate.

Table 1 shows the dielectric constants of chalcocite, copper oxide/hydroxide and kaolinite (Josann et al., 1936). It indicates that the formation of kaolinite coating on chalcocite surface will decrease the dielectric constant and the capacitance. The impedance Z of a capacitor is given in Eq. (4):

$$Z = {}^{-j}\!/_{\omega C} \quad (4)$$

Where $j = \sqrt{-1}$, ω is the angular frequency of the AC voltage. Therefore, the decrease of capacitance of surface layer can be reflected by the increase of impedance values.

Table 7.1 Dielectric constants of various materials

Mineral	Dielectric Constant
Chalcocite	>81
Copper oxide (Cuprite)	16.2
Kaolinite	11.18

Fig 7.3 shows the EIS (Bode plots) of chalcocite surface in background solution with the electrode pre-oxidized at 0 mV, 200 mV, and 400 mV. It can be seen that the impedance of chalcocite was much larger at 200 mV than at 0 mV at the low frequency region due to the formation of $Cu(OH)_2$/CuO layer. Further increasing the oxidation potential to 400 mV slightly increased the impedance value. This is consistent with the potential range for the oxidation of chalcocite through CV studies in Fig 7.1 where the moderate oxidation of chalcocite occurred over a potential range from 0.05 V to 0.25 V.

The formation of a continuous surface layer may cause a change to the capacitance. Since the impedance of a capacitor is inversely proportional to the capacitance, the decrease in electrode capacitance can be conveniently observed in Bode plots with an increase in impedance in the low frequency range.

The EIS of the pre-oxidized chalcocite electrode at 400 mV with the addition of 10% kaolinite in the solution is shown in Fig 7.4. The impedance of chalcocite in the presence of kaolinite was higher than that in the absence of kaolinite in the low frequency range. Obviously, kaolinite with the lower dielectric constant coated the oxidized chalcocite surface.

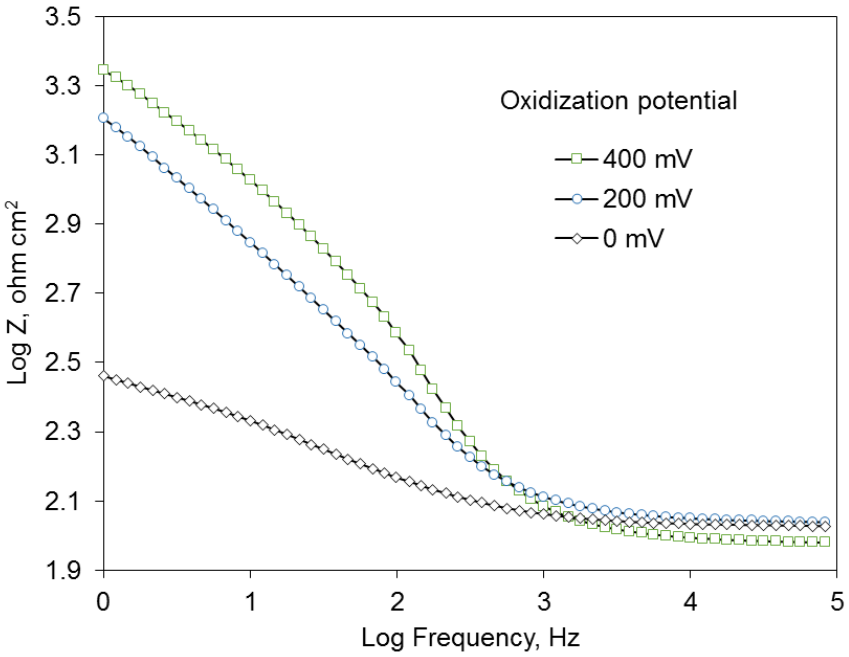

Fig 7.3 EIS (Bode plots) of chalcocite in the background solution with the electrode pre-oxidized at 0 mV, 200 mV and 400 mV

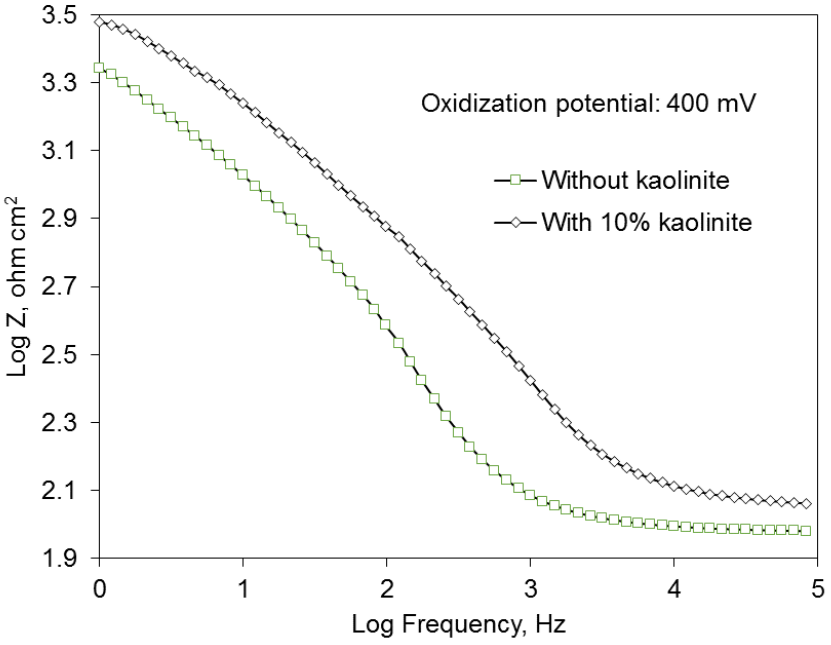

Fig 7.4 EIS (Bode plots) of chalcocite in DI water with the electrode pre-oxidized at 400 mV in the absence and presence of kaolinite

7.3.2 The effect of cations and anions on EIS of chalcocite in the absence of kaolinite

The EIS of the pre-oxidized chalcocite electrode at 400 mV in 0.34 M LiCl, NaCl and KCl solutions in the absence of kaolinite was investigated. Fig 7.5 shows that the impedance of chalcocite in these electrolyte solutions was very similar in the low frequency range. Compared to the impedance of chalcocite in DI water (Fig. 4) in the low frequency range (e.g., at Log Frequency = 0), the impedance of chalcocite in these three electrolyte solutions was lower. Since the oxidized chalcocite surface is positively charged at pH 7, anions in the solution are attracted to the chalcocite surface by electrostatic attraction, which may reduce the impedance of chalcocite. It is consistent with the study of Wei et al. (1992) showing that the dielectric constant of RbCl, CsCl or LiCl solution was higher than that of pure water.

The similar effect of LiCl, NaCl and KCl on the impedance of oxidized chalcocite surface is expected because of the same anion Cl^- associated with different cations.

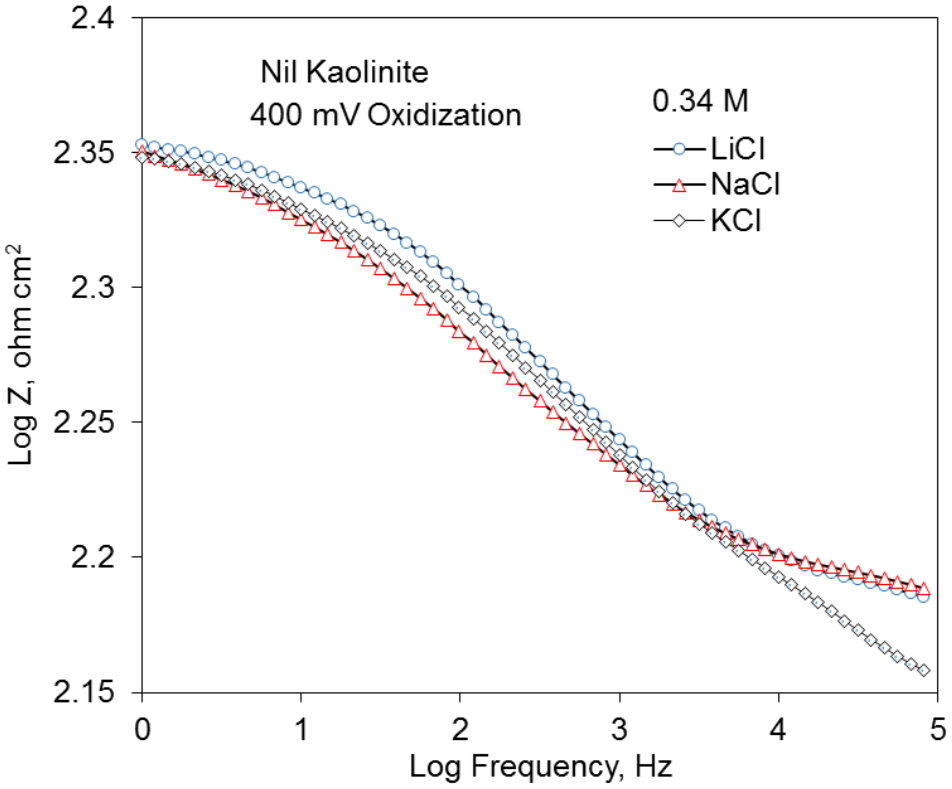

Fig 7.5 EIS (Bode plots) of chalcocite in 0.34 M LiCl, NaCl and KCl solutions with the electrode pre-oxidized at 400 mV in the absence of kaolinite

Fig 7.6 shows the EIS of chalcocite in NaF, NaCl and NaI solutions. Similarly, compared to the impedance of chalcocite in the low frequency range in DI water as shown in Fig 7.5, the impedance of chalcocite in these three electrolyte solutions was lower, indicating that the impedance of chalcocite decreased with the addition of electrolytes. It is interesting that the impedance of chalcocite was higher in NaF solution than in NaCl and NaI solutions, in general. For example, at Log Frequency = 0, the log value of chalcocite impedance in NaF solution was 2.55 ohm cm^2 which is higher than that in NaCl and NaI solutions (2.35 and 2.31 ohm cm^2, respectively).

Since the anion in the solution is attracted to the positive chalcocite surface by electrostatic forces, the impedance measurements suggest that F^- could be less adsorbed on chalcocite surface than Cl^- and I^-. Tadros and Lyklema (1968) and Sonnefeld (1995) reported that the adsorption sequence of monovalent cations on

silica surface follows the Hofmeister series with larger ions adsorbing in greater quantities than smaller ions. As known, SCN^- is also a large anion in Hofmeister series. However, it is not part of saline water and may complex with copper ion. Due to the difference to other anions, SCN^- has not been investigated.

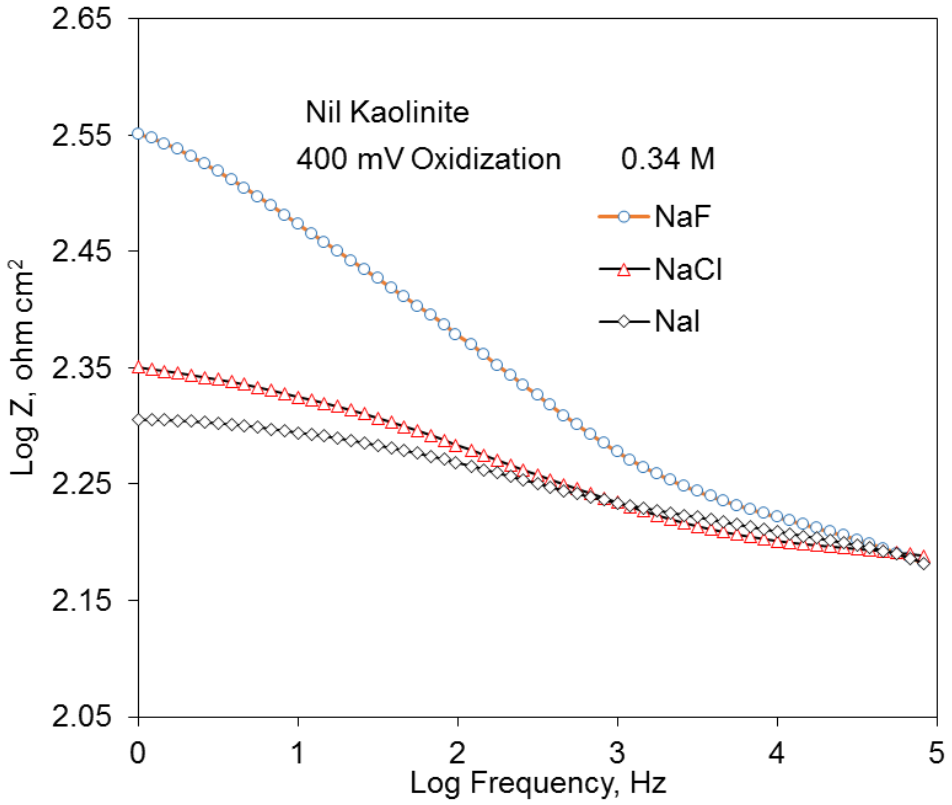

Fig 7.6 EIS (Bode plots) of chalcocite in 0.34 M NaF, NaCl and NaI solutions with the electrode pre-oxidized at 400 mV in the absence of kaolinite

7.3.3 The effect of cations and anions on EIS of chalcocite in the presence of kaolinite

The previous study reported that larger ions improved chalcocite flotation in the presence of kaolinite more than smaller ions. In this study, the effects of different cations (K^+, Na^+ and Li^+) and anions (I^-, Cl^- and F^-) on the EIS of chalcocite were examined.

Fig 7.7 shows the EIS of chalcocite in 0.34 M LiCl, NaCl and KCl solutions in the presence of 10% kaolinite. As can be seen, NaCl, LiCl and KCl all reduced

the impedance of chalcocite in the presence of kaolinite, indicating the mitigation of kaolinite slime coating from chalcocite surface. However, the three cations (Na^+, Li^+ and K^+) affected the impedance of chalcocite differently. Compared to the impedance of chalcocite in DI water in the presence of kaolinite, at the same concentration of 0.34 M, KCl generated the lowest impedance while LiCl only slightly reduced the impedance. To understand the different extent of cations in mitigating the kaolinite coating from chalcocite surface, the impedance of chalcocite in each electrolyte solution in the absence and presence of kaolinite as shown in Figs. 5 and 7, respectively, was compared. In general, the impedance of chalcocite was higher in the presence of kaolinite in each electrolyte solution. At the Log Frequency = 0, the differences in log value of impedance in the absence and presence of kaolinite were 0.57, 0.85 and 0.99 ohm cm^2 in KCl, NaCl and LiCl solution, respectively. It is clear that K^+ was superior to Na^+ and Li^+ in mitigating kaolinite slime coating on chalcocite surface, and produced a surface more close to the one without the slime coating. These EIS measurements are also in an agreement with the previous flotation results showing that chalcocite flotation in the presence of kaolinite was improved in a decreasing order of K^+, Na^+ and Li^+.

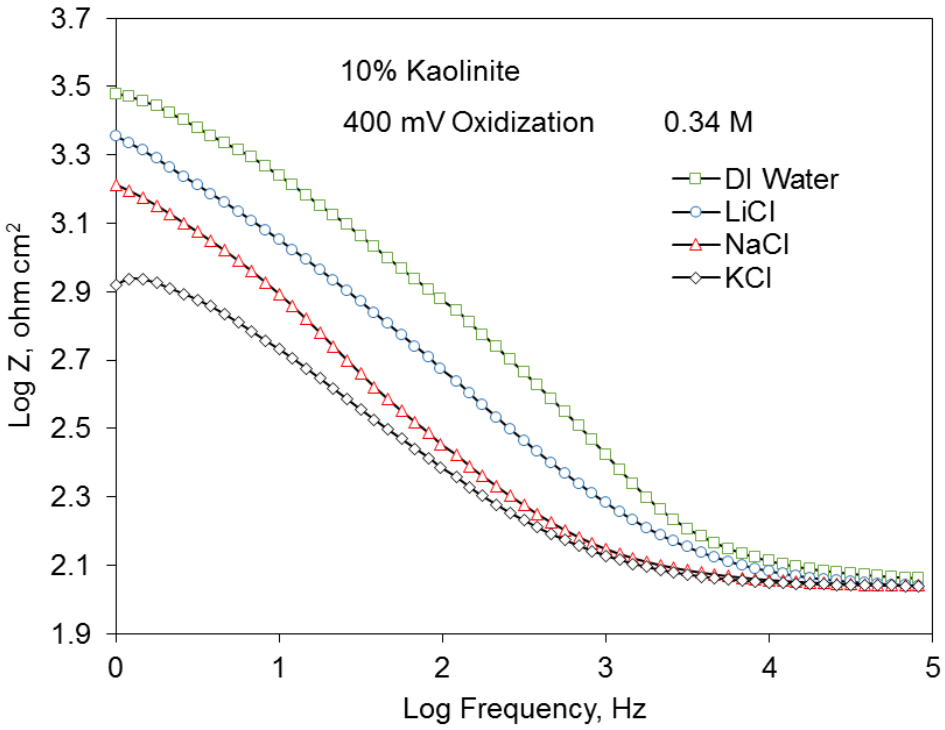

Fig 7.7 EIS (Bode plots) of chalcocite pre-oxidized at 400 mV in the presence of 10% kaolinite in 0.34 M LiCl, NaCl, and KCl solutions (the Bode plot of chalcocite with 10% kaolinite in DI water is also given for a comparison)

As previously mentioned in Chapter 6, negative effect of kaolinite coating and reduced the impedance by the order of K^+ > Na^+ > Li^+ was known as the Hofmeister series. As reported by Tadros and Lyklema (1968) and Sonnefeld (1995), the adsorption sequence of monovalent cations on silica surface follows the Hofmeister series with larger ions adsorbing in greater quantities than smaller ions. Sonnefeld (1995) proposed the stern layer thickness increased with the increase of the ion radius resulting in more ions adsorption. Franks (2002) measured the zeta potential of silica surface in the presence of K^+, Na^+ and Li^+ and found that the zeta potential increased with the cations following the Hofmeister series as well. At alkaline pH, silica had less negative zeta potential with K^+ than with Na^+ and Li^+ in line with the adsorbed amount. In this study, more K^+ may be adsorbed on the negatively charged kaolinite than Na^+ and Li^+ resulting in less electrostatic attraction between kaolinite and oxidized chalcocite.

Similarly, the effect of different anions on the EIS of chalcocite in the presence of 10% kaolinite was investigated. The results are shown in Fig 7.8. Compared to the impedance of chalcocite in DI water, at the same concentration of 0.34 M, NaI generated the lowest impedance while NaF only slightly reduced the impedance. Again, to understand the different extent of anions in mitigating kaolinite coating from chalcocite surface, the EIS of chalcocite in the absence and presence of kaolinite in each electrolyte solution as shown in Figs7. 6 and 7.8, respectively, was compared. In general, the impedance of chalcocite in the presence of kaolinite was higher in each electrolyte solution. At the Log Frequency = 0, the differences in the log value of impedance in the absence and presence of kaolinite were 0.40, 0.85 and 0.91 ohm cm^2 in NaI, NaCl and NaF solution, respectively. Obviously, I^- mitigated slime coating on chalcocite surface more than Cl^- and F^- and produced a surface closer to the one in the absence of kaolinite. This should be due to greater quantities of larger anions adsorbed on positively charged chalcocite surface, as discussed previously. It is consistent with the flotation tests in Chapter 6 showing that chalcocite flotation in the presence of kaolinite was improved more with I^- than Cl^- and F^-.

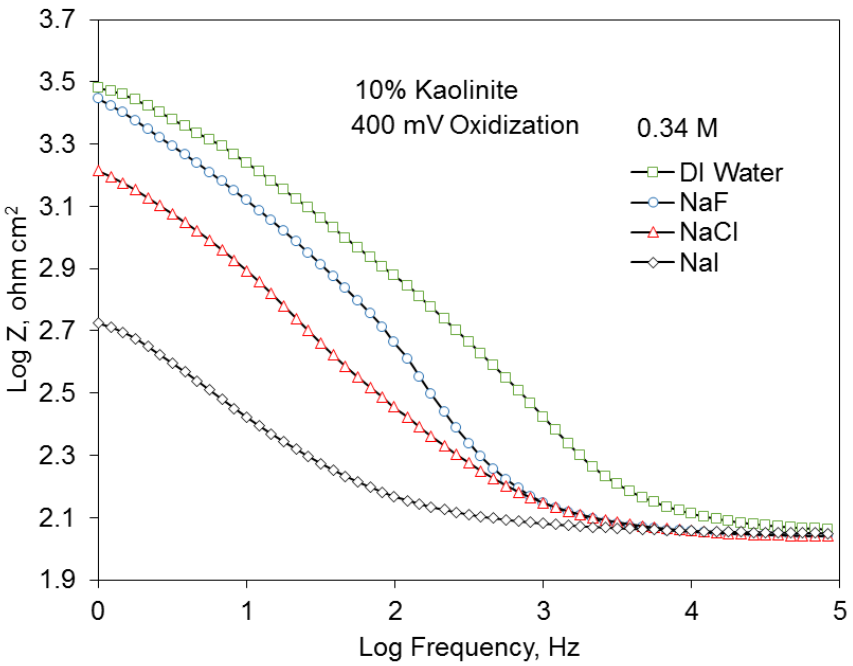

Fig 7.8 EIS (Bode plots) of chalcocite (pre-oxidized at 400mV) in the presence of 10% kaolinite in 0.34 M NaF, NaCl and NaI solutions (the Bode plot of chalcocite with 10% kaolinite coating in the absence of electrolyte is also given for a comparison)

7.4 Modelling of electrochemical impedance spectrum data

The impedance spectrum can be modelled by an electrical circuit with physical elements (Lin and Say, 1999; Pang et al., 1990; Venter and Vermaak, 2008). In this study, based on the criteria of simplicity and electrochemical interpretation, the electrical circuit shown in Fig 7.8 was used to model a simple charge transfer process at the mineral/solution interface. In this circuit, R_s represents the solution resistance and R_{ct} represents charge transfer resistance. The capacitance due to double layer charging and/or possible surface layers is represented by C_{dl} in place of an ideal capacitor. C_{dl} can provide a useful modelling element containing various disturbances due to the physical nature of electrode surface and reactions (surface roughness, "leaky" capacitor, non-uniform current distribution, etc.) (Ekmekçi et al., 2010; Venter and Vermaak, 2008). The surface heterogeneity and roughness of the electrode surface is indicated by a parameter n, usually varying between 0.5 and 1 (Bevilaqua et al., 2004; Guo et al., 2015).

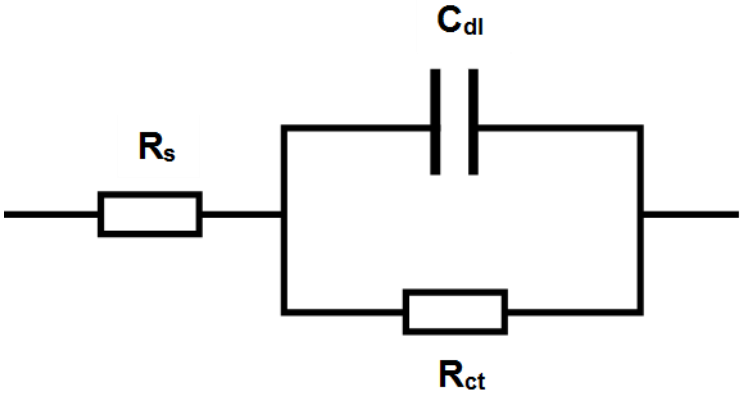

Fig 7.9 The electrical circuit that models the impedance spectrum

To further investigate the kaolinite adsorption on oxidized chalcocite surface in DI water and electrolyte solutions, the EIS data of oxidized chalcocite in the absence and presence of kaolinite were fitted to the proposed electrical circuit using computer program Zview. The extracted model parameters from the equivalent circuit in the absence and presence of kaolinite are given in Tables 7.2 and 7.3, respectively. In both tables, the resistance R_s representing the solution resistance was not greatly affected due to the use of buffer solution in all cases.

Table 7.2 The extracted model parameters by fitting the EIS data in DI water and 0.34 M electrolyte solutions in the absence of kaolinite to the equivalent circuit.

Ion	R_s (Ω cm^2)	R_{ct} ($k\Omega$ cm^2)	C_{dl} (μF cm^{-2})	n
DI Water	90.2	2.3	5.1	0.65
Li^+	110.5	1.5	28.6	0.51
Na^+	118.9	1.3	25.5	0.52
K^+	109.0	1.3	28.2	0.52
F^-	99.6	1.7	18.7	0.62
Cl^-	118.9	1.3	25.5	0.53
I^-	94.0	0.5	28.3	0.56

The experimental error is 1.3–2.8% for R_s, 5.9–10.1% for R_{ct} and 6.4–9.9% for C_{dl}.

In table 7.2, R_{ct} was higher in DI water than all electrolyte solutions, indicating the higher impedance in DI water. In the presence of Li^+, Na^+ and K^+, R_{ct} was similar (varying from 1.5 to 1.3 kΩ cm2), indicating the similar charge transfer between the oxidized chalcocite electrode and the electrolyte interface. R_{ct} was 1.7, 1.3 and 0.5 kΩ cm2 in the presence of F^-, Cl^- and I^-, respectively. The decreasing trend of R_{ct} indicates that the charge transfer was improved by electrolytes, following the order of $F^-<Cl^-<I^-$. C_{dl} was lower in DI water than electrolyte solutions, which reflects the absence of ions in DI water. C_{dl} in the presence of Li^+, Na^+ and K^+ was similar due to the same anion Cl^- absorbed on the oxidized chalcocite surface. An increasing trend of C_{dl} in the presence of F^-, Cl^- and I^- on the oxidized chalcocite surface was due to the greater quantity of a larger anion absorbed on the electrode surface.

In table 7.3, R_{ct} was 3.9 kΩ cm^2 in DI water in the presence of kaolinite which was higher than that in the absence of kaolinite (2.3 kΩ cm^2 in Table 7.2). It demonstrates that kaolinite was adsorbed on oxidized chalcocite surface and increased the difficulty in charge transfer. The decreasing trend of R_{ct} in the presence of Li^+, Na^+ and K^+ indicates that the improved charge transfer with electrolytes follows the order of $Li^+<Na^+<K^+$, due to stronger mitigation of kaolinite coating by larger cations as a result of greater adsorbed quantities of larger cations on the negatively charged kaolinite surface. Similarly, the decreasing trend of R_{ct} was found in the presence of F^-, Cl^- and I^-, due to stronger mitigation of kaolinite coating by larger anions as a result of greater adsorbed quantities of larger anions on the positively charged chalcocite surface.

The dielectric constant for kaolinite is 11.18 which is significantly smaller than that of oxidized chalcocite (>81) (Josann et al., 1936). Therefore, low C_{dl} in DI water reflects the existence of the adsorbed kaolinite. Compared to the C_{dl} values in DI water, the C_{dl} values in electrolyte solutions all increased, indicating less kaolinite absorbed on chalcocite surface. C_{dl} increased in the presence of electrolytes, following the order of $Li^+<Na^+<K^+$ and $F^-<Cl^-<I^-$ due to more large ions absorbed on mineral surface.

Table 7.3 The extracted model parameters by fitting the EIS data in DI water and 0.34 M electrolyte solutions in the presence of kaolinite to the equivalent circuit.solutions in the absence of kaolinite to the equivalent circuit.

Ion	R_s (Ω cm^2)	R_{ct} (kΩ cm^2)	C_{dl} (μF cm^{-2})	n
DI Water	99.0	3.9	4.0	0.55
Li^+	98.6	3.0	8.0	0.53
Na^+	104.2	1.9	11.0	0.58
K^+	103.9	0.8	14.2	0.59
F^-	106.7	2.9	6.9	0.60
Cl^-	104.2	1.9	11.0	0.58
I^-	110.4	0.7	40.4	0.60

The experimental error is 0.9–3.0% for R_s, 3.7–5.0% for R_{ct} and 4.5–9.2% for C_{dl}.

7.5 Conclusions

In this study, for the first time, the electrochemical impedance spectroscopy (EIS) was applied to investigate the slime coating effect and its mitigation on mineral surface. The results show that the impedance was lower in saline water than in tap water, indicating that the electrolyte mitigated slime coating. It is consistent with the flotation results showing that in tap water, the kaolinite coating on chalcocite surface occurs as a result of the electrostatic attraction, leading to the depression of chalcocite flotation. With the addition of electrolytes to the flotation system, the flotation of chalcocite can be improved due to slime coating being mitigated as a result of the reduction of electrostatic attraction between particles by electrolytes. In addition, for the cations (Li^+, Na^+ and K^+) and anions (F^-, Cl^- and I^-) in this study, larger ions can reduce slime coating in the presence of

kaolinite more than smaller ions presumably due to the adsorbed quantity of larger ions on mineral surfaces resulting in greater decreases in electrostatic attraction.

Chapter 8 Conclusions and future work

8.1 Conclusions

This thesis focuses on understanding the mechanism of clay minerals slime coating on copper sulphide minerals and the mitigation of slime coating effect in flotation by electrolytes. The main findings from this study are summarised in this chapter:

(1) The effect of clay minerals on the flotation of copper sulphide minerals

Results of batch flotation tests on open pit ore and underground ore indicated the overall copper flotation recovery of open pit ore was lower than that of underground ore due to the low chalcocite recovery from the open pit ore which contained bentonite. In the absence of bentonite, both chalcopyrite and chalcocite single minerals displayed good floatability in the flotation. However, chalcocite flotation was much more depressed than chalcopyrite in the presence of bentonite after grinding.

(2) The mechanism of clay slime coatings on copper sulphide minerals

It was found that the surface oxidation of chalcopyrite and chalcocite occured and changed the surface properties during grinding. Chalcocite was strongly oxidized while chalcopyrite was slightly oxidized after normal grinding with stainless steel media. The slightly oxidized chalcopyrite surface remained negatively charged after grinding at pH 9.0 and entropically repulsive from bentonite slime particles. In contrast, the strongly oxidized chalcocite surface became positively charged after grinding at the same pH and electrostatically attractive to bentonite particles. It well explained the different flotation behaviour between chalcocite and bentonite in the presence of bentonite.

(3) The mitigation of clay slime coatings on copper sulphides in the flotation by electrolytes

This study showed that electrolytes might mitigate kaolinite slime coating on chalcocite flotation. In tap water, the kaolinite coating on the chalcocite surface was responsible for the depression of chalcocite flotation. With the addition of electrolytes to the flotation system, the flotation of chalcocite was improved. In addition, it was found that larger size ions might improve chalcocite flotation in the presence of kaolinite more than smaller size ions.

(4) The mechanism of mitigation effect of electrolytes on clay minerals slime coating

The electrochemical impedance spectroscopy was applied to investigate how the electrolytes mitigate kaolinite slime coating on chalcocite particle surface. The results showed that with the addition of electrolytes, kaolinite slime coating might be mitigated as a result of the reduction of electrostatic attraction between particles by electrolytes. Larger ions might reduce slime coating in the presence of kaolinite more than smaller ions due to the decrease of the electrostatic attraction between chalcocite and kaolinite.

8.2 Recommendations for future works

To further establish the slime coating mitigation on sulphide minerals flotation, the following work is recommended:

(1) Study the mitigation of chalcocite surface oxidation

This study revealed that chalcocite oxidation might be an important contributing factor to the poor flotation of open pit copper ore. It is recommended to investigate the copper ore surface oxidation issue during grinding in the

Australian copper mining industry and how the reagent scheme could be adjusted accordingly to optimize the copper recovery.

(2) Investigate the clay slime coating mitigation on other main base metals

This study established the clay slime coating mitigation on chalcocite mineral. The possibility of clay slime coating mitigation on other main base metals is promising. Therefore, the isoelectric points of other common sulphides and oxides of metal minerals (such as lead, zinc, nickel, tin etc.) may be tested and compared with this study on chalcocite. Investigations on the mitigation of clay slime coating on these minerals are recommended.

(3) Study the influence of chalcopyrite and chalcocite oxidized layer thickness on slime coating

The thickness of the oxidised layer on copper mineral surface may quantify the formation of the oxidised layer. It could be combined with a time-dependent measurement of impedance to determine the kinetics of oxide layer formation.

List of Reference

Abramov, A., Avdohin, V.M., 1998. Oxidation of Sulfide Minerals in Benefication Processes. CRC Press. 135-136.

Abramov, A.A., Forssberg, K.S.E., 2005. Chemistry and optimal conditions for copper minerals flotation: Theory and practice. Mineral Processing and Extractive Metallurgy Review 26(2), 77-143.

Andreu, R.; Molero, M.; Calvente, J.; Carbajo, J. J. 1993. Generalization of the UDCA theory and its application to the analysis of the ion-free layer thickness. Journal of Electroanalytical Chemistry 358, 49–62. Arnold, B.J., Aplan, F.F., 1986. The effect of clay slimes on coal flotation, part ii: the role of water quality. International Journal of Mineral Processing 17, 243–260.

Bandini, P., Prestidge, C.A., Ralston, J., 2001. Colloidal iron oxide slime coatings and galena particle flotation. Minerals Engineering 14 487-497.

Barzyk, W., Malysa, K., Pomianowski, A., 1981. The influence of surface oxidation of chalcocite on its floatability and ethyl xanthate sorption. International Journal of Mineral Processing 8, 27-29.

Battersby, B.J., Sharp, J.C.W., Webb, R.I., Barnes, G. T., 1994. Vitrification of aqueous suspensions from a controlled environment for electron microscopy: an improved plunge-cooling device. Journal of Microscopy 176, 110-120.

Ben-Naim, A., 1974. Water and Aqueous Solutions. Introduction to a Molecular Theory, New York: Plenum Press.

Bhuiyan, L. B.; Blum, L.; Henderson, D. J. 1983. The application of the modified Gouy-Chapman theory to an electrical double layer contain-ing asymmetric ions. The Journal of Chemical Physics 78, 442–445.

Biegler, T. and Horne, M.D., 1985. Electrochemistry of surface oxidation of chalcopyrite. Journal of the Electrochemical Society 132(6), 1363-1369.

Bockris, J.O'M. and Reddy, A.K.N., 1970. Modern Electrochemistry. Plenum: New York. 2.

Bremmell, K.E., Fornasiero, D., and Ralston, J., 2005. Pentlandite-lizardite interactions andimplications for their separation by flotation. Colloids and Surfaces A 252, 207- 212.

Brigatti, M.F., Galan, E., Theng, B.K.G., 2006. Structures and mineralogy of clay minerals. In: Bergaya, F., Theng, B.K.G., Lagaly, G. (Eds.), Handbook of Clay Science. Amsterdamn, the Nertherlands, 19-86.

Buckley, A.N., Woods, R., 1983. X-ray photoelectron spectroscopic investigation of the tarnishing of bornite. Australian Journal of Chemistry 36 (9), 1793-1804.

Buckley, A.N., Woods, R., 1984. An X-ray photoelectron spectroscopic study of the oxidation of chalcopyrite. Australian Journal of Chemistry 37 (12), 2403-2413.

Castro, S., Uribe, L., Laskowski, J.S., 2014, Depression of inherently hydrophobic minerals by hydrolysable metal cations: molybdenite depression in seawater. XXVII International Mineral Processing Congress-IMPC 2014, Flotation Chemistry Chapter, Santiago, Chile, October 20-24, 2012, pp. 207-217.

Chander, S., 1991. Electrochemistry of sulphide flotation: Growth characteristics of surface coatings and their properties, with special reference to chalcopyrite and pyrite. International Journal of Mineral Processing 33(1-4), 121-134.

Chawla, S.K., Sankarraman, N., Payer, J.H., 1992. Diagnostic spectra for XPS analysis of Cu–O–S–H compounds. Journal of Electron Spectroscopy 61, 1-18.

Chen, G., Grano, S., Sobieraj, S., Ralston, J., 1999b. The effect of high intensity conditioning on the flotation of a nickel ore, part 2: Mechanisms. Minerals Engineering 12, 1359-1373.

Chen, G., Tao, D., 2004. Effect of solution chemistry on floatability of magnesite and dolomite. International Journal of Mineral Processing 74 (1-4), 343-357.

Chen, X., 2014. The Effect of Regrinding Chemistry and Particle Breakage Mechanisms on Subsequent Cleaner Flotation. Doctoral thesis, Queensland University, Brisbane.

Christine L. Henry and Vincent S. J. Craig. 2008. Ion-Specific Influence of Electrolytes on Bubble Coalescence in Nonaqueous Solvents. Langmuir 24, 7979-7985.

Collins, K.D., 2004. Ions from the Hofmeister series and osmolytes: eVects on proteins in solution and in the crystallization process. Methods 34, 300–311.

Craig, V. S. J., Ninham, B. W., Pashley, R. M. J., 1993. The effect of electrolytes on bubble coalescence in Water. Physical Chemistry 97, 10192-10197.

Craig, V. S. J., Ninham, B., Pashley, R.M.J., 1993. Effect of electrolytes on bubble coalescence. Nature 364, 317-319.

Crundwell, F.K., 1988. The influence of the electronic structure of solids on the anodic dissolution and leaching of semiconducting sulphide minerals. Hydrometallurgy 21(2), 155-190.

Dasgupta, S., 1991. Adsorption behavior of macromolecules on colloidal magnetic oxide particles: Interfacial interaction and dispersion characteristics. Progress in Organic Coatings 19, 123-139.

Deroubaix, G., Marcus, P., 1992. X-ray photoelectron spectroscopy analysis of copper and zinc oxides and sulphides, Surface and Interface Analysis 18, 39-46.

De Wet, J.R., Pistorius, P.C., Sandenbergh, R.F., 1997. The influence of cyanide on pyrite flotation from gold leach residues with sodium isobutyl xanthate, International Journal of Mineral Processing. 49, 149-169.

Deryagin, B.V., Landau, L.D., 1941. Theory of the stability of strongly charged lyophobic sols and of the adhesion of strongly charged particles in solution of electrolytes. Acta Physicochimica URSS 14:633-62.

Deryagin, B. V., Dukhin, S. S., Rulev, N. N., 1982. Kinetic theory of the flotation of small particles, Russian Chemical Reviews 51, 51-67.

Duarte, A.C.P., and Grano, S.R. 2007. Mechanism for the recovery of silicate gangue minerals in the flotation of ultrafine sphalerite. Minerals Engeering 20, 766-775.

Eadington P., 1977. Study of oxidation layers of surfaces of chalcopyrite by use of Auger electron spectroscopy. Transactions of the Institutions of Mining and Metallurgy. 86, 186-189.

Edwards, G.R., Kipkie, W.B., and Agar, G.E., 1980. The effect of slime coatings of the serpentine minerals, chrysotile and lizardite on pentlandite flotation. International Journal of Mineral Processing 7, 33-42.

Ekmekçi, Z., Becker, M., Tekes, E.B., Bradshaw, D., 2010. An impedance study of the adsorption of CuSO4 and SIBX on pyrrhotite samples of different provenances. Minerals Engeering 23, 903-907.

Ekmekci, Z., Demirel, H., 1997. Effects of galvanic interaction on collectorless

flotation behaviour of chalcopyrite and pyrite. International Journal of Mineral Processing 52 (1), 31-48.

Emsley, J., 2003. Nature's building blocks: an A-Z guide to the elements. Oxford University Press. pp. 121-125. ISBN 978-0-19-850340-8. Retrieved 2 May 2011.

Fairthorne, G., Fornasiero, D., Ralston, J., 1997. Effect of oxidation on the collectorless flotation of chalcopyrite. International Journal of Mineral Processing 49, 31-48.

Fairthorne, G., Brinen, J.S., Fornasiero, D., Ralston, J., 1998. Spectroscopic and electrokinetic study of the adsorption of butyl ethoxycarbonyl thiourea on chalcopyrite. International Journal of Mineral Processing 54, 147-163.

Faro T. M. C., Thim G. P., Skaf M. S., 2010. A Lennard-Jones plus Coulomb potential for Al^{3+} ions in aqueous solutions. The Journal of Chemical Physics 132, 114509.

Fornasiero, D., Eijt, V., Ralston, J., 1992. An electrokinetic study of pyrite oxidation. Applied Surface Science 62 (1-2), 63-73.

Forssberg, E., Sundberg, S., Zhai, H., 1988. Influence of different grinding methods on floatability. International Journal of Mineral Processing 22 (1-4), 183-192.

Franks, F.Water, 1972. A comprehensive treatise, New York: Plenum Press.

Franks, G.V., 2002. Zeta potentials and yield stresses of silica suspensions in concentrated monovalent electrolytes: isoelectric point shift and additionalattraction. J. Colloid Interf. Sci. 249, 44−51.

Frank, H. S. & Wen, W. Y., 1957. Structural aspects of ion-solvent interaction in aqueous solutions: a suggested picture of water structure. Discussions of the Faraday Society 24, 133-140.

Fullston, F., Fornasiero, D., Ralston, R., 1999. Zeta potential study of the oxidation of copper sulphide minerals. Colloids and Surfaces 146 (1-3), 113-121.

Gardner, J.R. and Woods, R., 1979. An electrochemical investigation of the natural flotability of chalcopyrite. International Journal of Mineral Processing 6 (1), 1-16.

Gaudin, A.M., Fuerstenau, D.W., Miaw, H.L., 1960. Slime-coatings in galena flotation. CIM Bull 53, 960-963.

Ghosh, P., 2004. Coalescence of Air Bubbles at Air-Water Interface. Chemical Engineering Research and Design 82, 849-854.

Ghosh, P., 2009. Colloid and Interface Science. PHI Learning, New Delhi. pp. 136.

Glew, D. N., 1962. Aqueous solubility and the gas-hydrates, the methane-water system 1. The Journal of Physical Chemistry 66, 605-609.

Gonçalves, K.L.C., Andrade, V.L.L. and Peres, A.E.C., 2003. The effect of grinding conditions on the flotation of a sulphide copper ore. Minerals Engineering 16 (11), 1213-1216.

Grahame, D.C., 1947. The electrical double layer and the theory of electrocapillarity. Chemical Reviews. 41, 3, 441-501.

Grano, S., 2009. The critical importance of the grinding environment on fine particle recovery in flotation. Minerals Engineering 22, 386-394.

Guo, B., Peng, Y., Espinosa-Gomez, R., 2015. Effect of free cyanide and cuprous cyanide on the flotation of gold and silver bearing pyrite. Minerals Engineering 71, 194-204.

Guo,H., Yen,W.T., 2003. Pulp potential and floatability of chalcopyrite. Minerals Engineering 16 (3), 247-256.

Gurney, R. W.Ionic., 1953. Processes in Solution. New York: McGraw-Hill.

Guy, P.J., Trahar, W.J., 1984. The influence of grinding and flotation environments on the laboratory flotation of galena. International Journal of Mineral Processing 12 (1-3), 15-38.

Guy, P.J. and Trahar, W.J., 1985. The Effects of Oxidation and Mineral Interaction on Sulphide Flotation Flotation of Sulphide Minerals. K. S. E. Forssberg. Amsterdam, The Netherlands, Elservier: 91-100.

Hancer M., Celik M.S., Miller J.D., 2001. The significance of interfacial water structure in soluble salt flotation systems. Journal of Colloid and Interface Science 235(1), 150-161.

Hasted, J.B., Ritson, D.M., and C. H. Collie, C.H., 1948. Dielectric Properties of Aqueous Ionic Solutions. Parts I and II. The Journal of Chemical Physics 16, 1.

Hayes, R.A., Price, D.M., Ralston, J. and Smith, R.W., 1987. Collectorless Flotation of Sulphide Minerals. Mineral Processing and Extractive Metallurgy Review 2 (3), 203-234.

Helmholtz, H. (1853), Ueber einige Gesetze der Vertheilung elektrischer Ströme in körperlichen Leitern mit Anwendung auf die thierisch-elektrischen Versuche, Annalen der Physik und Chemie (in German), 165 (6), 211–233.

Henry, C. L.; Dalton, C. N.; Scruton, L.; Craig, V. S. J., 2007. Ion-Specific Coalescence of Bubbles in Mixed Electrolyte Solutions. Journal of Physical Chemistry C 111, 1015.

Heyes, G.W. and Trahar, W.J., 1977. The natural flotability of chalcopyrite. International Journal of Mineral Processing 4(4), 317-344.

Heyes, G.W. and Trahar, W.J., 1979. Oxidation-Reduction effects in the flotation of chalcocite and cuprite. International Journal of Mineral Processing 6 (3), 229-252.

Hirajima, T., Mori, M., Ichikawa, O., Sasaki, K., Miki, H., Farahat, M. and Sawada, M., 2014. Selective flotation of chalcopyrite and molybdenite with plasma pre-treatment. Minerals Engineering 66–68 (0), 102-111.

Hitoshi, O., Tamas, R., 1993. Structure and dynamics of hydrated ions. Chemical Reviews. 93 (3), 1157-1204.

Hofmeister, F., 1888. Zur Lehre von der Wirkung der Salze, Archiv fur Experimentelle Pathologie und Pharmakologie (Leipzig), 24, 247-260; translated in Kunz, W., Henle, J., and Ninham, B.W., 2004.' Zur Lehre von der Wirkung der Salze' (about the science of the effect of salts: Franz Hofmeister's historical papers, Current Opinion in Colloid and Interface Science, 9, 19-37.

Israelachvili, J. N., 1991. Intermolecular and surface forces, 2nd ed. Academic Press, London/San Diego.

Josann, L., RosnNnor, Z., and Duornv T. S., 1936, The Dielectric Constant of Mineral Powders. Rensselaer Polytechnic Institute Engineering and Science Series, No. 52, The American Mineralogist 21(2).

Jungwirth, P. and Cremer, P.S., 2014, Beyond Hofmeister. Nature Chemistry 6, 261-263.

Kang, K.C., Praveen Ling, P., Park, K., Choi, S.J., Lee J.D., 2014. Seawater desalination by gas hydrate process and removal characteristics of dissolved ions (Na^+, K^+, Mg^{2+}, Ca^{2+}, B^{3+}, Cl^-, $SO4^{2-}$). Desalination 353, 84–90.

Kelebek, S. and Smith, G.W., 1989. Electrokinetic properties of a galena and chalcopyrite with the collectorless flotation behaviour. Colloids and Surfaces 40, 137-143.

Kotlyar, L.S., Sparks, B.D., Schutte, R., 1996. Effect of salt on the flocculation behaviour of nano particles in oil sands fine tailings. Clays Clay Minerals 44 (1), 121-131.

Kulikov, B. F., Zyev, V. V., Vainshenker, I. A., and Mitenkov, G. A., 1985. Minerals Handbook of the Beneficiation Technologist, Moscow, Russia, Nedra Press (in Russian).

Kunz W., 2010. Specific ion effects. World Scientific Publishing Co., Singapore. Pp.50.

Lagaly, G., 1993. From clay minerals to colloidal clay mineral dispersions. In: Dobias, B. (Ed.), Coagulation and Flocculation. Theory and Applications. Marcel Dekker Inc., New York, pp. 427-494.

Lascelles, D., Finch, J.A., 2002. Quantifying accidental activation. Part I. Cu ion production. Minerals Engineering. 15 (8), 567-571.

Legrand, D.L., Bancroft, G.M., Nesbitt, H.W., 1997. Surface characterization of pentlandite, $(Fe, Ni)_9S_8$, by X-ray photoelectron spectroscopy. International Journal of Mineral Processing 51, 217-228.

Linge H. G., 1976. A study of chalcopyrite dissolution in acidic ferric nitrate by potentiometric titration. Hydrometallurgy. 2, 51-64.

Liu, J., Xu, Z., Masliyah, J., 2005a. Interaction forces in bitumen extraction from oil sands. Journal of Colloid and Interface Science 287, 507-520.

Liu, J., Xu, Z., Masliyah, J., 2005b. Interaction forces in bitumen extraction from oil sands. Journal of Colloid and Interface Science 287 (2), 507-520.

Luckham, P.F., Rossi, S., 1999. The colloidal and rheological properties of bentonite suspensions. Advances in Colloid and Interface Science 82 (1-3), 43-92.

Marcus, Y., 2015. Ions in solution and their solvation. John Wiley & Sons, Inc., Hoboken, New Jersey. 136.

Martinez J. M., Pappalardo R. R., and Marcos E. S., 1999. First-Principles Ion−Water Interaction Potentials for Highly Charged Monatomic Cations. Computer Simulations of Al^{3+}, Mg^{2+}, and Be^{2+} in Water. Journal of the American Chemical Society. 121 (13), 3175.

McIntyre, N.S., Cook, M.G., 1975. X-ray photoelectron studies on some oxides and hydroxides of cobalt, nickel, and copper, Analytical Chemistry 47, 2208-2213.

Mielczarski, J. and Suoninen, E., 1988. XPS study of the oxidation of cuprous sulphide in aerated aqueous solutions. Colloids and Surfaces 33, 231-237.

Mielczarski, J.A., Mielczarski, E., Cases, J.M., 1998. Influence of chain length on adsorption of xanthates on chalcopyrite. International Journal of Mineral Processing 52 (4), 215-231.

Mikhlin, Y.L., Tomashevich, Y.V., Asanov, I.P., Okotrub, A.V., Varnek, V.A. and Vyalikh, D.V., 2004. Spectroscopic and electrochemical characterization of the surface layers of chalcopyrite (CuFeS2) reacted in acidic solutions. Applied Surface Science 225(1-4), 395-409.

Moayedi, H., Huat, B.B.K., Kazemian, S., Daneshmand, S., Moazami, D. 2011. Electrophoresis of Suspended Kaolinite in Multivalent Electrolyte Solution. International Journal of Electrochemical Science 6, 6514 – 6524.

Natarajan, K.A., 1996. Laboratory studies on ball wear in the grinding of a chalcopyrite ore. International Journal of Mineral Processing 46 (3-4), 205-213.

Nemethy, G., Scheraga, H. A., 1962. Structure of Water and Hydrophobic Bonding in Proteins. II. Model for the Thermodynamic Properties of Aqueous Solutions of Hydrocarbons. The Journal of Chemical Physics 36, 3401-3417.

Nesbitt, H.W., Muir, I.J., 1994. X-ray photoelectron spectroscopic study of a pristine pyrite surface reacted with water vapour and air. Geochimica et Cosmochimica Acta 58, 4667–4679.

Nikita, P., Nikolay, S., Valery, Y., Eugeny, F.J., Eugeny, F., 2015. Terahertz Spectroscopy Applied for Investigation of Water Structure. The Journal of Physical Chemistry B 119, 12664−12670.

Niu, Y., Sun, F., Xu, Y., Cong, Z., Wang. E., 2014. Applications of electrochemical techniques in mineral analysis. Talanta 127, 211-218.

Nsib, F., Ayed, N., Chevalier, Y., 2006. Selection of dispersants for the dispersion of carbon black in organic medium. Progress in Organic Coatings 55, 303-310.

Nsib, F., Ayed, N., Chevalier, Y., 2007. Comparative study of the dispersion of three oxide pigments with sodium polymethacrylate dispersants in alkaline medium. Progress in Organic Coatings 60, 267-280.

Omta A.W., Kropman M.F., Woutersen S., Bakker H.J., 2003. Negligible effect of ions on the hydrogen-bond structure in liquid water. Science, 301, 347-349.

Ozlem B., Zafir E., Metin C., and Yasemin O., 2012. The effect of water chemistry on froth stability and surface chemistry of the flotation of a Cu-Zn sulfide ore. International Journal of Mineral Processing 102-103, 32-37.

Pang, J., Briceno, A., and Chander, S., 1990. A Study of Pyrite/Solution Interface by Impedance Spectroscopy. Journal of The Electrochemical Society 137 (11), 3447-3455.

Pang, X.F., 2014. Water Molecular Structure and Properties. Singapore, World Scientific Publishers.

Parsons, R.; Zobel, F., 1965. The interphase between mercury and aqueous sodium dihydrogen phosphate. Journal of Electroanalytical Chemistry 9, 333–348.

Pashley, R. M. & Karaman, M. E. Applied colloid and surface chemistry, Chichester, West Sussex, England ; Hoboken, N.J.: J. Wiley; 2004.

Paulson, O., Pugh, R.J., 1996, Flotation of inherently hydrophobic particles in aqueous solutions of inorganic electrolytes. Langmuir 12 (20), 4808-4813.

Peabody, A.L., Abramov, A.A. and Avdokhin, V.M., 1997. Oxidation of sulphide minerals in benefication processes. Australia, Gordon and Breach Science Publishers.

Peng,Y., Grano, S., Ralston,J., Fornasiero,D., 2002. Towards prediction of oxidation during grinding I. Galena flotation, Minerals Engineering 15, 493-498.

Peng, Y., Grano, S., Fornasiero, D., Ralston, D., 2003a. Control of grinding conditions in the flotation of chalcopyrite and its separation from pyrite. International Journal of Mineral Processing 69 (1-4), 87-100.

Peng, Y., Grano, S., Fornasiero, D., Ralston, J., 2003b. Control of grinding conditions in the flotation of galena and its separation from pyrite. International Journal of Mineral Processing 70 (1-4), 67-82.

Peng, Y., Ourriban, M., 2006. Roles of metal oxidation species in the flotation of fine sulphide minerals. In: Xu, Z., Liu, Q. (Eds.), Proceedings of Sixth UBC-McGill-U of A Biennial Symposium on Interfacial Phenomena in Fine Particle Technology. Montreal, Canada, pp. 345-359.

Peng, Y., Bradshaw, Smart, R.Sc., 2010. Reducing the Deleterious Impacts of Clay Particle Interactions with Valuable Minerals in Copper and Gold Processing. ARC Linkage Project Report.

Peng, Y., Grano, S., 2010. Effect of grinding media on the activation of pyrite flotation. Minerals Engineering 23 (8), 600-605.

Peng, Y., Grano, S., 2010. Dissolution of fine and intermediate sized galena particles and their interactions with iron hydroxide colloids. Journal of Colloid and Interface Science 347, 127-131.

Peng, Y., Grano, S., 2010. Inferring the distribution of iron oxidation species on mineral surfaces during grinding of base metal sulphides. Electrochimica Acta 55, 5470-5477.

Peng, Y., Grano, S., 2010. Effect of iron contamination from grinding media on the flotation of sulphide minerals of different particle size. International Journal of Mineral Processing 97, 1-6.

Peng,Y., Zhao,S, 2011. The effect of surface oxidation of copper sulphide minerals on clay slime coating in flotation. Minerals Engineering 24 (2011) 1687-1693.

Peng,Y., Zhao,S., Bradshaw.D., 2012. Role of saline water in the selective flotation of fine particles. Water in Mineral Processing: Proceedings of the First International Symposium. 2012 SME Annual Meeting, Seattle, USA, (61-72). 19 - 22 February.

Peng, Y., Bradshaw, D., 2012. Mechanisms for the improved flotation of ultrafine pentlandite and its separation from lizardite in saline water. Minerals Engineering 36-38, 284-290.

Permien, T., Lagaly, G., 1994. The rheological and colloidal properties of bentonite dispersions in the presence of organic compounds IV. Sodium montmorillonite and acids. Applied Clay Science 9 (4), 251-263.

Philipsea, A.P., Tuinier, R., Kuipersa, B.W.M., Vrija, A M. Vis, M., 2017. On the Repulsive Interaction Between Strongly Overlapping Double Layers of Charge-regulated Surfaces. Colloid and Interface Science Communications 21 10-14.

Pietrobon, M.C., Grano, S.R., Sobieraj, S., 1997. Recovery mechanisms for pentlandite and MgO bearing gangue minerals in nickel ores from Western Australia. Minerals Engineering 10, 775-786.

Priest, C., Stevens, N., Sedev, R., Skinner, W., Ralston, J., 2008. Inferring wettability of heterogeneous surfaces by ToF-SIMS. Journal of Colloid and Interface Science 320 (2), 563-568.

Rand, B., Pekenc, E., Goodwin, J.W., Smith, R.W., 1980. Investigation into the existence of edge-face coagulated structures in Na-montmorillonite suspensions. Journal of the Chemical Society, Faraday Transactions 1 76, 225-235.

Rumball, J.A. and Richmond, G.D., 1996. Measurement of oxidation in a base metal flotation circuit by selective leaching with EDTA. International Journal of Mineral Processing 48(1-2), 1-20.

Russel, W.B., Saville, D.A. and Schowalter, W. R. 1989. Colloidal Dispersions, Cambridge University Press, 265.

Sato, M., 1960. Oxidation of sulphide ore bodies, II. Oxidation mechanisms of sulphide minerals at 25°C. Economic Geology 55, 1202-1231.

Scheffel, R.E., 2002. Copper heap leach design and practice. In: Mular, A.L., Halbe, D.N., Barratt, D.J. (Eds.), Mineral Processing Plant Design, Practice, and Control. Littleton, Colo, pp. 1571-1585.

Schmickler, W., Santos, E., 2010. Interfacial Electrochemistry. Springer, pp. 41.

Schwierz, N., Horinek, D., Netz, R.R., 2010. Reversed anionic Hofmeister series: The interplay of surface charge and surface polarity. Langmuir. 26, 7370-7379.

Schoonheydt, R.A., Johnston, C.T., 2006. Surface and interface chemistry of clay minerals. In: Bergaya, F., Theng, B.K.G., Lagaly, G. (Eds.), Handbook of Clay Science. Amsterdamn, The Nertherland, pp. 87-114.

Senior, G.D., Trahar, W.J., 1991. The influence of metal hydroxides and collector on the flotation of chalcopyrite. International Journal of Mineral Processing 33 (1-4), 321-341.

Sillitoe,R., Petersen,R., 1996. Andean Copper Deposits: New Discoveries, Mineralization, Styles and Metallogeny, Littleton, CO.

Smart,R.St.C., 1991. Surface layers in basemetal sulphide flotation, Minerals Engineering 4, 891-909.

Smith, J. M., Qin, Z., Shoessmith, D. W., 2009. Electrochemical Impedance Studies of the Growth of Sulphide Films on Copper. 17th International Corrosion congress. Paper No. 11, 1-9.

Sondi, I., Milat, O., Pravdic, V., 1997. Electrokinetic potentials of clay surfaces modified by polymers. Journal of Colloid and Interface Science 189 (1), 66-73.

Sonnefeld, J., 1995. Surface charge density on spherical silica particles in aqueous alkali chloride solutions. Colloid and Polymer Science 273, 932-938.

Soga,I., 2001. Polydispersity and Functional Group Distribution of Dispersant Polymer: Adsorption Properties and Magnetic Paint Dispersion. Journal of Colloid and Interface Science 240, 622-629.

Somasundaran,P., Runkana,V., 2003. Mathematical modeling of flocculation and dispersion of colloidal. International Journal of Mineral Processing 72, 33-55.

Song,S., Lopez-Valdivieso, A., Martinez-Martinez, C., Torres-Armenta, R., 2006. Improving fluorite flotation from ores by dispersion processing. Minerals Engineering 19, 912-917.

Spångberg D. and Hermansson K., 2004. Many-body potentials for aqueous Li^+, Na^+, Mg^{2+}, and Al^{3+}: Comparison of effective three-body potentials and polarizable models. The Journal of Chemical Physics. 120, 4829.

Spitzer, J. J., 1983.The effect of ionic sizes on the potential distribution in the double layer in the absence of specific adsorption Journal of Colloid and Interface Science 92, 198–203.

Swartzen-Allen, S.L., Egon, M., 1974. Surface and colloid chemistry of clays. Chemical Reviews 74 (3), 385-400.

Tadros, Th. F., and Lyklema, J., 1968. Adsorption of potential-determining ions at the silica-aqueous electrolyte interface and the role of some cations. Journal of Electroanalytical Chemistry 17 (3-4), 267-275.

Theodoor, J., Overbeek, G., 1990. The role of energy and entropy in the electrical double layer. Colloids and Surfaces 51, 61-75.

Tjipangandjara, K.F., Huang, Y.B., Somasundaran, P., Turro, N.J., 1990. Correlation of alumina flocculation with adsorbed polyacrylic acid conformation. Colloids and Surfaces 44, 229-236

Todd, E.C., Sherman, D.M., Purton, J.A., 2003. Surface oxidation of chalcopyrite (CuFeS2) under ambient atmospheric and queous (pH 2-10) conditions: Cu, Fe L- and O K-edge X-ray spectroscopy. Geochimica et Cosmochimica Acta 67 (12), 2137-2146.

Tolley, W., Kotlyar, D., Van Wagoner, R., 1996. Fundamental electrochemical studies of sulphide mineral flotation. Minerals Engineering 9 (6), 603-637.

Trahar, W.J., 1981. A rational interpretation of the role of particle size in flotation. International Journal of Mineral Processing 8, 289-327.

Uribe, L., Gutierrez, L., Janusz S. Laskowski, J.S., 2017. Role of calcium and magnesium cations in the interactions between kaolinit and chalcopyrite in seawater. Physicochemical Problems of Mineral Processing. 53(2), 737−749.

Valleau, J. P.; Torrie, G. M. J. 1982. The electrical double layer. III. Modified Gouy - Chapman theory with unequal ion sizes. The Journal of Chemical Physics 1982, 76, 4623–4630.

Van Olphen, H., 1964.Internal mutual flocculation in clay suspensions. Journal of Colloid Science 19, 313-322.

Vane, L.M., Zang, G.M., 1997. Effect of aqueous phase properties on clay particle zeta potential and electro-osmotic permeability: implications for electro-kinetic soil remediation processes. Journal of Hazardous Materials 55 (1-3), l-22.

Vaughan, D.J., Becker, U. and Wright, K., 1997. Sulphide mineral surfaces: Theory and experiment. International Journal of Mineral Processing 51(1-4), 1-14.

Velasquez, P., Leinen D., Pascual J., Ramos-Barrado, J.R., Cordova, R., Gomez, H., Schrebler, R., 2001. XPS, SEM, EDX and EIS study of an electrochemically modified electrode surface of natural chalcocite (Cu2S). Journal of Electroanalytical Chemistry 501, 20-28.

Verwey, E.J.W., Overbeek, J.Th.G., 1948. Theory of the stability of lyophobic colloids: the interaction of sol particles having an electric double layer. Elsevier, Amsterdam.

Wagner,C.D., Riggs,W.M., Davis,L.E., Moulder,J.F., Muillnbery,G.E., 1979. Handbook of X-ray Photoelectron Spectroscopy, Perkin Elmer Corporation, Eden Prairie, Minn., USA.

Walker, G.W., Stout Iii, J.V. and Richardson, P.E., 1984. Electrochemical flotation of sulphides: Reactions of chalcocite in aqueous solution. International Journal of Mineral Processing 12(1-3), 55-72.

Wang,Q., Heiskanen,K., 1992. Dispersion selectivity and heterocoagulation in apatite-hematite-phlogopite fine particle suspensions II. Dispersion selectivities of the mineral mixtures. International Journal of Mineral Processing 35, 133-145.

Wei, Y., Chiang, P., and Sridhar, S., 1992. Ion size effects on the dynamic and static dielectric properties of aqueous alkali solutions. The Journal of Chemical Physics 96 (6), 4569.

Weissenborn, P., Pugh, R.J. 1995. Surface Tension and Bubble Coalescence Phenomena of Aqueous Solutions of Electrolytes. Langmuir 11, 1422-1426.

Wellham, E. J.; Elber, L.; Yan, D. S. 1992. The role of carboxy methyl cellulose in the flotation of a nickel sulphide transition ore. Minerals Engineering 5 (3-5), 381.

Wiese, J., Harris, P., Bradshaw, D., 2005. The influence of the reagent suite in the flotation of ores from the Merensky reef. Mineral Engineering 18, 189–198.

Wilhelm, E., Battino, R., Wilcock, R. J., 1977. Low-pressure solubility of gases in liquid water. Chemical Reviews 77, 219-262.

Yarar, B., 1988. Gammar flotation: A new approach to flotation, using liquid vapour surface tension control. Edited by Castro, S. H., Alvarez, J., Elsevier Publishing: Amsterdam, Chapter 3, Froth Flotation, 41.

Ye, X., Gredelj, S., Skinner, W., Grano, S.R., 2010. Evidence for surface cleaning of sulphide minerals by attritioning in stirred mills. Minerals Engineering 23 (11-13), 937- 944.

Ye,X., Gredelj,S., Skinner,W., Grano,S.R., 2010. Regrinding sulphide minerals - breakage mechanisms in milling and their influence on surface properties and flotation behavior. Powder Technology 203, 133-147.

Yin Q., Kelsall G.H., Vaughan D.J., England K.E.R., 1995. Atmospheric and electrochemical oxidation of the surface of chalcopyrite (CuFeS2). Geochimica et Cosmochimica Acta. 59(6), 1091-1100.

Yin, Q., Vaughan, D.J., England, K.E.R., Kelsall, G.H. and Brandon, N.P., 2000. Surface oxidation of chalcopyrite (CuFeS2) in alkaline solutions. Journal of the Electrochemical Society 147(8), 2945-2951.

Yoon, R. H., 1982. Flotation of Coal Using Micro-Bubbles and Inorganic Salts. Mining Congress Journal 68 (12), 76.

Zachwieja, J.B., McCarron, J.J., Walker, G.W. and Buckley, A.N., 1989. Correlation between the surface composition and collectorless flotation of chalcopyrite, Journal of Colloid and Interface Science 132(2), 462-468.

Zhang, M., Peng, Y., 2015. Effect of clay minerals on pulp rheology and the flotation of copper and gold minerals. Minerals Engineering 70, 8-13.

Zhang, Z., Liu J., Xu Z., Ma L., 2013. Effects of clay and calcium ions on coal flotation. International Journal of Mining Science and Technology. 23 (5), 689-692.

Zhao, H., Bhattacharjee, S., Chow, R., Wallace, D., Masliyah, J.H., Xu, Z., 2008. Probing surface charge potentials of clay basal planes and edges by direct force measurements. Langmuir 24 (22), 12899-12910.